REPUBLIC OF TURKEY

ACIBADEM MEHMET ALI AYDINLAR UNIVERSITY

INSTITUTE OF HEALTH SCIENCES

DEVELOPMENT OF ANTIMICROBIAL PEPTIDES SPECIFIC TO BIOFILM FORMATION BACTERIA AND BINDING TO CATHETER SURFACE

TUBA POLAT

MASTER THESIS

DEPARTMENT OF MEDICAL BIOTECHNOLOGY

SUPERVISOR

Assist. Prof. Nihan ÜNÜBOL

CO SUPERVISOR

Assist. Prof. Erkan MOZİOĞLU

ISTANBUL 2021

REPUBLIC OF TURKEY

ACIBADEM MEHMET ALI AYDINLAR UNIVERSITY

INSTITUTE OF HEALTH SCIENCES

DEVELOPMENT OF ANTIMICROBIAL PEPTIDES SPECIFIC TO BIOFILM FORMATION BACTERIA AND BINDING TO CATHETER SURFACE

TUBA POLAT

MASTER THESIS

DEPARTMENT OF MEDICAL BIOTECHNOLOGY

SUPERVISOR

Assist. Prof. Nihan ÜNÜBOL

CO SUPERVISOR

Assist. Prof. Erkan MOZİOĞLU

ISTANBUL 2021

DECLARATION

I hereby declare that; this thesis has been written by me based on the data obtained in line with the scientific rules and ethical principles of responsible conduct of research. All information, data, comments, analyses have been collected and processed through scientific, academic writing style, and literature used have been duly shown by giving reference to the sources by the publication ethics. I also announce and emphasize that I have not violated any rules secured by patent and copyrights whilst the conduct and writing of this research.

03.02.2021

Tuba POLAT

ACKNOWLEDGMENTS

I would like to thank my dear advisor, Assist. Prof. Nihan ÜNÜBOL and my co-advisor, Assist Prof. Erkan MOZİOĞLU, for their guidance, contributions, encouragement and supports during this research. I would like to gratefully thank our head of department, Prof. Dr. Tanıl KOCAGÖZ, who has vast knowledge and whom I always apply for his experiences. Again, I would like to thank Assist Prof. Özgül GÖK, Assist Prof. Tuğba Arzu ÖZAL ILDENIZ and Assoc. Prof. Özge CAN for their contribution to my work. Furthermore, I would like to thank my father, who is my greatest chance as a daughter and thank my mother whom I took as a role model in my life. I am grateful to all my family, dear lab mates whom we worked together until night and my dear close friends for being with me in this process.

This study was supported by TUBITAK Chemistry and Biology Research Support Group with the 118Z859 coded project, Development of antimicrobial catheters by using peptide antibiotics specific to biofilm formation with new binding strategies.

TABLE OF CONTENTS

DECLARATION ..... **iii**

ACKNOWLEDGMENTS ..... **iv**

TABLE OF CONTENTS ..... **v**

LIST OF ABBREVIATION AND SYMBOLS ..... **ix**

LIST OF FIGURES ..... **xii**

LIST OF TABLES ..... **xv**

SUMMARY **1**

ÖZET **2**

1. BACKGROUND AND AIM OF THE STUDY **4**

2. INTRODUCTION **6**

2.1. Antimicrobial Peptides 6

2.1.1. Peptide biosynthesis and chemical synthesis 7

2.1.2. Natural AMPs 9

2.1.2.1. Animal AMPs 10

2.1.2.2. Plant AMPs 12

2.1.2.4. Bacterial AMPs 15

2.1.3. Structure of AMPs 16

2.1.4. Protecting human cells from the effect of AMPs 17

2.1.5. Antibacterial effect of AMPs 18

2.1.6. Bacterial resistance mechanisms to AMPs 21

2.1.7. Molecular modeling methods for determining the effectiveness of antimicrobial peptides 24

2.2. Biofilm 25

2.2.1. Biofilm formation in bacteria 26
2.2.1.1. Quorum sensing 28
2.2.2. Other biofilm-forming species 29
2.2.3. Detection methods of biofilm formation 30
2.2.4. Medical biofilms 31
2.2.5. AMPs to combat bacterial biofilm 33
2.2.6. Self-Assembly ability of peptides 34
3. MATERIALS AND METHODS 35
3.1 Materials 35
3.2. Peptide Design 38
3.3. Molecular Modeling of Peptides 40
3.4. Solid Phase Chemical Synthesis of Designed Peptide Antibiotics 41
3.5. HPLC (High-performance liquid chromatography) and Lyophilization 43
3.5.1 Analytical HPLC 43
3.5.2 Semi-prep HPLC 44
3.5.3. Lyophilization 45
3.6. Peptide Concentration 46
3.7. Liquid Chromatography–Mass Spectrometry (LC/MS) 47
3.8. Detection of Antibacterial Activity (MIC) 48
3.9. Protease Resistant Assay 50
3.10. SEM (Scanning Electron Microscope) Imaging 50
3.11. Detection of Hemolysis 51
3.12. Detection of Cytotoxicity 52
3.13. Detection of Biofilm Inhibition and Eradication 53
3.13.1. Agar and broth preparation 54
3.13.2. Minimum biofilm inhibition assay (MBIC) 54

3.13.3. Minimum biofilm eradication concentration assay (MBEC) 58
3.14. Peptide Characterization and Self-assembly (FT-IR) 59
3.14.1. Slicon catheter surface cleaning protocol 59
3.14.2. Peptide characterization 60
3.14.3. Peptide self-assembly by drip method 60
3.14.4. Peptide self-assembly with the soaking method in peptide solution 61
3.15. Peptide Self-Assembly EDS Analysis 61
4. RESULTS 62
4.1. Peptide Design 62
4.2. Molecular Modeling of Peptides 63
4.3. HPLC 64
4.3.1. Analytical HPLC 65
4.3.2. Semi-preparative HPLC 66
4.4. Peptide Concentration Assay 68
4.5. LC / MS 69
4.6. Detection of Antibacterial Activity (MIC) 74
4.7. SEM Images 76
4.8. Protease Resistant Assay 79
4.9. Detection of Hemolysis 82
4.10. Detection of Cytotoxicity 83
4.11. Detection of Minimum Biofilm Inhibition and Eradication 85
4.11.1 Minimum Biofilm Inhibiton Assay 85
4.11.2. Minimum Biofilm Eradication Assay 89
4.12. Peptide Characterization and Self-assembly (FT-IR & SEM) 90
4.12.1. Peptide characterization 90
4.11.2. Self-Assembly by Drip Method 91

4.12.2.1. Self-assembly by drip method at 25°C 91
4.12.2.2. Self-assembly by drip method at 37°C 92
4.12.3. Self-assembly with soaking method in peptide solution..... 93
4.12.4. Self-assembly EDS analysis..... 95
5. DISCUSSION AND CONCULUSION..... 97
6. REFERENCES..... 102
7. CURRICULUM VITAE..... 117

LIST OF ABBREVIATION AND SYMBOLS

α	Alpha
Aa	Amino Acid
AAMPs	Anionic Antimicrobial Peptides
ACN	Acetonitrile
AMP	Antimicrobial Peptides
APD	Antimicrobial Peptide Database
Arg	Arginine
ATP	Adenosine Triphosphate
β-	Beta
BHIA	Brain Heart Infusion Agar
BHIB	Brain Heart Infusion Broth
CAMPs	Cationic Antimicrobial Peptides
c-di- GMP	(3'-5')-cyclic dimeric guanosine monophosphate
CFU	Colony-forming unit
CPPs	Cell-penetrating peptides
CRA	Congo Red Agar
CRB	Congo Red Broth
CSLM	Confocal Scanning Laser Microscopy
CV	Crystal Violet
dH_2O	Distilled Water
DMEM	Dulbecco's Modified Eagle Medium

DMF	Dimethylformamide
DMSO	Dimethyl Sulfoxide
DNA	Deoxyribo Nucleic Acid
E.coli	*Esherichia coli*
EDS	Energy Dispersive X-ray Spectroscopy
EPS	Extracellular polymeric substances
FA	Formic Acid
FBS	Fetal Bovine Serum
θ-	Gama
HC_{50}	Hemolytic concentration that lysis 50 % of cells
hCAP	Human Cationic Antimicrobial Peptide
HDPs	Host Defence Peptides
HeLa	Henrita Lacks Cell
HNP	Human Neutrophil Peptide
HPLC	High-Performance Liquid Chromatography
IIS	Innate Immune System
kDa	Kilodalton
LC/MS	Liguid Chromotography /Mass Spectrometry
LEAP-1	Liver Expressed Antimicrobial Peptide
Leu	Leucine
Lys	Lysine
MBEC	Minimal Biofilm Eradication Concentration
MBIC	Minimal Biofilm Inhibiton Concentratiton

MHA	Müeller Hinton Agar
MHB	Müeller Hinton Broth
MIC	Minimal Inhibition Concentration
µg	microgram
µl	microliter
mg	miligram
MRSA	*Methicillin resistant S.aureus*
P.aeuroginosa	*Pseudomonas aeuroginosa*
pI	Isoelectronic Point
RP-HPLC	Reverse Phase High Performance Liquid Chromatography
QS	Quorum Sensing
RPM	Revolutions Per Minute
S.aureus	*Staphylococus aureus*
SEM	Scanning electron microscopy
SPPS	Solid Phase Peptide Synthesis
TCP	Tissue Culture Plate
TFA	Trifluoroacetic Acid
TIS	Triisopropyl Silane
TM	Tube Method
TSA	Triptic Soy Agar
TSB	Triptic Soy Broth
VMD	Visual Molecular Dynamics

LIST OF FIGURES

Figure 1. Chemical and biological peptide synthesis 7
Figure 2. Circular chart of AMPs by source 9
Figure 3. hCAP18 and its truncated form LL-37 peptide 10
Figure 4. Antimicrobial peptide mechanism of action on bacterial cell membrane after adsorbtion 20
Figure 5. Monolayer (a) and multilayer (b) biofilm structure 27
Figure 6. The Biofilm Formation Steps 55
Figure 7. NET2 peptide PEPFOLD 3D structure 62
Figure 8. Positioning of the NET1 peptide on the bacterial membrane and in water 63
Figure 9. After the NET1 peptide molecule is positioned on the bacterial membrane and in water, the result of the molecular simulation for ~ 46 ns 64
Figure 10. NET1 1 mg/ml 65
Figure 11. NET2 1 mg/ml 65
Figure 12. NET3 1 mg/ml 66
Figure 13. NET4 1 mg/ml 66
Figure 14. NET1 10 mg/ml semi-preparatif HPLC 67
Figure 15. NET2 10 mg/ml semi-preparatif HPLC 67
Figure 16. NET3 10 mg/ml semi-preparatif HPLC 67
Figure 17. NET4 1 mg/ml semi-preparatif HPLC 68
Figure 18. Peptide concentration standard curve 68
Figure 19. NET1 peak wiev 0.2 mg/ml 70
Figure 20. NET1 peak content 70
Figure 21. NET2 peak wiev 0.2 mg/ml 71
Figure 22. NET2 peak content 71
Figure 23.NET3 peak wiev 0.2 mg/ml 72
Figure 24. NET3 peak content 72
Figure 25. NET4 peak wiev 0.2 mg/ml 73
Figure 26. NET4 peak content 73

Figure 27. Antibiogram of 1 mg/ml NET1, NET2, NET3, NET4 peptides 74
Figure 28. NET1, NET2, NET3, NET4 peptides MIC assay w/ *E.coli NTCC 13846* epi -white chemidoc image 75
Figure 29. *E.coli* 5.000X, 25.000X, 200.000X SEM images 76
Figure 30. *E.coli* NET1 16 µg/ml 100.000X, 120.000X, 150.000X SEM images ... 77
Figure 31. *E.col*i NET2 128 µg/ml 25.000X, 150.000X, 120.000X SEM images ... 77
Figure 32. *E.coli* NET3 16 µg/ml 25.000X, 100.000X, 150..000X SEM images 78
Figure 33. *E.coli* NET4 32 µg/ml 25.000X, 100.000X, 120.000X SEM images 78
Figure 34. NET1 peptide proteinase K assay HLC results 80
Figure 35. NET2 peptide proteinase K assay HLC results 80
Figure 36. NET3 peptide proteinase K assay HLC results 81
Figure 37. NET4 peptide proteinase K assay HLC results 81
Figure 38. NET1, NET2, NET3, NET4 and Triton X-100 % lysis rates 82
Figure 39. Cytotoxicity rates for NET1, NET2, NET3, NET4, Magainin 2 and only cell in Hela cell line 83
Figure 40. Cytotoxicity rates for NET1, NET2, NET3, NET4, Magainin 2 and only cell in 3T3 cell line 83
Figure 41. % Cytotoxicity rates for NET1, NET2, NET3, NET4, Magainin 2 and only cell in HaCaT cell line 84
Figure 42. MHCRA black colony biofilm formation *S.aureus ATCC25923, S.aureus ATCC29213, S.aureus MRSA, E.coli ATCC25922, E.coli ATCC13846* bacteria strains on MHCR w/os, MHCR w/g, MHCR w/s, MHCR w/f 86
Figure 43. Serial dilituon of bacteria effect on CRB black colour occuring 87
Figure 44. The NaClO and Ciproflaxxain treatment at 0. h and 7. hour by Congo red method 88
Figure 45. a) NET1 b) NET2 c) NET3 d) NET4 peptides FT-IR 90
Figure 46. Peptide self-assembly on catheter at 25°C FT-IR results a) NET1 washed b) NET1 c) NET2 washed d) NET2 e) NET3 washed f) NET3 g) NET4 washed h) NET4 92
Figure 47. Peptide self-assembly on catheter at 37°C FT-IR results a) NET1 washed b) NET1 c) NET2 washed d) NET2 e) NET3 washed f) NET3 g) NET4 washed h) NET4 93

Figure 48. Self-assembly with soaking method in NET1 peptide solution at 37°C FT-IR results 94
Figure 49. Self-assembly with soaking method in NET1 peptide solution at 37°C FT-IR results, zoom in Figure 48 94
Figure 50. 6.4 mg/ml NET1 peptide self-assembly on catheter at 37°C a) NET1 washed b) NET1 95
Figure 51. 10 mg/ml NET1 peptide self-assembly on catheter at 37°C a) NET1 washed b) NET1 95

LIST OF TABLES

Table 1. The equipments used during the study and their brands 35
Table 2. The chemicals used during the study and their brands..... 36
Table 3. Designed peptide sequences and their properties..... 39
Table 4. Amino acid quantities required for peptide synthesis 42
Table 5. Analytical HPLC conditions 44
Table 6. Semi-prep HPLC conditions 45
Table 7. LC/MS protonetion; m/z ratio calculation of peptides..... 48
Table 8. Pure peptide concentrations (mg/ml) 69
Table 9. MIC values of NET1, NET2, NET3, NET4 peptides 75
Table 10. Minimum Biofilm Inhibition Values (ug/ml) by CV method..... 85
Table 11. Dark sport formation on MHCRA with different carbon sources..... 87
Table 12. Minimum Biofilm Inhibition Values (ug/ml) by CRB- MBIC method 89
Table 13. Minimum Biofilm Eradication Concentration (ug/ml) by CV method..... 90
Table 14. FT-IR wavenumbers and infrared peaks 91
Table 15. EDS analytics based on N % to detect self-assembled peptide rate..... 96

SUMMARY

Today, the resistance developed by bacteria against antibiotics poses a great difficulty in the prevention and treatment of nosocomial infections. However, antimicrobial peptides (AMPs), which bacteria cannot develop resistance specifically, but can only resist with the proteases or biofilm-forming mechanism in their structure, have become a current area of interest. It is aimed to improve the activities of these peptides by synthetic production. The activities and toxic effects of peptides, which have the same sequence in alpha-helix structure but synthesized by combining 2 different amino acid forms in 4 different ways, were compared. As a result, it was seen that the use of D- and L-form amino acids together increased the antibacterial activity 4-32 times. MIC (Minimum Inhibition Concentration) values also remain in the safe range for IC_{50} and HC_{50} values. While the lowest antibacterial activity is seen in the peptide consisting entirely of L-form amino acids, peptide antibacterial activity consisting entirely of D-form amino acids is located in the middle segment between these peptides. For biofilm inhibition, NET3 peptide with D-arginine in its structure showed better activity, while NET1 peptide with D-leucine in its structure showed better activity in removing the biofilm. Thereupon, the CRB-MIC experiment was developed in order to find the true biofilm inhibition concentration by real time monitoring. After taking these results, peptides which are expected to bond spontaneously with no chemical or intermediate linker is needed called as self-assembly, since they are amphipathic and alpha-helix structure, showed surface binding though with low efficiency.

Key words: Antimicrobial Peptides, Antibiofilm Peptides, Biofilm, Biofilm Structure, Peptide Self Assembly

ÖZET

Biyofilm Oluşturan Bakterilere Özgü Antimikrobiyal Peptitlerin Geliştirilmesi ve Kateter Yüzeyine Bağlanması

Günümüzde bakterilerin antibiyotiklere karşı geliştirdiği direnç özellikle hastane enfeksiyonlarının önlenmesi ve tedavisinde büyük güçlük oluşturmaktadır. Bununla beraber bakterilerin özel olarak direnç geliştiremedikleri, fakat yapılarında bulunan proteazlarla veya biyofilm oluşturma mekanizması ile ancak karşı koyabildiği antimikrobiyal peptitler (AMP) güncel olarak ilgi gören çalışma alanı oluşturmuştur. Bu peptitlerin sentetik olarak üretilmesi ile aktivitelerinin geliştirilmesi amaçlanmaktadır. Alfa heliks yapısında aynı diziye sahip fakat 2 farklı aminoasit formunun 4 farklı şekilde kombinlenmesi ile sentezlenen peptitlerin aktiviteleri ve toksik etkileri karşılaştırılmıştır. Bunun sonucunda D- ve L- form aminoasitlerin beraber kullanımının antibakteriyel aktiviteyi 4-32 kat artırdığı görülmüştür. MİK (Minimum İnhibisyon Konsantrasyon) değerleri, IC_{50} ve HC_{50} değerleri için de güvenli aralıkta kalmaktadır. En düşük antibakteriyel aktivite tamamen L-form amino asitlerden oluşan peptitte görülürken, tamamen D-form aminoasitlerden oluşan peptit antibakteriyel aktivite bu peptitler arsında olarak orta segmente yer almaktadır. Biyofilm inhibisyonu için bu peptitlerden yapıısnda D-arjinin bulunan NET3 peptidi daha iyi aktivite gösterirken, biyofilmin ortadan kaldırılmasında yapısında D-lösin bulunan NET1 peptidi daha iyi aktivite göstermiştir. Bunun üzerine gerçek biyofilm inhibisyon konsantrasyonunu bulmak amacıyla gerçek zamanlı izleme ile CRB-MIC deneyi geliştirilmiştir. Bu sonuçlar alındıktan sonra, hiçbir kimyasal veya ara bağlayıcı olmadan kendiliğinden bağlanması beklenen peptitler, amfipatik ve alfa-heliks yapıları oldukları için kendiliğinden-bağlanma olarak adlandırılan metodla düşük verimlilikle de yüzey bağlanması göstermiştir.

Anahtar Sözcükler: Antimikrobiyal Peptitler, Antibiyofilm Peptitler, Biyofilm, Biyofilm Yapısı, Peptit Kendiliğinden Bağlanma

1. BACKGROUND AND AIM OF THE STUDY

In order to reduce or eliminate hospital infections that have increased rapidly in recent years, urgent solutions based on new approaches are required. For example, today, 40% of hospital infections are urinary tract infections and 80% of these infections are caused by catheters. Especially when it is necessary to use it for more than a week, microorganisms can create biofilms on the catheter surface. While biofilm makes the response to treatment with antibiotics difficult, it can trigger bigger problems by helping the development of microorganisms resistant to these antibiotics. After this stage, microorganisms, that have become resistant to antibiotics, become a new threat to not only the patient using the catheter but also to the whole world by starting with the places where the patient is treated. This infection, which has shown up in hospitals, calls hospital infection. For the fighting with this, the first target is the catheters that are the source itself. There are serious studies regarding the production of catheters from materials that prevent the attachment of microorganisms or directly kill microorganisms or coat their surfaces with antimicrobial molecules. However, since all these efforts are limited to the use of molecules whose antibiotic properties are known, their ability to gain resistance to these antibiotics has improved.

It is not effective enough on bacteria. Antimicrobial peptides, which are more effective due to their ability to kill microorganisms, use a different metabolic pathway, are taking their place in the scientific literature as new options. New generation antimicrobial peptides were selected by the director of this project during his doctoral study. They were found to have much higher antimicrobial effects compared to their counterparts in the literature, and they have been published. Our first goal in our proposed project is to develop new peptide antibiotics specific to bacteria that cause the most catheter infections and determine their effectiveness with

in vitro studies, molecular models, and also to investigate their mechanisms of action by molecular modeling. Our second goal is to develop new strategies for our peptide antibiotics, which we have developed previously, to bind to the catheter surfaces, and maintain their effectiveness and perhaps even show better antimicrobial activity. Thus, it is aimed to reduce catheter-induced hospital infections with the catheters that are coated with new generation peptide antibiotics.

2. INTRODUCTION

2.1. Antimicrobial Peptides

Antimicrobial peptides (AMPs) are oligopeptides consisting of less than 50 and more than 10 amino acids and have a wide range of effects on viruses, bacteria and some parasites. Some peptides play a role in the innate immune system (IIS). and have antimicrobial activity in all living things, from bacteria to humans, to prevent the growth or to inhibit their harmful activities (1). A large part of these peptides is structurally simple but functionally highly complex molecules. Today, the peptide group designed for use in bacteria is called antibacterial peptides and constitutes the largest subgroup of AMPs. The basis of the peptide designs, which are made especially for bacteria, is making bacteria to generate resistance against antibiotics. Unlike interacting with the positively charged eukaryotic cell wall, these peptides that interact with the bacterial wall which is negatively charged are called cationic peptides, in other words, they are called host defense peptides (HDPs) (2).

AMPs kill target cells by their intracellular mechanisms and by affecting the cell membrane. When the mechanisms, which are affected in the cell, are examined, inhibition of intracellular DNA and protein synthesis, disruption of cell wall synthesis, and targeting of enzymatic activities can be given as examples (3,4). AMPs are less target-specific than other antibacterials. It works well despite this unspecificity. This limitation of specificity positively makes it difficult to develop resistance to AMPs (4).

2.1.1. Peptide biosynthesis and chemical synthesis

In organic chemistry, peptide synthesis occurs by linking multiple amino acids via amide bonds which are also known as peptide bonds. The reaction for peptide formation is known as the condensation reaction. In the condensation reaction, water is released during the combination of two small molecules to form a large molecule. This reaction takes place between the carboxyl group of one amino acid and the amino group of another. In biological systems, both ribosomal (RNA mediated) and non-ribosomal (thioester mediated) peptide biosynthesis proceeds from N- to C-terminus by ligation at the activated peptide C-terminus, also without protecting group unlike chemical peptide synthesis shown in Figure 1 (5).

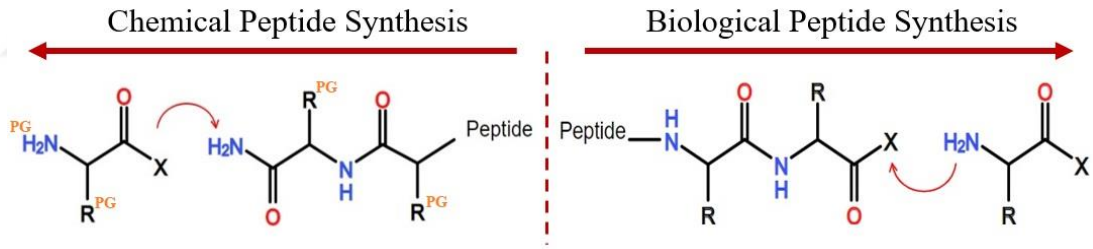

Figure 1. Chemical and biological peptide synthesis PG: Protecting group, R: amino acid side group, X: added amino acid [modified according to Canavelli P et al. 2019 (6) via Sigma Aldrich Substructure Search Page Software]

Gene-encoded AMPs are synthesized by mammals, birds, amphibians, insects, plants and many microorganisms (6). AMPs are primarily synthesized as the precursor protein in ribosomes and undergo post-translational modifications to form a mature protein. In prokaryotes, peptides are obtained by cleaving the precursors

synthesized by ribosome or by a process independent of the ribosome (7). In mammals, AMPs are synthesized in phagocytes and mucosal epithelial cells (lehler) and constitutes a large part of the IIS. According to their primary structure, they are often cationic and amphiphilic. Mostly they can kill bacteria by permeability break of the negatively charged cell wall. Besides their antimicrobial activity, they also have antiviral, antiparasitic and anticancer activity (8).

AMPs are usually synthesized with signal sequences at the N- terminal ends. Defensins are synthesized as pre-proteins. They are containing about 95 residues. The first 19-residue is a signal sequence at the N-terminal and it is typical for defensins. The following 40-45-residue is an anionic prosequence. The signal sequence allows the preprotein to target the endoplasmic reticulum, but the anionic prosequence's biological role is not yet known. Due to its anionic structure, it may be able to imitate the bacterial cell wall and protect the peptide structure, allowing it to enter the cell (9).

In contrast to peptide biosynthesis, the binding of two amino acids starting from C- terminus in solid-phase peptide synthesis (SPPS). SPPS generally consists of 3 stages. For the protected amino acid to bind with the next amino acid, it is necessary to deprotection, activation of the carboxyl end, and binding of the next amino acid. Protective groups for amino groups most commonly used in peptide synthesis are the 9-fluorenylmethyloxycarbonyl group (Fmoc) and t-butyloxycarbonyl (Boc) Some amino acids carry functional groups in the side chain that must be specifically protected from reacting with incoming N-protected amino acids. Unlike the Boc and Fmoc groups, the peptides need to be stable throughout peptide synthesis, although they are removed during the final deprotection (10). After the peptide synthesis is carried out as a solid phase resin-bound, the cleavage step is done to separate the

peptide from the resin and to deprotect the side groups in the peptide sequence. TFA (trifluoroacetic acid) in the cleavage solution provides this (11).

2.1.2. Natural AMPs

AMP production is a feature that is found in many living life forms (12). Originally isolated from insect hemolymph, amphibian skin secretions and mammalian phagocytes, AMPs caught the attention of researchers because of their capability to inhibit the growth of various microorganisms. As new AMPs began to emerge, they were understood to be universal and evolutionarily ancient elements of the IIS. The current rates are given in Figure 2, according to The Antimicrobial Peptide Database (APD) (13).

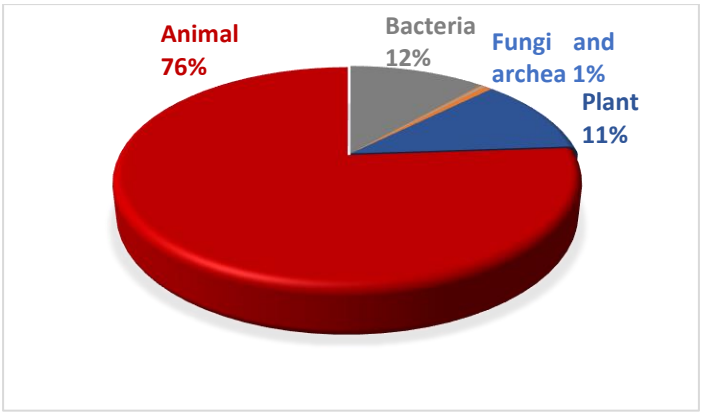

Figure 2. Circular chart of AMPs by source

2.1.2.1. Animal AMPs

HDPs are protecting the human body from microbial infections existing in tissues and human layers such as eyes, skin, mouth, lung intestines and urinary tract (14). AMPs are divided into 4 families, human cathelicidins, human defensins, human dermicidine and human hepcidins. Human cathelicidins are one gene multiple peptides and were isolated in 1898 (15). Like defensins, they exist primarily as precursor proteins, then form active AMPs with proteolytic cleavage. The cathelicidin domain located at the N terminal distinguishes these AMPs from other peptide families (16). The 18 kDa human cationic antibacterial protein hCAP18 (human cationic antimicrobial protein), also called cleaved form; active form LL-37 (17). The LL-37 peptide has 30 amino acid signal sequence and 101 amino acid cathelicidin at the N terminal of the peptide (18). After cleavage step of cathelicidin domain and signal peptide, peptide reaches its active form (Figure 3) (19). LL-37 was first found in leukocytes and testis and then realized that it is located in a large variety of cells, tissues and body fluids. When the bacterial production increase in sinus epithelial, LL-37 production is also increasing. Cathelicidins were also detected in chicken and three fish (20,21).

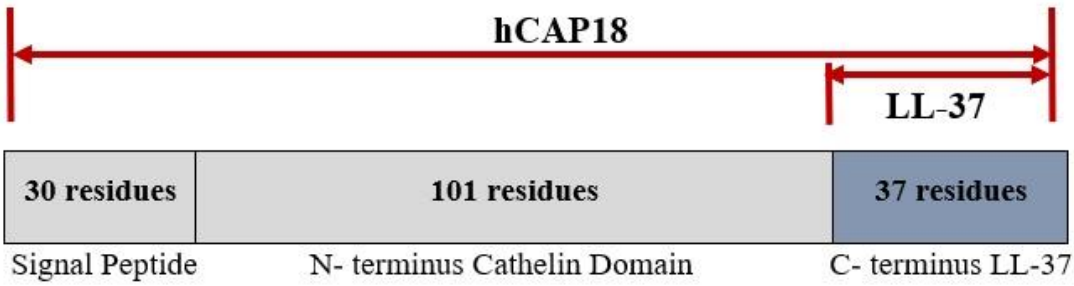

Figure 3. hCAP18 and its truncated form LL-37 peptide [modified according to Polcyn-Adamczak M and Niemir ZI 2014 (1) via Microsoft Power Point]

HDPs are often referred to as precursor proteins and are released by the mature form protease process. Human defensins are a large group of 4-kDa open-ended cysteine- and arginine-rich peptides and also they have complex three-dimensional structures (22). In mammals, defensins are divided into two groups; α-defensins and β- defensins and both including 3 disulfide bonds between cysteine residues. α-defensins are 29-35 residues long, while β-defensins are 38-42 in length. In addition to these, non-human primates contain θ-defensins as another group. In θ-defensins have three disulfide bonds as well as α- and β-defensins, they are formed by end-to-end binding of two truncated α-defensins. They have a ring structure by joining these 18 residue pieces end to end (23,24) α-defensins have been found in the "neutrophils and some macrophages of humans, monkeys, and several rodent species". The α-defensins in humans and mice are expressed and secreted in the gut by secretory epithelial cells of small intestinal crypts with a putative host defense function (24). Lehler group discovered and isolated the human defensins group's human neutrophil peptides from human blood in 1985. There are three human neutrophil peptides, which have a nearly identical sequence, named HNP-1, HNP-2, HNP-3. All three peptides have CYCRIPACIAGERRYGTCIYQGRLWAFCC common amino acid sequence, HNP-1 also has alanine (A) amino acid and HNP-3 has aspartic acid (D) at the beginning of the sequence. This aspartic acid residue makes HNP-3 less active than other peptides in killing *S.aureus, P. aeuroginosa* and *E.coli.* After four years, in 1989, HNP-4 was discovered and purifed by Lehler and collagues. HNP-4's amino acid sequence differs more from the other three peptides. HNP-1, HNP-2, and HNP-3 also detected in peripheral blood leukocytes , spleen and thymus (25). Every mammal species, which was discovered so far, has β-defensins. It was found in the respiratory tract and tongue of cattle and leukocytes of chickens (26). However, in other species, β-defensins are expressed mostly by epithelial cells that cover various organs and play an important role in the host defense of the respiratory tract (27).

Histadins family AMP's histidine-rich peptides that are secreted into human saliva by the salivary glands (28). In 1988, histatins 1, 3 and 5 were purified from

human saliva and antimicrobial activities were tested. All three histatins show killing activity in pathogenic yeast, bacteria and *C.albicans*. Histatin genes are located on chromosome 4, band q13 but only histatin 1 and 3 are gene-encoded, other histatins were produced by cleaving these peptides (29).

The latest found human AMP family is hepcidins, liver expressed antimicrobial peptide (LEAP-1) was isolated in 2000. DTHFPICIFCCGCCHRSKCGMCCKT amino acid sequenced LEAP-1 is a cysteine rich peptide and found from urine besides of liver. Unlike other human AMPs, human dermcidin is an anionic peptide and it is constitutively expressed in human sweat. The level of the peptide of dermcidin does not increase with infection, it is the same in healthy and sick people (30).

2.1.2.2. Plant AMPs

Plant AMPs are an important component of the barrier defense system of plants species. It has activities against phytopathogens and pathogenic bacteria for humans. AMPs, like in other species, act by interacting with the phospholipid layer of pathogens and disrupting cell stability (31). Besides this, the other component of the plant defense system is cell-penetrating peptides (CPPs). CPPs, as the name suggests, are capable of introducing into cells when the variety of cargoes by the interaction of specific receptors with membrane phospholipids (32). According to their electric charge, plant AMPs can be divided into two groups as anionic (AAMPs) and cationic peptides (CAMPs). Plant AMPs have been isolated from neoplastic cells of a wide variety of species of roots, seeds, flowers, stems and leaves and are known to exhibit

activities against phytopathogens against human, viruses, bacteria, fungi, protozoa, large parasites and organisms that are pathogenic to humans (33).

The main families of AMPs comprise defensins, thionins, lipid transfer proteins, cyclotides, snakins, and hevein-like proteins, according to amino acid sequence homology. Despite the significant differences in amino acid sequences of plant AMPs, significant similarities are seen in their tertiary structure. Among the basic structural features of AMPs are the high content of cysteine and / or glycine and the presence of disulfide bridges. It is known that especially loaded amino acids in plant AMPs play an important role in antimicrobial activity against pathogenic bacteria. As is known, the mechanism of action of AMPs in plants consists of three basic models; carpet model, perforation and embedment model in the membrane (34). Although pathogen interactions are still unclear in terms of the specificity of plant AMPs, it is thought to be associated with thionine activity found in plant AMPs and containing aspartic residues (31).

Thionins are a family of AMPs with low molecular weight, arginine, lysine and cysteine-rich, contain two antiparallel α helices and an antiparallel double-stranded β-sheet with three or four conserved disulfide linkages, and positively charged at neutral pH (35). Thionins are toxic to most of the species of bacteria, fungi and yeast. More than 100 thionin sequences have been discovered in more than 15 plant species. For example, Wheat endosperm crude purothionin is effective against bacteria such as *Pseudomonas solanacearum, Xanthomonas phaseoli* (36), while Wheat endosperm α-purothionin acts against *Rhizoctonia solani* fungus (37).

2.1.2.3. Amphibian AMPs

The skin of Amphibians is the largest source, especially for AMPs, with many biologically active peptides. Due to the presence of cutaneous glands on amphibian skin surfaces, HDPs can be released on condition of anxiety, injury, and electrical or norepinephrine stimulation (38). There may be more than one hundred various peptides generated by more than 6600 identified species of anuran Amphibians (39). AMP diversity is quite high in amphibians, there are AMPs with very different peptide sequences. Therefore, peptide sequences have been used as a taxonomic tool between *Ranagenus* (40) and *Littoria* families species to classify antimicrobial peptides (41). Based on structural similarities, two groups of peptides have been identified: linear cationic peptides and cationic peptides with a disulfide bond at the carboxyl end. Linear cationic represents amphipathic peptide, magainin isolated from *Xenopus laevis* (42). Presently, AMPs are classified into 12 well established families "nigrocin-2, japonicin-1, japonicin-2, palustrin-2, brevinin-1, brevinin-2, esculentin1, esculentin-2, ranacyclin, ranatuerin-1, ranatuerin-2, and temporins" (43). Brevinin-1, esculentin-1, esculentin-2 and temporin peptides are found in both Eurasian and North American ranid frogs. Ranatuerin-2, and palustrin peptides are found in North American frogs, and brevinin-2 and japonicin peptides are found only in Eurasian frogs (44). An important part of peptides is produced by frogs of the genus *Rana* (45). Esculentins are isolated from European frog *Rana esculenta*, as an example, esculentin-1 has 46 amino acid length with a disulfide bond between cysteines 40 and 46, and one of the longest AMPs (46). The native peptide of esculentin-1 display very high antimicrobial activity (minimum inhibitory concentration (MIC ; Minimal Inhibition Concentration < 1 μM) against a whole range of human pathogens, comprising *E. coli, S. aureus, P. aeruginosa, and C. albicans* (47). There are more than a thousand types of amphibian AMPs that differ from each other with amino acid sequences, but still not clear that all of them are gene-encoded or degradation products (48,49)

2.1.2.4. Bacterial AMPs

The AMPs that bacteria produce are called bacteriocidin. There are 177 species of bacteriocins with different sequences. These are produced by Gram-positive bacteria, lactic acid bacteria, Gram-negative bacteria and halophile archaea (50). While it is part of the body's IIS against microorganisms in higher organisms, AMP production in bacteria provides a selective advantage to bacteria. Bacteriocidins are synthesized by bacteria to kill other bacterial species. As with eukaryotic AMPs, bacterial AMPs are consisting of 5-50 amino acids, cationic, amphiphilic or hydrophobic properties (51). Since the target organism is bacteria, positive charge and hydrophobicity are important in disturbing the cell wall stability. Besides this, there are some important differences between bacteriocidins and eukaryotic cell AMPs; bacteriocidins have a high effect on target with pico or nanomolar concentrations while eukaryotic AMPs are needed within higher concentrations. Another important difference is most bacteriocidins have a very narrow target spectrum and being active only a few species/genera closely related to the producer, while eukaryotic AMPs are usually targeted at a large group of bacteria and less specific. Due to these important differences, bacteriocidins are seen as promising antimicrobial agents such as extending the shelf life of food products and infection treatment (52).

Bacteriocins are divided into two main groups; Class I consists of small molecules (less than 5 kDa) presenting post-translational changes; Class II consists of peptides with unmodified amino acids (51). The structural differences of the molecules determine the number of AMPs, the active antimicrobial agent and even the spectrum against susceptible bacteria. Bacterial AMPs are encoded by genes and released as AMP after posttranslational modifications are completed. Most proteins

are hydrophobic, so it has been suggested that bacteriocin synthesis is membrane dependent (53).

Bacteriocins are extremely powerful bactericidal agents. Bacteriocin resistance is independent of antibiotic resistance and cross-resistance has not been noted so far. In many studies, it has been observed that bacteriocins can not only create pores but also interact with receptors in the cell. Based on the cationic properties of bacterial AMPs, pore formation starts with electrostatic interactions between the peptide and the negatively charged bacterial surface (50). Pore formation in the membrane is achieved by inserting the hydrophobic domain of the C-terminal into the cytoplasmic membrane (54). Changing membrane permeability leads to a total or partial distribution, resulting in energy depletion and cell death. Some bacteriocins show antimicrobial activity by inhibiting cell wall biosynthesis rather than forming membrane pores (55).

2.1.3. Structure of AMPs

AMPs are divided into 4 main groups according to their structure; extended AMPs, β-hairpin or loops, β-sheet, and α helical. Extended AMPs don’t have a secondary structure since including glycine, proline, tryptophan or histidine amino acids in their composition. We can show indolicidin, histadines and drosocin as examples among this group of peptides (56).

Peptides in the β-sheet group are characterized by two or more β-strands formed by disulfide bonds. α-, β- and θ- defensins are in this group (57–59). AMPs have a hairpin structure interconnected by a type II-turn, and stabilized by disulfide bonds formed between the β-strands, such as lactoferricin B from bovine milk, θ- defensin-1 from rhesus monkey leukocytes, tigerinin-1 from frog skin segretion (60). β-hairpin peptides may have 1,2,3 and 4 disulfide bonds in their structure depending on the amount of cysteine amino acids (61).

Due to their amphipathic characteristic AMPs can form α-helical structure and they are widespread in nature. Magainin II, human cathelicidin LL-37, frog distincin and mellitin are some of this group of peptides (62). α-helical AMPs are usually unstructured in an aqueous solvent, but in the presence of membranes, they fold into amphipathic α-helices. When the α-helical AMPs contact with the negatively charged bacterial membrane and reach the required amount, they can insert into it and form transmembrane pores, causing the membrane to become unstable leads to subsequent depolarization and cell death (63).

2.1.4. Protecting human cells from the effect of AMPs

Since the cell membranes of eukaryotic cells that produce AMPs have a different fat composition than the bacterial cell membrane, this difference is protected from AMPs targeting the cell membrane. While there are anionic groups on the outside of the bacterial cell membranes, in the eukaryotic cell membrane, anionic groups are located on the cytoplasm side. It is known that AMPs act through the attachment of positively charged amino acids to the anionic face of the sensitive microbial cell membrane, thanks to their cationic structure. Another reason the peptides cannot

target the eukaryotic cell membrane is that the unprocessed precursor form of the peptide is capped at the cationic groups of the peptide until it is proteolytically removed. The storage of peptides in neutrophil granules in inactive precursor forms is also thought to be an additional mechanism for protection (64–66)

Since bacteria producing AMPs have cytoplasmic membranes resistant to their peptides, they do not need protection mechanisms as in eukaryotes (67,68). This mechanism in bacteria has one or two components that function completely differently. The first is an immune protein that is thought to function by interfering with the peptide's ability to disrupt the normal membrane structure and functionality, but its mechanism is not exactly clear, but it binds to the cell membrane with a fat modification and inhibits the action of the peptide. The second immune component, on the other hand, is an outwardly directed ABC transporter system and rapidly expels the peptide from the cytoplasmic membrane after binding from the environment, thus preventing the peptide from accumulating in the membrane (69).

2.1.5. Antibacterial effect of AMPs

AMPs act by some known strategies as interacting by the cell membrane and formation of pores, accompanied by increased ion permeability, depolarization, interruption of the cellular events, and resulting in cell death. Positively charged antimicrobial peptide structure is attracted by anionic phospholipids, lipopolysaccharides, or teichoic acids. Thus, there is an accumulation of AMPs on the cell surface (70). When the accumulated AMPs reach the threshold value, they can act on three mechanisms in the cell membrane. These are the barrel-stave model,

the wormhole (or toroid pore) model, and the carpet model (34). These models are described in the mechanism of an action title.

Generally, cationic AMPs are known to target anionic bacterial membranes. Human AMPs can target and interact with a variety of molecules either on the cell surface (including membranes) or within cells and exhibit antimicrobial activity (8). The molecular targets of AMPs are not limited to bacterial membranes. Human AMPs have been shown to inhibit cell wall synthesis by many researchers. This effect is one of the common mechanisms of AMPs (8). Apart from this, there are also AMPs with proteins that recognize specific fats or carbohydrates in the cell membrane, although they are uncommon (71).

Human cathelicidin LL-37 is known to disrupt bacterial membranes. Membrane breakdown occurs in three stages. In the first stage, the cationic peptide recognizes and covers the anionic surface of bacteria. The amphipathic helical cationic peptide targets anionic bacterial membranes. In the second stage, LL-37 binds to the outer membrane and crosses the outer membrane. In the last stage, it reaches the inner membrane and is connected here (8). At high concentrations, the peptide may micelize, disrupting membranes or forming pores by taking a vertical position (72).

It is known that some peptides produced from DNA binding histone 2A inhibit nucleic acid synthesis by binding DNA and thus exhibit antimicrobial effect (73). Also, proteins that inhibit elastase and cathepsin L are known to exhibit antibacterial activity by binding nucleic acids (8). The antibacterial mechanism of action of AMPs can occur with many different mechanisms. For example, human LL-37 may first damage the bacterial cell membrane and then bind to DNA to prevent bacteria from

reproducing (73). Many models have shown that some peptides increase cell permeability against small molecules by inducing the flow of ATP in bacteria and exhibit antibacterial activity by causing ion imbalance. Again, to combat bacterial infection, it has been reported that some AMPs act on immune cells and stimulate the immune system to increase the fight against infection (8). However, it is still unclear how immune system molecules and AMPs work together to kill bacteria (74).

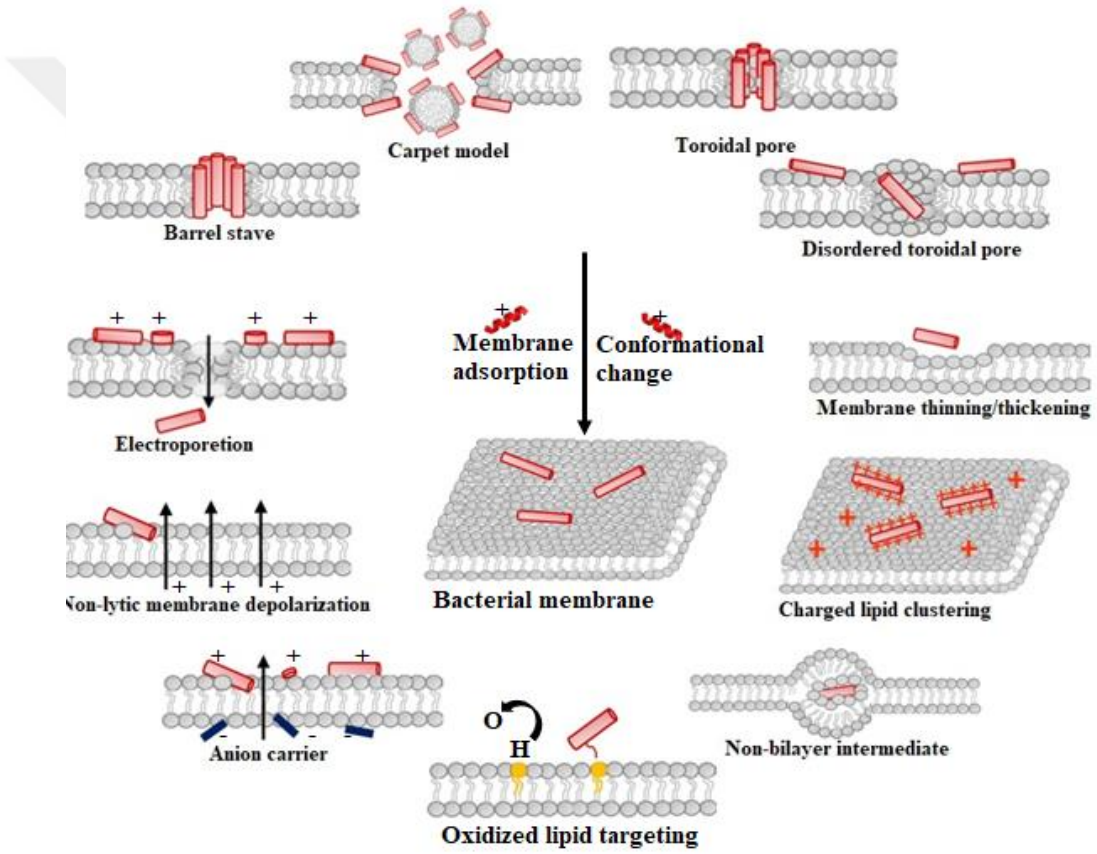

Figure 4. Antimicrobial peptide mechanism of action on bacterial cell membrane after adsorbtion [modified according to Nguyen et al. 2011 (3) via Microsoft Word]

When AMPs with a positive net charge interact with the negative charged bacteria membrane, it may cause pore formation on the membrane surface such as barrel stave and toroidal pore. Besides, it may cause the ion balance of the membrane to be disrupted, such as anion carrier, electroporation, non-litic membrane depolarization. It may cause thinning of the bacterial cell wall or cause the lipid layer on the membrane surface to become positive and form lipid clumps (3) (Figure 4).

2.1.6. Bacterial resistance mechanisms to AMPs

Today, antibiotic resistant is a major public health problem because of the wrong and overuse of antibiotics. The AMPs have many powerful reasons to replace antibiotics such as rapid killing effect (nanoseconds), low antibacterial resistance developing comparing to antibiotics and being effective on multidrug-resistant bacteria. The development of AMP resistance has been proposed, but it will be less likely than classical antibiotics, due to the main target these molecules have, the bacterial cytoplasmic membrane, and consequently the need to rebuild this membrane. Although some mechanisms of resistance to native AMPs have been identified [e.g. up-regulation of outflow pumps, membrane and cell envelope changes, proteolytic degradation of peptides, biofilm formation and lipopolysaccharide (LPS) modification (75).

The development of resistance to AMPs makes it difficult to treat infectious diseases. For this reason, it is very important to understand the resistance mechanism. Mechanisms of AMP resistance include "proteolytic degradation or sequestration of secreted proteins (keeping them in a separate part), an impedance of exopolymer and biofilm matrix molecules, blocking of membrane exchange with the cell surface, and

removal of AMPs from the cell membrane by pumps". AMPs usually target the anionic bacterial membrane. The interaction between the positive peptide and the membrane is defined as "electrostatic interaction". The next step is hydrophobic interaction. This interaction occurs between the amphipathic region of the peptide and membrane phospholipids (76). The mechanism of action of these peptides is often rigid once the threshold concentration is reached, leaving the target organism less capable of adapting or developing resistance to AMPs. The mechanisms by which AMPs can pass through microbial membranes are not common to all peptides and appear to depend on both peptide properties and molecular properties of lipid membrane composition (77).

Proteases are the first defense mechanisms AMPs encounter when interacting with bacteria. Proteolytic degradation of AMPs by extracellular enzymes is a simple but effective way of providing microorganisms resistance to AMPs (78). Proteases, which are host cell proteins, act on AMPs by macroglobulin or they secrete dermatan sulfate that inactivates AMPs (77). one of the most effective protease groups is the omptin family, aspartate protease found in the outer membrane of Gram-negative bacteria, and has been shown to break down many AMP members (79). Along with the omptin family of proteases, metalloproteases also inactivate AMPs and play an important role in protecting gram-negative bacteria against AMPs. It has been emphasized that the inactivation of AMPs by proteases is highly dependent on the structure of the target peptide (80). Along with proteolysis, sequestration has an important role in resistance to extracellular protein-mediated AMPs. Staphylokinase is one of the most prominent extracellular AMP sequestration molecules. It links *S.aureus* and alpha-defensins (HNP-1 and 2) (81). Moreover, binding to LL-37 enhances staphylokinase-dependent plasminogen activation, indicating that staphylokinase plays an important role in pathogenesis (80).

Bacterial biofilm is a composition of surface-bound bacterial cells embedded in a matrix of extracellular proteins, extracellular DNA, and exopolysaccharides (EPS) (82). Biofilm-forming bacteria show higher resistance to antibiotics and AMPs (80). This strong resistance is thought to be due to the reduction of AMPs in biofilm leaching (83). It is thought to be due to the decrease (83). EPS and capsular polysaccharides (CPS) inhibit AMPs from their activity by capturing or repelling them (84). Capsules found in some bacteria also play an important role in the sequestration of AMPs. In particular, the hyaluronic acid capsule and M protein abolish the antibacterial activities of AMPs (85). Genetic overexpression of acylated polysaccharides containing anionic sugars such as gulukronic acid and mannuronic acid plays a role in AMP resistance in biofilms (80). Some gram-negative bacteria are protected from the action of AMPs by the presence of an extracellular capsule containing poly-gamma-glutamic acid (PGA), a glutamic acid homopolymer that prevents surface attachment and protects bacteria from phagocytosis (86). However, bacteria with this capsule are also more difficult to form biofilms than other bacteria (87). However, it should be noted that AMPs can be an alternative to traditional antibiotics in the treatment of biofilm-related infection. The mode of action of AMPs is usually bactericidal, whereas many traditional antibiotics are generally bacteriostatically effective and target fast-growing bacteria. Therefore, their effectiveness against biofilms is (87,88) However, because biofilm internal stress creates resistance to AMPs, the use of AMPs in the treatment of biofilm control or biofilm-presence infections with natural or synthetic AMPs becomes difficult (89). A new study has shown that D-alanylation, which is widely used by various gram-positive bacteria, increases cell wall density, and this causes a decrease in electrostatic repulsion and surface permeability and reduces the effectiveness of AMPs (90).

Bacterial biofilm is a composition of surface-bound bacterial cells embedded in a matrix of extracellular proteins, extracellular DNA, and exopolysaccharides (EPS) (82). Biofilm-forming bacteria show higher resistance to antibiotics and AMPs (80).

This strong resistance is thought to be due to the reduction of AMPs in biofilm leakage (83). Human AMPs target the bacterial peptidoglycan precursor, fat II, to block cell wall biosynthesis. Bacteria AMPs also generally use oil II to create pores in the membrane. Another way of developing resistance to AMP in Gram-negative bacteria is to increase the hardness of the outer membrane by adding extra acyl chains to fat A (80).

2.1.7. Molecular modeling methods for determining the effectiveness of antimicrobial peptides

Molecular modeling is the general name given to all methods used to predict (imitate) the actual structure and behavior of molecules, either theoretically or computationally in computer environment (91). While ab initio (quantum) modeling is used to determine the 3-dimensional structures containing a limited number of atoms with minimum energy, methods such as "molecular dynamics" or "docking" can be used to model microscopic interactions in systems with many more atoms and more than one molecule. In quantum modeling, the structure of molecules, electronic charge distributions, angles between atoms and similar parameters can be calculated using the probability functions of the presence of electrons in atoms depending on the distance from the center of the nucleus. In molecular dynamics, the Born-Oppenheimer approach is valid, that is, the movements of atomic nuclei can be thought independently of electron movements, which allows the classical laws of physics to be used. Molecular dynamics; It is a type of modeling that predicts the movement of molecules by calculating with certain algorithms how they actually behave in environments such as water or inside the membrane (92). The solution of Newton's equation of motion F = m.a is based on the principle that a body with mass accelerates when a force is applied. The force here is formed as a result of the interaction between atoms in molecules and / or between them. The force acting on

each atom is usually derived from the potential energy that depends on the position vector of each particle. This potential energy consists of the sum of the potential energy of the non-bonding ones and the potential energies of the bonding ones, which are empirically defined as the Lennard-Jones potential function. The potential energy of the bonders, the bond between bonded pairs of atoms energy consists of the energies of the bond angles made by the three atoms and the torsional energies of the four bound atoms. Depending on these, the Cartesian coordinate information of each atom after each time step in molecular dynamics is calculated by different versions of Verlet's algorithm (93) (94). The docking modeling method, on the other hand, uses the region where smaller molecules, generally called a linker, bond with the lowest energy on a large molecule called a receptor and this is another molecular modeling method used to numerically calculate the amount of energy. In the docking modeling method, genetic or Lamarckian genetic algorithms are used. Different molecular modeling methods such as Monte Carlo, Multiscale modeling, Network Modeling are also used. Computer modeling methods are like a bridge between microscopic time and distance scales and macroscopic experiments in the laboratory. The details behind some of the results obtained in the experiments can be explained by computational modeling methods. As you can compare a modeling result with experimental results. It is possible to examine very difficult or impossible environments with simulation methods in the laboratory environment.

2.2. Biofilm

The biofilm structure is a structure that allows bacteria to survive in various environmental conditions, mostly composed of an extracellular matrix, with a maximum microorganism density of 10 % (95). Biofilms can occur on environmental abiotic surfaces such as minerals, shells of dead organisms, or air-water interfaces. They can also occur on biotic surfaces in natural environments such as plants, other

microbes, and animals. In the human body, bacteria are found in biofilms essentially in every niche they colonize. These include both pathogenic and non-pathogenic skin flora, pathogenic and non-pathogenic oropharyngeal and nasal flora, commensal and pathogenic intestinal flora, and bacteria adhering to endovascular structures such as natural and prosthetic heart valves, central venous catheters, and endovascular thrombosis (95). Cells within biofilms typically produce EPS (Extracellular polymeric substance) components, which are a polymeric combination of EPS proteins, lipids, and DNA (deoxyribonucleic (96,97) bacteria reach a high density in a region, starvation is started and biofilm formation begins with the attachment of free-floating microorganisms to a surface (98). Pathogenic bacteria that cause infection to attach to the surface using structures such as pili and flagella as well as physical forces and form a thin layer. Ambient pH, temperature, nutrient and oxygen content are important factors in biofilm formation. It is assumed that biofilm bacteria express stress response genes that protect themselves from antibiotics, host immune factors and environmental toxins, due to environmental stresses such as nutrition, pH, temperature, etc. (99). In addition to protecting bacteria, the biofilm structure also provides a simple environment for the bacteria to attach to the surface (100).

2.2.1. Biofilm formation in bacteria

In the environments, bacteria are directed into or out of the biofilm by environmental signals. Once it reaches the surface, the bacteria can bind as single cells or clusters of cells. If single cells stick to the surface, a monolayer biofilm is formed. The monolayer biofilm is also defined as a biofilm in which bacteria only bond to the surface (Figure 5). A multilayer biofilm is formed if bacteria are bound as clusters of cells and in this form, bacteria attach to both the surface and neighboring bacteria. Multilayer biofilm often occurs together with an extracellular matrix that can contain exopolysaccharides, proteins, and DNA (95).

The first colonist bacteria of a biofilm can initially adhere with weak van der Waals forces and hydrophobic effects (101,102) binding occurs when, over time, the attractive forces become stronger than the repulsive forces. Bacteria usually perform these attachments on medical devices and living tissues containing binding molecules such as fibronectin, fibrinogen and (103,104). And the maturation step starts by adhering cells grow and mature by interacting with each other with the production of autoinductive signals that result in the expression of biofilm specific genes (103). Increased production of autoinductor molecules corresponds to signal cues that aid in virulence and gene regulation (105). At this stage, bacterial cells begin to secrete EPS surrounding the cells, thereby stabilizing the biofilm network and protecting themselves from antibacterial agents (103). After biofilm mature, the dispersion phase begins, which is the mechanism by which bacteria expand from one part of the body to another and spread the infection. With the formation of the biofilm, the bacteria establish a physical barrier to themselves, besides, the bacteria within the biofilm structure make some transcriptional changes, initiating quorum sensing communication among themselves, and activating the resistance mechanism against antibiotics and other antimicrobial/antibiofilm properties (106).

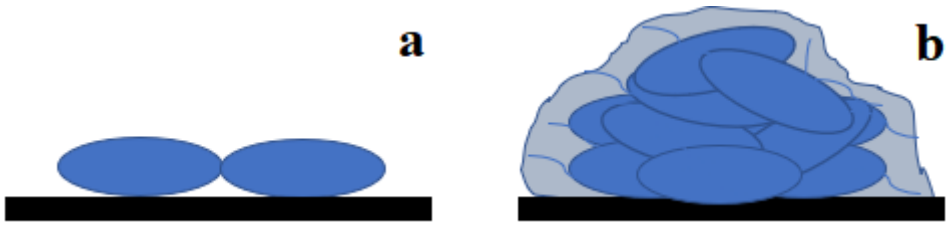

Figure 5. Monolayer (a) and multilayer (b) biofilm structure [modified according to E.Karatan, P.Watnick. 2009 (2) via Microsoft Word]

2.2.1.1. Quorum sensing

Bacterial gene regulation in response to cell population density called quorum detection is accomplished by the production, secretion and subsequent detection of extracellular signal molecules called autoinductors (107). QS was first reported in 1970 in Gram-negative rod-shaped *Vibrio fisheri* bacteria exhibiting bioluminescence when relatively high cell density reached (108). Bacteria primarily initiate signaling for biofilm formation. This signaling takes place through autoinductors. Due to the increase in cell density over time, the levels of these autoinductors in the environment increase. This increase determines not only biofilm formation but also many behaviors of the bacteria such as virulence and sporulation. Bacteria either enter the spore form or form biofilms as a defense (109–112). Gram-positive bacteria often use specific peptides as autoinducers. these peptides have different sequences due to their specificity. Also, they are usually modified after transplantation. Gram-negative bacteria use acylated homoserine (113–116)

The bacteria forming the biofilm structure according to the environmental conditions go into the stationary phase. Transition to the stationary phase significantly changes gene expression patterns to ensure long-term cell survival in the absence of nutrients. Therefore, starvation is the main signal that regulates transition into the stationary phase. Transition to the stationary phase, some bacteria form a resistant spore structure and thus survive in such environmental conditions, while bacteria that cannot form a spore structure form the biofilm structure with various signaling. For example, while *B.subtilis* is a bacterium that can form a spore structure, *E.coli* forms a biofilm structure. For non-sporulating bacteria such as *E.coli*, the stationary phase results in increased resistance to a range of environmental stresses such as high osmolarity, oxidative agents and high temperatures (117,118)

The transition to the stationary phase is driven by key transcription factors whose activity or production is stimulated by starvation. Bacteria synthesize low molecular weight signaling molecules released from cells to communicate with other microorganisms. The released "auto-inducing" signal molecules direct a process called quorum sensing (QS) (119,120). Quorum sensing is a cell-cell communication process between bacteria according to cell density and allows to the regulation of gene expression accordingly (121). An important part of an intracellular signaling molecule is bis- (3'-5')-cyclic dimeric guanosine monophosphate (c-di-GMP). This second messenger c-di-GMP regulates various complex bacterial processes such as biofilm formation, motility, virulence, cell cycle, differentiation and other processes. It stimulates the biosynthesis of the adhesins and exopolysaccharide matrix substances that provide adhesion to the surface in the biofilm structure and prevents the motility patterns of bacteria: It controls the transition between the "lifestyles" of bacteria associated with motile planktonic and immobile biofilms (122,123)

2.2.2. Other biofilm-forming species

Although it is known that the biofilm structure is widely produced by bacteria, they are not the only creatures that make up this structure. Especially in strains belonging to *S.aureus* bacteria, a high rate of biofilm formation is seen. Also, eukaryotic biofilm structures are encountered (124–126) Examples of biofilm-forming eukaryotes are fungi and microalgae. Fungal biofilm structures are frequently encountered in human and plant infections, which causes antifungal resistant fungal infection to become much more resistant (127,128)

Biofilms formed by eukaryotic algae and cyanobacteria are formed on contact surfaces in various land and water environments. The energy source of these creatures is light as the name suggests (129). By reducing the carbon dioxide ratio in the environment, they provide organic substrate and oxygen, this process also feeds the biofilm formation process. Because of these beneficial properties, there is an increasing interest in the application of Phototrophic biofilms, for example in wastewater treatment, bioremediation, aquaculture and biohydrogen production inbuilt wetlands (130).

2.2.3. Detection methods of biofilm formation

Since access to the bacteria, which occurs after the biofilm is formed, is limited, it is very important to inhibit this structure before it occurs (131). The methods used to determine the biofilm structure are aimed at staining the biofilm matrix or detecting signal molecules involved in the biofilm-forming mechanism between bacteria. Congo Red Agar / Broth method, Modified Christen's method (Cristal violet dyeing), dye elution technique and latex agglutination methods can be given as examples (132). In addition to this, the real-time monitoring of biofilm inhibition (RT-MBIC) method is used for pseudomonas strains based on the fluorescent luminescence feature (133).

There are many methods for detecting biofilm. The first of these is Cristal violet (CV) dyeing. Although this method is simple and inexpensive, it is not a specific method. In addition to the biofilm structure, it also dyes bacteria and the environment in the environment. At the same time, since the method has many give and take steps, the resulting biofilm also damages and affects the result (134). Tissue Culture

Plate (TCP) method, which requires a CV staining step, is also widely used (135). In addition, Congo red agar (CRA) method is also used to detect strong biofilm-producing strains. This method allows the formation of black colonies in the presence of c-di-GMP molecules produced by QS. Also, the Congo red broth (CRB) method we created with the development of the CRA method is described in 3.11.4. (136). In addition, the presence of biofilm structure can be detected with microscopes such as SEM (137), confocal scanning laser microscopy (CSLM) (138).

2.2.4. Medical biofilms

After a bacterium attaches to the surface, depending on the environmental conditions, the extracellular secretion it produces as well as dividing and multiplying is called biofilm. The biofilm structure forms an extracellular matrix in which the bacteria protect themselves. This structure is three dimensional and consists of extra polymers in gelatin form. From a medical point of view, biofilm structure is a very suitable structure to form on the surface of implants. Implants can be permanent in the body or can be inserted and removed for a short time. For example, while dental implants are permanent, catheters are implants that can be worn daily or for a maximum of two weeks. In particular, direct contact of the intrabody catheter structures with the living surface facilitates the formation of biofilms on these surfaces. Since the biofilm structure forms a protective envelope around the bacteria, it reduces its sensitivity to antibiotics and HDPs. For this reason, it becomes almost impossible to remove and treat the biofilm. Hospital-acquired infections are called nosocomial infections and *Staphylococcus epidermis* is shown among the bacteria that cause these infections most (139).

Cystic fibrosis is a major cause of biofilm-associated infections, morbidity and mortality, and financial cost, including lung infection, chronic and recurrent otitis media, chronic wounds, and implant and catheter-related infections. Chronic biofilm-based infections are persistent to conventional antibiotic therapy and are not often impaired by host immune responses such as phagocytosis, despite the persistent presence of host inflammation (139). Biofilm disease can be divided into three main types “device-associated biofilm disease; non-device related chronic biofilm disease; and biofilm-related device failure” (140).

Device-associated biofilm diseases are due to the use of implanted medical devices such as “Pacemakers and prosthetic heart valves, vascular prostheses, electric dialyzers, intravenous catheters, permanent urinary catheters, chest implants, urethral stents, endotracheal tubes, peritoneal dialysis catheters and contact lenses”. Some of these devices come with a high risk of biofilm-associated infection, along with their remarkable (140,141) These infections can affect the quality of life or be fatal. Bacterial colonization of these devices can occur rapidly by host-produced conditioning films such as platelets, plasma and tissue proteins (within 24 hours) (142). When a medical device is implanted in the human body, it becomes an area where host cells and microbes compete for access while fulfilling its purpose of rescuing the normal functions of vital organs. Device-associated nosocomial infections begin with the colonization of the material surface of the medical device, followed by the microorganism resulting in the formation of a biofilm (143). Experimental studies have reported that cells separated from biofilms have a greater association with cytotoxicity and mortality than equivalent planktonic (144,145)

Biofilm disease not associated with implanted devices are “chronic airway infection, chronic obstructive lung diseases, tuberculosis, chronic wound infections, chronic otitis media, chronic sinusitis, endocarditis, osteomyelitis, dental caries,

bacterial prostatisis and cystic fibrosis" (146). Biofilm-related device malfunction also occurs within 4 weeks after the removal of an implant in the body (147).

2.2.5. AMPs to combat bacterial biofilm

AMPs can also have an effect on biofilms. They can exhibit an inhibitory or eliminating effect at different stages of biofilm formation. They also provide an inhibitory effect on direct biofilm binding on peptide coated surfaces (148,149). For example, the Nisin A peptide is effective, whereas the MRSA strain is capable of forming biofilms. Nisin A is a polycyclic AMP. This peptide can pierce the biofilm structure and reach buried bacteria and disrupt the membrane structures (150). It is known that LL-37 peptide also disrupts the QS system which is one of the stages of biofilm formation and causes (149,151).

AMPs can cause degradation of the EPS structure. Degradation of this structure causes bacteria to become vulnerable. Hepcidin AMP targets intercellular adhesion (PIA) and disrupts the biofilm structure. (152). Biofilm formation is coordinated by the icaADBC locus in staphylococci. Human β-defensin 3 is known to slow down or inhibit biofilm formation by decreasing the expression of these genes (153).

2.2.6. Self-Assembly ability of peptides

Some peptides, especially peptides with alpha-helix or beta-sheet structure and showing amphipathic properties, may exhibit the ability to hold between themselves and with the surface on which they are located. Self-assembly is called self-assembly without using any chemicals or linkers in the environment. Peptides showing sel-assembly are generally amphipathic in their structures by containing ionic and hydrophobic groups. In antimicrobial peptides, positively charged cationic amino acids such as R or K are preferred as the counterpart of these ionic amino acids (154). The reason for this is to maximize the peptide membrane interaction as mentioned in the previous titles. Besides the properties of the peptide, the ionic strength of the solvent and the peptide concentration also affect it. The excess of ionic power in the environment causes hydrogenation formation. For this, the reproduction of ionic and hydrophobic amino acid residues used in the structure of peptides in aqueous environment supports the formation of self-assembly (154).

Nowadays, antimicrobial peptides have come to the fore in addition to antibiotic treatments to prevent catheter-based hospital infections. In the light of all this information, it is aimed to design peptides with high antibacterial effect and low cytotoxicity in this thesis. For this, amino acids in D and L form were used and it was aimed to keep the HC50 value low while increasing the antibacterial effect. Peptides, whose design and biological activities were studied, were tried to be attached to the catheter surface by self-assembly method, thus it was aimed to prevent the formation of infection on the peptide-coated catheter surface.

3. MATERIALS AND METHODS

3.1 Materials

The equipment used during the study is given in the Table 1.

Table 1. The equipments used during the study and their brands

EQUIPMENT	**BRAND**
Peptide Synthesizer	CEM Liberty Blue
Peptide Razor	CEM
HPLC	Agilent
Pure Water Device	Advantage Milli-Q
CO_2 Incubator	Thermo Scientific
Biosafety Cabinets	Thermo Scientific
15-50 ml Falcons	Thermo Scientific
Eppendorfs	Thermo Scientific
Sonicator	Isolab
Scanning Electron Microscope	Thermo Scientific-Quattro
-20 Freezers	Kirsh Froster
-80 Freezers	GFL
Microplate Reader	Thermo scientific Varioscan
Water Bath	Thermo Digital
Precision Weighing	Isolab

Freeze Dryer (lyophilizer)	Labconco

Table 1. The equipments used during the study and their brands (continued)

C18 Analytical HPLC Column	**Agilent**
C18 Semi-preparative HPLC Column	Agilent
96 well microplate	TPP / Cellstar

The equipment used during the study is given in the Table 2.

Table 2. The chemicals used during the study and their brands

CHEMICAL	**BRAND**
F moc L-aminoacids	Sigma-Aldrich
F moc D-aminoacids	Novabiochem
Oxyma	Sigma-Aldrich
Rink Amide Resin	Sigma-Aldrich
Acentonitrile HPLC grade	Merck
Dicloromethane	Carlo Erba
Diethyl ether	Carlo Erba
N,N'-Dimethylformamide (DMF)	Merck
N,N'-Diisopropylcarbodiimide (DCM)	Merck
Piperidine	Merck
Triisopropylsilane (TIS)	Across
Trifluoroacetic acid (TFA)	Sigma
Dulbecco's Modified Eagle Medium (DMEM)	Sigma

Table 2. The chemicals used during the study and their brands (continued)

Fetal Bovine Serum (FBS)	Thermo Sci
Penicillim-Streptomycin	Thermo Sci
Phospate Buffered Saline (PBS)	GenerMarkBio
Triton X-100	Merck
DMSO	Merck
Trypsin EDTA 25%	Thermo Sci
NaCl	Merck
Mueller Hinton (MH) agar	Oxoid
Mueller Hinton (MH) broth	Oxoid
Tris base	Sigma
Ampicillin	GenemarckBio
MTT Assay	Sigma Cell Proliferation Kit I (MTT)
Peptide Concentration Assay	Pierce™ Quantitative Fluorometric Peptide Assay
Proteinase K	GeneMarck
Tris Buffered Saline (TBS)	Sigma
NaClO	Emplura
Congo Red	Sigma (BCB25091)
D-Fructose	Bioshop
Sucrose	Merck
D-Glucose monohydrate	Sigma Aldrich
Tyrptone Soya Broth	Oxoid
Brain Heart Infusion Broth	Sigma Aldrich
Gram Stain Set	Chembio
Crystal Violet	Cembio

3.2. Peptide Design

The most important part of the new AMPs design is increasing the antimicrobial activity and decreasing the hemolysis. So that target to phospholipid layer, makes AMPs need to positive net charge for best interaction (155). Besides net charge, the helicity is the key point for lipid pore formation or leakage. Reach to best α-helicity within amphipathic features, gives satisfactory results (156). As intended in the thesis title, new peptides with antimicrobial activity have been designed following the literature review. In these designs, the LL-37 antimicrobial peptide, which is the only peptide from the cathelicidin group, was taken as an example. Except for the LL-37 signal sequence, it consists of a precursor sequence of 19.3 kDa and 18 amino acids; This sequence has an α-helix structure and gives the peptide antimicrobial activity property (157). In the review of AMPs, it was observed that the peptides were hydrophobic and positive (+) charged (158). The cationic part provides binding to the bacterial cell wall beside the hydrophobic part provides to cross the membrane structure. When all this information is evaluated, in the peptide design, hydrophobic and positively charged amino acids and 10-20 amino acid long peptides forming the α-helix structure are designed. In addition to the L-amino acid form in nature, the D-amino acid form is also used in peptide antibiotics. The use of D-amino acid makes the peptide more stable, as well as protecting it against proteases and thereby affecting its (159,160) One of the most important points in peptide design is the termination of the peptide with the amide group. The amide group at the C-terminal end has been found to have an effect on increasing membrane permeability, as the peptide causes the membrane to approach more upright and be taken up into the cell more quickly. In addition, it shows activity in peptide resistance to proteases (161).

R, K and H amino acids are generally used to provide a positive charge in the structure of antimicrobial peptides. Although K and R amino acids are positively

charged, they are frequently used amino acids in the structure of synthetic peptides due to their hydrophobic nature. The use of the twin-arginine motif in peptides enhances the membrane-peptide interaction. It has been determined that the R amino acid protonates the membrane surface and the K amino acid has the effect of deprotonating the membrane surface (162). The twin-arginine motif also facilitates membrane translocation (163). Within the scope of all this information, 4 peptide sequences were designed using D and L-form amino acids (Table 3). The sequence, amino acid contents (aa), hydrophobicity ratios, net charge at pH 7.0, pI points and molecular weights are listed in table 3.

Table 3. Designed peptide sequences and their properties

	Peptide sequence	**Aa content**	**Hydrophobicity**	**Net charge**	**pI value**	**Molecular weight g/mol**
NET1	RLLLRLLRRLLRLLLR-NH_2	D-leu L-arg	% 62,5	+6	13,2	2085,75
NET2	RLLLRLLRRLLRLLLR-NH_2	L-leu L-arg	% 62,5	+6	13,2	2085,75
NET3	RLLLRLLRRLLRLLLR-NH_2	L-leu D-arg	% 62,5	+6	13,2	2085,75
NET4	RLLLRLLRRLLRLLLR-NH_2	D-leu D-arg	% 62,5	+6	13,2	2085,75

The aim of using this combination of a different form of amino acids is to decrease the hemolysis and increase the antibacterial activity. According to researches, the peptide has amphipathic features more effective than hydrophobic features. To gain the amphipathiticity to peptide should be used the polar or positively charged amino acids with nonpolar or hydrophobic amino acids (156). For

representing positive charge and hydrophobicity respectively R and L amino acids preferred (164). We used positively charged and hydrophobic amino acids in our designs for our peptides to be hydrophobic to approach the membrane and to interact better with the negatively charged cell membrane. Both L- and D- forms of amino acids were used in our peptide sequence for resistance to proteases, lower cytotoxicity and higher antimicrobial activity.

3.3. Molecular Modeling of Peptides

The 3-dimensional structures of the peptides were obtained using the PEP-FOLD3 server (165) and molecular dynamic models were performed by running the CHARMM27 force field parameters and NAMD 2.11 software in parallel (166). The placement of peptide molecules on the POPE membrane at a certain distance was done using VMD (Visual Molecular Dynamics) software (167). The reason for choosing POPE membrane is that PE (Phosphatidylethanolamine) lipids are generally more on the cytoplasmic side of the bacterial membrane, and PE lipids are frequently used to mimic the bacterial membrane (168). In the first report, 4 identical peptide molecules were positioned so that the distance between them and the distance between them and the peptides to the bacterial membrane was approximately 10 Å to observe the orientation or attitude of the peptides to both each other and the membrane, but this report focuses on solving the problem in the parameterization of the NET1 peptide and a larger simulation. (The simulation box can be optimized in the future.) The method for the NET1 peptide in which the D and L amino acids are in mixed form is fitted and ready to be used for other peptides that will contain amino acids in similar mixed form.

There are many unnatural atom positions as we artificially put together the lipid system provided by the VMD's membrane insert. For this reason, before running the molecular dynamics algorithm, in order to bring the system to the minimum local energy, a 2 ps minimization is followed by a stabilization phase that takes 0.5 ns and includes restricted peptides. Since the system is not in equilibrium, a simulation was first performed in which everything except lipid tails (water, ions, protein, lipid head groups) was fixed. In the literature, 0.5 ns was found to be sufficient at this stage (169). After this simulation, another simulation step was performed in which 2 ps minimization and 0.5 ns lipids were free but the water was restricted, and then all restrictions were removed and a 0.5 ns balancing model was performed and the lipid ends became irregular. After the peptides reach equilibrium, the whole system is ready to operate with molecular dynamics. The simulation performed for the NET1 peptide is ~ 46 = ~ 50ns long. The outputs obtained as a result of the molecular dynamic simulation performed were analyzed by visualizing them with the VMD program.

3.4. Solid Phase Chemical Synthesis of Designed Peptide Antibiotics

CEM Liberty Blue® peptide synthesizer was used in peptide synthesis. Amounts of amino acids, resin (Rink amide proTide), activator (DIC), activator base (oxyma), washing (DMF; dimethylformamide) and deprotection (piperidine) solutions were made on the computer by device program. Amino acid amounts and resin amount were calculated depending on the resin range. The calculated amount of resin was kept in 10 ml DMF or a minimum of half an hour and the resin was swelled. Table 4 shows how much of the amino acid is used in each synthesis and how many ml of DMF it dissolves. Peptide synthesis was initiated after the resin, amino acids and all other solutions were loaded on the synthesis device and a synthesis took 2 to 3 hours (170).

Table 4. Amino acid quantities required for peptide synthesis

	Resin Range (mmol)	Amino acid amounts g / ml
NET1	0.05	2.6 gr L-arg + 20 ml DMF 1.14 gr D-leu + 16 ml DMF
NET2	0.05	2.6 gr L-arg + 20 ml DMF 1.14 gr L-leu + 16 ml DMF
NET3	0.05	2.6 gr D-arg + 20 ml DMF 1.14 gr L-leu + 16 ml DMF
NET4	0.05	2.6 gr D-arg + 20 ml DMF 1.14 gr D-leu + 16 ml DMF

Razor® device for cleavage was set to 38 °C and a cleavage cocktail was prepared. Consisting of 4.75 ml of TFA, 125 µl of TIS (triisopropyl silane) and 125 µl of dH_2O cleavage cocktaile were added to the peptide and kept at 38 °C for 45 minutes. As stated in the synthesis program of the device, the duration of the cleavage phase was determined by adding half an hour to 3 arginine in the peptide structure and 5 minutes for each arginine after 3 arginine. After the cleavage phase was completed, 15 ml of cold diethyl ether was added to the peptide collected from the filtered falcon by the vacuum of the device and it was centrifuged for 3 minutes at 4000 rpm (revolutions per minute). This stage was repeated 3 times. Lastly, the liquid other than the peptide pellet was poured and the falcon lid was pulled open and the peptide was obtained in powder form by keeping in the fume cupboard every other day (170).

3.5. HPLC (High-performance liquid chromatography) and Lyophilization

The peptides synthesized with the CEM Liberty Blue® peptide synthesizer obtained ~ 95% pure with a firm and device warranty. HPLC is a method used for purity and accuracy analysis of peptides and proteins. Common usage reasons are sensitivity, easy adaptability to quantitative determinations, and suitability for separation of non-volatile or temperature-degradable compounds (171).

3.5.1 Analytical HPLC

The analytical HPLC was done by the C8 HPLC column (172). The C8 column is used specifically for peptides and suitable for reverse-phase HPLC (RP-HPLC). A (0.05% TFA in dH_2O) and B (0.25% TFA in acetonitrile) solutions used in the mobile phase were prepared. After the peptide is injected into the column, 5% B is passed through the column for 5 minutes, allowing the column to reach equilibrium. The peptide is then run from a wide range of hydrophobicity (5-80% in 30 minutes). After the peptide is expected to be detected in this range, after 30 minutes, 100% B is passed through the column to remove any residue in the column and wash the column. The synthesized peptide antibiotics were first prepared for reverse phase HPLC, 2 mg/ml and carried out in the analytical column, and the approximate hydrophobicity was calculated according to the peak position.

Table 5. Analytical HPLC conditions

Time (m)	% A	% B	Flow rate
0.00	95	5	0.2 ml/min
5.00	95	5	0.2 ml/min
5.01	95	5	0.2 ml/min
35.00	20	80	0.2 ml/min
35.01	0	100	0.2 ml/min
40.00	0	100	0.2 ml/min

3.5.2 Semi-prep HPLC

Semi-preparative HPLC was started for purification. Despite 95% purity the peak seen was collected and purified. A (0.05% TFA in dH_2O) and B (0.25% TFA in acetonitrile) solutions used in the mobile phase were prepared. Alternatively, water-insoluble peptides before purification were dissolved in DMSO and loaded onto the column. Subsequently, 10 mg/ml was prepared, run on the semi-preparative C-18 column, and pure peaks were collected (172) (Figure14, Figure 15, Figure 16, Figure 17).

Table 6. Semi-prep HPLC conditions

Time (m)	% A	% B	Flow rate
0.00	95	5	4 ml/min
5.00	95	5	4 ml/min
5.01	95	5	4 ml/min
35.00	20	80	4 ml/min
35.01	0	100	4 ml/min
40.00	0	100	4 ml/min

3.5.3. Lyophilization

Since the pure peptide solution collected in the collector consists of TFA, ACN (acetonitrile) and dH_2O, it was diluted with water in a ratio of 1: 3 (ACN / dH_2O) to reduce the rate of acetonitrile, an organic solvent. Lyophilization process is a process that allows the substance to be dried by freezing the product in solution or suspension and subsequent removal of the gas phase formed by sublimation (173). The diluted peptide solution was kept at -80 °C every other day or frozen with liquid nitrogen, and then the lyophilizer reached -80 ° C, frozen samples were placed in the device and the vacuum was turned on, after 2 days, peptides in powder form were obtained.

3.6. Peptide Concentration

Peptides taken from the lyophilizer were weighed on a precision scale, 1 ml of dH_2O was added, and dissolved by leaving the sonicator for 5-7 minutes. Water-insoluble peptides prior to lyophilization were determined to dissolve in water after lyophilization. Peptide concentrations were measured using the Pierce Quantitative Fluorometric Peptide Assay (Thermo Fisher) kit (174). Since the kit does not conform to water, the samples were diluted with 100 % ACN in a 1: 1 ratio of 10 µl so that the blank solvent was 50 % AcN. 10 µl of standards, blank and peptides were placed in each well of the 96-well black plate. 70 µl Fluorometric Peptide Assay Buffer was added to them and pipeted. 20 µl Fluorometric Peptide Assay Reagent was added and incubated in the dark for 5 minutes at room temperature. The standards specified by the kit are prepared by serial dilution. A curve graph was drawn with the absorbance measurement taken with standards included in the kit. Fluorometric (ex/em 390nm/475nm) absorbance value was entered on the Y-axis and the standard concentration corresponding to this value was entered on the X-axis (174) (Graph 1).

The absorbance value obtained by fluorometric reading was written in the equation given by the graph instead of Y and X value was found. Then, the peptide concentrations were calculated with the formula below, the peptide concentrations obtained were calculated by converting from µm to mg/ml with the formula and used in further experiments (174) (Table 8).

Concentration (mg /ml) = [Peptide molecular weight (da) × Concentration (µm)]/ 1000

3.7. Liquid Chromatography–Mass Spectrometry (LC/MS)

LC / MS is a combination of liquid chromatography and mass spectrometry. The sample carried out in the liquid phase also allows for mass analysis. LC / MS allows the samples to be divided into fragments according to the m / z ratio by ion bombardment, the accuracy of the sample is proven according to the agreement of these fragments with m / z calculations (175).

Peptides are divided into fragments while detected by the LC/MS method. These fragments are separated according to the ionic charge of the peptide. Z (charge) indicates the degree of ionization. Peptides that are fragmented during this ionization can be spliced, or FA from solution can be added to any fragmented. The effect of various solvent compositions such as Formic acid (FA) is calculated also in table 7. In Table 7 the ionization degrees and masses of the peptide, ionization degrees and masses of the peptide when 1, 2 or 3 FA was added to the peptide were calculated. 60 g / mol was added for each FA. By comparing the peaks from LC / MS with the calculations here, the accuracy of the loaded peptide content is determined (176).

Table 7. LC/MS protonetion; m/z ratio calculation of peptides

NET1 NET2 NET3 NET4 Peptides					
	z (charge)	**m/z (mass/charge)**	**m/z**	**m/z**	**m/z**
m (molecular weight)	1	2085,75	2145,75	2130,75	2115,75
	2	1042,88	1102,88	1087,88	1072,88
	3	695,25	755,25	740,25	725,25
	4	521,44	581,44	566,44	551,44
	5	417,15	477,15	462,15	447,15
	6	347,63	407,63	392,63	377,63
	7	297,96	357,96	342,96	327,96
	8	260,72	320,72	305,72	290,72
2085,75 g/mol	9	231,75	291,75	276,75	261,75
	10	208,58	268,58	253,58	238,58
	11	189,61	249,61	234,61	219,61
	12	173,81	233,81	218,81	203,81
	13	160,44	220,44	205,44	190,44
	14	148,98	208,98	193,98	178,98

3.8. Detection of Antibacterial Activity (MIC)

The MIC (Minimum inhibition concentration) determines the minimum concentration of material studied that stops the growth of bacteria. Müeller Hinton agar (MHA) and Müeller Hinton broth (MHB) were prepared for use in the MIC experiment. For 1 liter MHB, 21 g MHB (sigma) in powder form was weighed and dissolved in 1 liter distilled water (dH_2O) and autoclaved at 121 °C for 15 minutes, and for MHA, 38 g of MHA was weighed in powder form, dissolved in 1 liter of water and autoclaved at 121 °C for 15 minutes. After the autoclave, the MHA medium was expected to cool to around 50-60 °C. The warmish MHA medium was

distributed to 25 ml in petri dishes. This procedure was performed in the hood and next to the fire to be sterile. Waited 10-15 minutes, the medium poured into the petri dishes was allowed to cool and solidify. The prepared petri dishes were parafilmed and stored at +4 °C until the experiment.

To determine whether the amide-terminated peptide produced had any antimicrobial susceptibility before proceeding to the MIC tests, the smear was planted in the Müeller Hinton Agar plate with *E.coli* and *S.aureus* strains free of gaps in the plate. Steril water; the solvent in which the peptide is dissolved, is added to a portion of the two-separated plate, and 1 mg/ml of the peptide is added to the other part and incubated in a 37 °C incubator overnight. The next day, it was observed that the solvent had no effect on the plate, but all four peptides formed a zone at a concentration of 1 mg/ml that had an effect on both *E.coli* and *S.*aureus. Figure 26 shows the zone of four peptides on five bacterial strains.

MIC was determined by serial dilution of the peptides whose effect was observed at a concentration of 1 mg/ml. The bacterial strains to be used were seeded in Müeller Hinton agar and incubated overnight at 37 °C. For experiment 0.5 McFarland bacterial suspension was prepared in MH broth, which is $1x10^8$ cfu /ml (colony-forming unit/ml), from the bacteria that growth the day before. And 40 µl of 0.5 McFarland bacteria are diluted in 4 ml MH broth (final cfu/ml 10^5). In the 96-well plate, serial dilutions of peptide antibiotics starting from 512 µg/ml up to 0.5 µg/ml were made in MH medium and added 5 µl of bacterial suspensions prepared on them. Incubated overnight at 37 °C and results were evaluated the next day (177). Ampicillin was used as positive controls. The MIC value of each peptide is given in Table 9.

3.9. Protease Resistant Assay

The peptide solution was prepared at a concentration of 1 mg/ml in tris-buffered saline (TBS buffer, pH = 7.6, Aldrich) with 10% DMSO. Proteinase K solution was prepared in TBS buffer that the stock solution was 1 mg/ml (enzyme activity = 30U/mg). 100 µl of the enzyme solution was added to 1 ml of peptide solution. It was incubated overnight at 37°C with shaking. The reaction was blocked by adding 1% TFA (100 µl) in water (178).

HPLC analyzes of peptide solutions with and without proteinase K enzyme were performed. Peptide solutions were first analyzed in 30 minutes in a range of 580% B with Linear gradient, with an analytical C18 Agilent tec(178)hnologies AdvanceBio Peptide Plus, 2.1 x 150mm, and 2.7µm, column. Two different mobile phases were used: A: 0.05% TFA / H20, B: 0.25% TFA / Acetonitrile.

3.10. SEM (Scanning Electron Microscope) Imaging

A scanning electron microscope (SEM) is a type of electron microscope that produces images of a sample by scanning the surface with a focused electron beam. Electrons interact with atoms in the sample, producing various signals containing information about the surface topography and composition of the sample (179).

The peptide concentration of 16 µg/ml, which is 8-16 times the MIC value, was used for NET1 and NET3 peptides. For NET4, 32 µg/ml concentration, which is 8 times its own MIC value, was used. For NET2, 128 µg/ml concentration, which is 2 times its own MIC value, was used. Bacteria concentrations were prepared at 10^5 cfu/ml and peptides were added at the specified concentrations and treated at 37 °C for 4-5 hours. After 5 hours, peptide treated bacteria 20 µl was dropped onto the dialysis membrane (FigurE 29, Figure 30, Figure 31, Figure 32). After fixation, images were taken in SEM microscope. *E.coli*, which was not treated with any factor of 10^5 cfu/ml, was used as a control (Figure 28) (180).

3.11. Detection of Hemolysis

A hemolytic activity test was performed to determine the concentration of the synthesized peptides in human red blood cells causing hemolysis. Tris-Saline (Sterile, 10 mM TRIS, 150 mM NaCl, pH 7.2) solution was prepared, autoclaved and sterilized. 30 µl of fresh human blood was taken and added to 10 ml of Tris-Saline solution and centrifuged for 5 minutes at 1500 rpm, the supernatant was discarded, the pellet was re-dissolved 10 ml of Tris-Saline and centrifuged, this step was repeated 3 times. In the last one, the pellet was dissolved in 10 ml of Tris-Saline and 100 µl was distributed to each well of the 96-well plate, in another 96-well plate serial dilution of peptides was performed in Tris saline and 100 µl added on the blood-tris solution in the first plate. Triton X-100 was used as a positive control (%100 lysis). Plate incubated at 37 °C for 30 minutes. After incubation, the 96-well plate was centrifuged at 1500 rpm for 10 minutes. The supernatant of each well was transferred to the new 96-well plate for spectrophotometric measurement. Hemolytic activities were analyzed by reading each well with a plate reader spectrophotometer device at 414 nm and the % lysis rate was calculated in Microsoft Excel according to the following formula (181).

% lysis = [OD 414 - OD 414 (blank)] / [OD 414 total lysis - OD 414 blank] x 100

3.12. Detection of Cytotoxicity

MTT Cell Proliferation Kit is the colorimetric assay based on the reduction of a yellow tetrazolium salt (3-(4,5-dimethylthiazol-2-yl)-2,5-diphenyltetrazolium bromide or MTT) to purple formazan crystals by metabolically active cells was used to evaluate the damage that peptides can cause in eukaryotic cells. The cell lines of HeLa (ATCC CCL-2), 3T3 (ATCC CRL-1658) and HaCaT (ATCC PCS-200-011) were revived under appropriate culture conditions and made ready for the experiment (182). Cells were incubated in a 5 % CO_2 incubator at 37 °C in Dulbecco's modified Eagle's Medium (DMEM) medium supplemented with 10% fetal bovine serum (FBS), 100 U / ml penicillin and 100 µg / ml streptomycin (183). After growth, the medium containing 80-85 % of the cells adhering to the bottom surface of the cell flasks, the medium was discarded without removing the cells. To remove cells well from the flask surface treating by trypsin, the cells were washed once with 1X phosphate buffer and discarded. Then, 0.25% Trypsin-EDTA has added it and it was kept in a 5 % CO_2 incubator for 10 minutes at 37 °C. After incubation, cells were suspended in DMEM containing FBS with a minimum amount of 3 times the amount of Trypsin. The collected cells were centrifuged at 500 g for 5 minutes. After centrifugation, the supernatant was discarded, and the underlying cell pellet was re-dissolved with DMEM. Cells were stained with trypan blue to perform cell count in hemocytometry. After cell counting, cells were seeded in 96-well plates, with 50.000 cells in 100 µl of medium in each well. It was incubated for 24 hours at 37 °C an incubator with 5 % CO_2 (182).

After 24 hours of incubation, peptide doses prepared 10X; starting from 640 μg/ml up to 10 μg/ml in the medium by serial dilution and then 10 μl added to wells. Final concentration of peptides reached to 64 μg/ml, 32 μg/ml, 16 μg/ml, 8 μg/ml, 4 μg/ml, 2 μg/ml, 1 μg/ml. After appropriate peptide antibiotic doses were added to the wells, the plate incubated for 18-24 hours in an incubator with 5 % CO_2 at 37 °C. Samples were worked in 3 replicates for each concentration. Cells incubated without peptide-treatment under the same conditions were used as a control. Magainin II, a known natural AMP that has no cytotoxic effects, was used as a positive control (184).

After incubation, the protocol of the MTT cytotoxicity kit was applied. 10 μl of the MTT labeling reagent (final concentration 0,5 mg/ml) was added to each well. Incubated the plate for 4 hours in the incubator with 5 % CO_2 at 37 °C. After 4 hours, 100 μl of the Solubilization solution was added into each well, and allow the plate to stand overnight in the incubator with 5 % CO_2 at 37 °C. After all these steps the results were analyzed by reading them with a 96-well plate reader at appropriate wavelengths (550 and 690 nm) (182).

3.13. Detection of Biofilm Inhibition and Eradication

In order to perform biofilm inhibition and eradication experiments, first of all, the best carbon source required for bacteria to form biofilm should be selected. This experiment is also performed with TSB and BHIB. Using MHB, the required carbon source has determined by the CRA method and the experiment has done.

3.13.1. Agar and broth preparation

38 g/l MHA for agar plates and 21 g/l MHB used for a broth preparation. 26.3 g/l glucose (mw: 180,156) to prepare CRA w/g, 50 g/l sucrose (mw: 342.3) to prepare CRA w/s (185), 26.3 g/l fructose (mw: 180.16) to prepare CRA w/f. The amount of sugar to be used is adjusted according to the amount of sucrose added. The final molarity was 0.146 M for all. It has finished by adding and 0.8 g/l Congo red dye. It is completed with water and autoclaved at 121 °C for 15 minutes, the agar plates are poured onto the plates and allowed to solidify. Then both are stored at +4 °C.

3.13.2. Minimum biofilm inhibition assay (MBIC)

For the biofilm inhibition experiment, bacterial strains were grown in MHB at 37 °C one day before. Bacteria were prepared 0.5 McFarland (1.5×10^8 cfu/ml) and diluted to 10^6 cfu/ml in MHB w/f (186) and 90 µl added to each well. Peptide concentrations prepared 10X; starting from 640 µg/ml up to 10 µg/ml in medium by serial dilution and then 10 µl added to wells. Final concentration of peptides reached to 64 µg/ml, 32 µg/ml, 16 µg/ml, 8 µg/ml, 4 µg/ml, 2 µg/ml, 1 µg/ml. Samples were worked in 3 replicates for each concentration and bacteria. 96 well F-bottom plate was used, the plate incubated in a 37 °C incubator overnight.

The next day for CV (Crystal violet) staining, the plate is inverted and the bacteria and media in the wells are poured into a container. The wells are washed 2-3

times with distilled water. After washing, 200 µl of 1 % CV solution is added to the wells, left for 15 minutes at ambient temperature in the dark. After 15 minutes, the wells are emptied by inverting the plate. It is washed 2-3 times with distilled water. To remove the remaining water in the washed wells, the plate is inverted and hit the filter paper several times. It is then left to dry in an oven at 45-50 °C. After a few hours, 200 µl of 33 % acetic acid solution is added to the wells to dissolve the dye and the biofilm layer. Pipetting is done and then the measurement is taken at 590 nm (187).

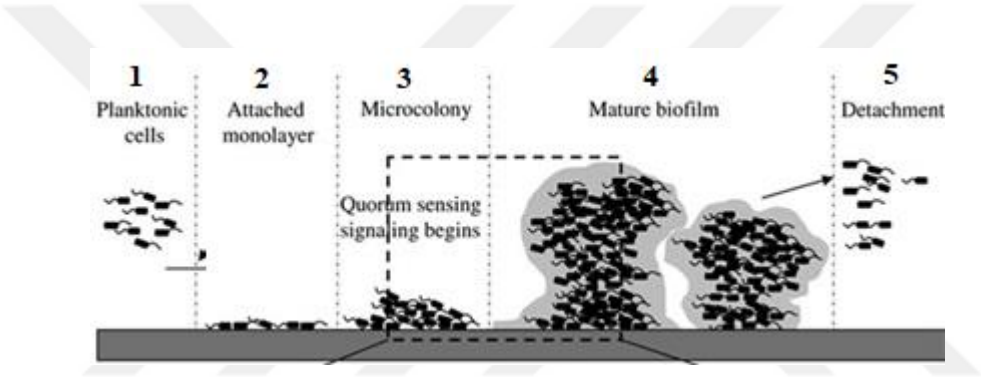

Figure 6. The Biofilm Formation Steps

During the literature review, the simultaneous addition of bacteria and peptide in biofilm inhibition study with the CV method and the difference of only 10-fold (for MIC 10^5, for MBIC 10^6) between the initial concentrations explains this difference between MBIC and MIC values. With the molecular modeling method, it is modeled that peptides show an antibacterial effect within nanoseconds. In addition, with SEM Imaging, it was reported that bacteria were damaged or killed after 3 hours of peptide treatment. Based on these results, the idea that the peptide added simultaneously with the bacteria for the biofilm inhibition experiment kills the bacteria in the plantonic phase as in seen Figure 6, and the bacteria that are not ready for biofilm formation

are inhibited by stopping or slowing down bacterial growth. Based on this idea, the congo red broth method, which contains congo red dye that interacts with the secondary metabolite of c-di GMP and creates color change, has been developed. While the CV method in the literature targets the 1st step in figure 7, the Congo rejection method targets the 3rd step. With this method, the bacteria are allowed to have the concentration that can form biofilms and the environment that the signal molecules contain, and the antimicrobial peptide added to the bacteria, which is ready for biofilm formation but not started, has been achieved with a true biofilm inhibition concentration. For the development of the method, the CRA (Congo red agar) method was inspired (188). With this method, bacteria producing strong biofilms were selected and the agar method was converted to the broth method. Biofilm formation in the invitro is triggered by the addition of a polysaccharide source that the bacteria can use. For this, glucose or sucrose is often added to the medium. Biofilm formation study was carried out primarily with *S.aureus ATCC25923, S.aureus ATCC29213, S.aureus MRSA, E.coli ATCC25922* and *E.coli ATCC13846* strains. For this, the bacteria were grown in Müeller Hinton Broth (MHB) at 37 °C one day before. Bacteria were prepared 0.5 McFarland (1.5×10^8 cfu/ml) in MHB and 10 µl dropped onto the MHCRA w/os (without sugar), MHCRA w/g (with glucose), MHCRA w/s (with sucrose), MHCRA w/f (with fructose) to determine the best carbon source triggering biofilm formation. Agar plates were incubated in a 37 °C incubator overnight and the next day the black colonies were observed (Figure 37). The most suitable polysaccharide source for bacteria to produce biofilm determined as fructose.

When the same method is applied to congo red broth, the conversion of red color to black color was measured as fluorescence at ex: 525 em: 625 nm by the varioscan device and the exact hour of biofilm formation was determined. Immediately before this hour, it was observed whether there was a real biofilm inhibition by adding antibiofilm agent to the bacteria that were already about to produce biofilms. Trials were performed with NaClO and Ciproflaxaxin antibiotics before peptides for

method optimization. Since it is known that the initial concentration only affects the time of black color formation, the study continued with the starting bacterial concentration of 0.5 Mcfarland in order to obtain faster results. To compare with the traditional CV staining method, the experiment with CRB was also performed in MHB w / s for CV staining. In NaClO application, it was diluted serially to 0.15% starting at 5% and was applied on the 0.5 Mcfarland bacteria at 0 hour first. For the true CRB method, NaClO was applied at the 7th hour, which is 1 hour before the black color formation. The same application was performed for the ciprofloxacin antibiotic at 0 and 7 hours. It was diluted from 200 µg to 6.25 µg. The next day, the values obtained from the variosacan were plotted and the true biofilm inhibition value was reached. This value was also observed with the eye as the point where the black color formation ends.

After optimization trials with ciproflaxaxin and NaClO peptides were also studied by congo red method. Bacteria were prepared 0.5 McFarland (1.5×10^8 cfu/ml) in MHB w/f (186) and 90 µl added to each well. The AMPs are added at the point where the bacteria reach a sufficient concentration to form a biofilm. For our bacteria the common point is set at the 8^{th} hour; 1 hour before the formation of black color. Because the black color cannot be reversed after it has formed and if the biofilm formation is inhibited at this point, the black color will not occur, 10 µl dH_2O was added to the last well as a positive control. Only MHCRB w/f and MHB were used as negative controls. 8 hours after the addition of AMPs, the bacteria were allowed to grow and reach the amount that would form a biofilm. Peptide concentrations prepared 10X; starting from 2560 µg/ml up to 10 µg/ml in the medium by serial dilution and then 10 µl added to wells. Final concentration of peptides reached to 256 µg/ml, 128 µg/ml, 64 µg/ml, 32 µg/ml, 16 µg/ml, 8 µg/ml, 4 µg/ml, 2 µg/ml, 1 µg/ml. Samples were worked in 3 replicates for each concentration and bacteria. 96 well F-bottom plate was used, the plate incubated in a 37 °C incubator overnight. Results are given in Table 12.

3.13.3. Minimum biofilm eradication concentration assay (MBEC)

For the biofilm eradication experiment, bacterial strains were grown in Mueller-Hinton (MH) broth at 37 °C one day before. Bacteria were prepared 0.5 McFarland in MHB w/f and 90 µl added to each well. 96 well F-bottom plate was used. For the formation of the biofilm structure, it was incubated in an overnight incubator without the addition of peptide. After 18-24 hours of incubation, peptide concentrations prepared 10X; starting from 1280 µg/ml up to 10 µg/ml in the medium by serial dilution and then 10 µl added to wells. The final concentration of peptides reached logarithmically 128 µg/ml to 1 µg/ml. Samples were worked in 3 replicates for each concentration and bacteria. Again the plate was incubated in a 37 °C incubator overnight (186).

The next day for CV (Crystal violet) staining, the plate is inverted and the bacteria and media in the wells are poured into a container. The wells are washed 2-3 times with distilled water. After washing, 200 µl of 1 % CV solution is added to the wells, left for 15 minutes at room temperature in the dark. After 15 minutes, the wells are emptied by inverting the plate. It is washed 2-3 times with distilled water. To remove the remaining water in the washed wells, the plate is inverted and hit the filter paper several times. Then it is left to dry in an oven at 45-50 ° C. After a few hours, 200 µl of 33 % acetic acid solution is added to the wells to dissolve the dye and the biofilm layer. Pipetting is done and then the measurement is taken at 590 nm (187).

3.14. Peptide Characterization and Self-assembly (FT-IR)

Some peptides are adsorbed to the surface on which they are located. This method is called self-assembly. In this thesis, the surface to be used for self-assembly is the silicone catheter. For examination, Fourier transforms infrared (FTIR) spectroscopy provides information about the various bonding types of molecules in a material. Whether the material processed on a surface is present or adsorbed on the surface can be understood with this method. This instrument can measure the wavelength range from 2.5 μm to 15 μm. Its equivalent wavenumber range is 4000 cm^{-1} to 660 cm^{-1}. It was analyzed the bonding types on the peptide treated catheter. To detect the peptide on the surface, it is necessary to detect the amide bond. The amide I bond in the frequency range from 1600 cm^{-1} to 1700 cm^{-1} and the amide II bond in the frequency range is 1548 cm^{-1} (189).

3.14.1. Slicon catheter surface cleaning protocol

The cylindrical silicone catheter is cut into 1 cm^2 pieces and the catheter surface is cleaned with the piranha solution. Piranha solution is the mixture of 1:1 (v/v) 98% H_2SO_4 + 27 % H_2O_2. These catheter pieces were treated with Piranha solution at room temperature for 20 mins. After 20 mins, silicon pieces abundantly rinsed with deionized water, dried under the airflow. After drying, silicon catheter pieces were placed for 4 hours at 70 C° under vacuum (190).

3.14.2. Peptide characterization

The peptide powder was loaded into the sample portion of the spectrometer for FT-IR examination of the peptides. This investigation enabled the detection of peptide bonds. Pioneering was provided for searching these bands later in the self-assembly experiment on the catheter.

3.14.3. Peptide self-assembly by drip method

20 µl of peptides prepared at a concentration of 4 mg / ml are dropped onto the inner surface of the catheter cleaned for self-assembly. With the dripping method, 2 different temperatures were tested for the self-assembly. Each peptide was studied in 2 repetitions for each temperature. Followed by 24 hours of incubation after dripping, one of these repeats was washed and the other was not applied anything. In the dripping method, which is the first method tried for self-assembly, 20 µl of the peptide was dropped to cover the entire inner face of the 1 cm2 catheter. The first two-repetitive sample set was incubated at room temperature and the other was incubated at 37 °C. After the peptides were dripped, they were kept overnight, and one of the two-repetitive peptides dropped catheters in each sample set was washed with solvent. In this way, it was tested whether the peptide was separated from the surface by washing. Using 2 different temperatures, it was tested which temperature is more ideal for bonding.

3.14.4. Peptide self-assembly with the soaking method in peptide solution

Peptides are prepared at a concentration from 0,25 mg/ml to 10 mg/ml and 1 ml pipetted in the 24 well plates and then the catheter piece was dropped into the peptide solution. It was ensured that the solution covered the entire surface. Catheters incubated at room temperature and 37 °C. After the peptides are kept overnight, one of the catheters that were worked twice and washed with ACN, the other is not washed. In this way, peptides are examined at 2 different temperatures and 2 different washes. The results are shown in Figure 43.

3.15. Peptide Self-Assembly EDS Analysis

In the result analysis of the self-assembly experiment of 4 peptides to the silicon catheter surface, no numerical result was taken in FT-IR measurement, and a peak-based evaluation was attempted. Subsequently, the percentages of carbon (C), nitrogen (N), oxygen (O), and silicon (Si) atoms on the catheter surface were calculated with the EDS analysis, which can give a more precise and numerical value. In the experiment, 4 peptides were tested at 25 °C and 37 °C, washed and unwashed, at 4 different conditions for each peptide. An empty catheter and an empty catheter washed with ACN were used as blanks. As the most important atom to be seen in these measurements is the nitrogen (N) atom, the adsorption rates of the peptide to the surface depending on the % change in the N atom were calculated. These rates are given in Table 15.

4. RESULTS

4.1. Peptide Design

The 3D structures of the designed peptide sequences in PEPFOLD have been previewed. Although the peptides we designed have the same sequence, they contain different forms of amino acids. Application of PEPFOLD3 gives the 3D structure of peptides using L-amino acid forms and cannot display D-amino acids. As it is known, since L- and D-forms of amino acids are mirror images of each other, the amino groups in our designs will not change their position in the alpha helix, but only the side groups of the direction of the amino acid will change. The three-dimensional structure of NET2, which we designed, in PEPFOLD3 is given in Figure 7 (191). Considering the orientation of the side groups of the peptide, it shows a corkscrew-like structure.

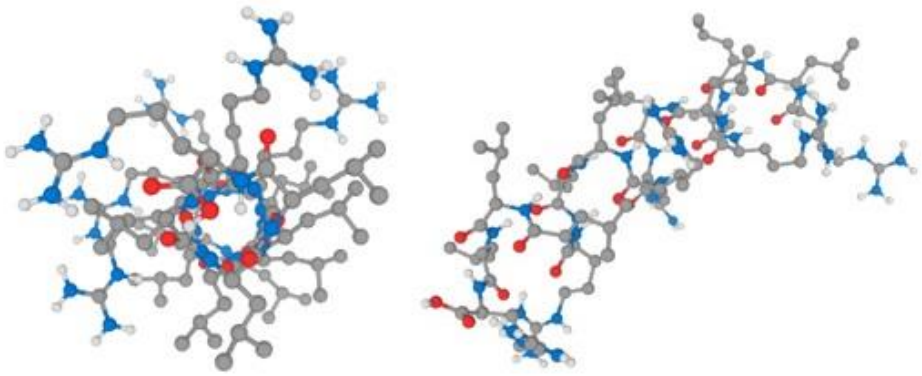

Figure 7. NET2 peptide PEPFOLD 3D structure

4.2. Molecular Modeling of Peptides

The positioning of the molecularly modeled NET1 peptide on the membrane is shown in Figure 8. In the simulation initiated after its positioning on the membrane, penetration of the peptide through the cell wall is observed after ~ 46 ns. This indicates that the peptide penetrates the bacterial cell wall quite quickly.

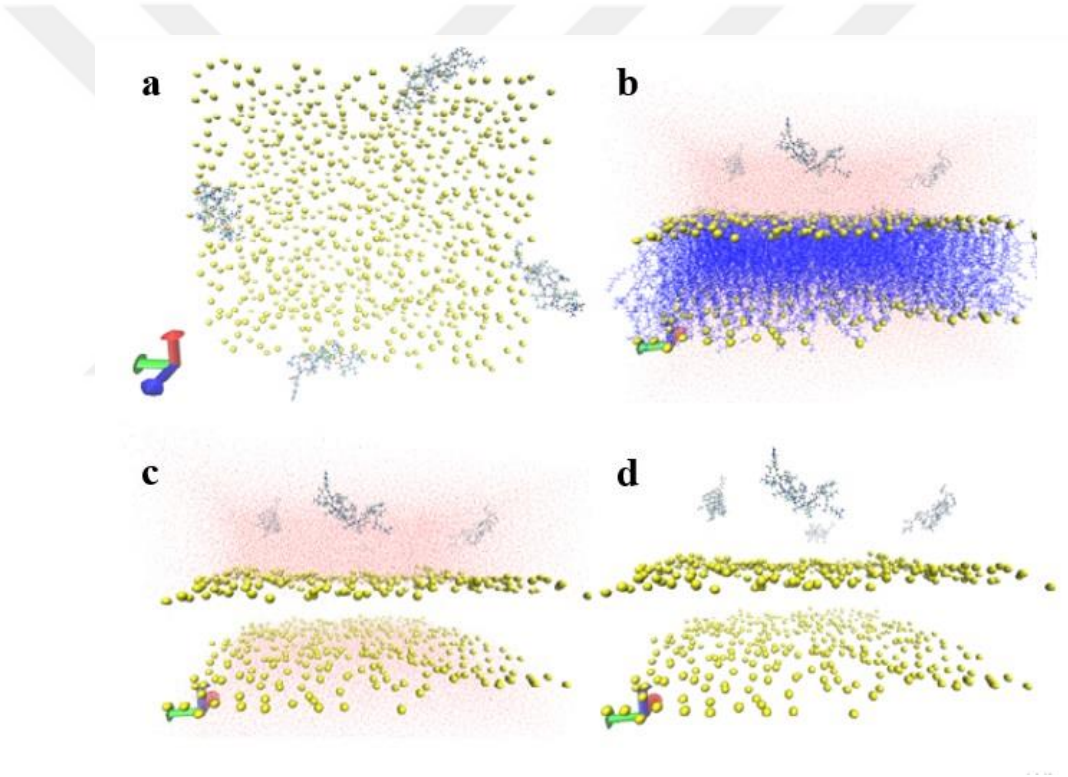

Figure 8. Positioning of the NET1 peptide on the bacterial membrane and in water

a) water and lipids covered, b) side view, c) side lipids covered view, d) lipids, and waters covered view. Water molecules are shown with red dots, phosphate molecules with bee VDW notation, membrane lipids with blue lines, peptide atoms with CPK notation

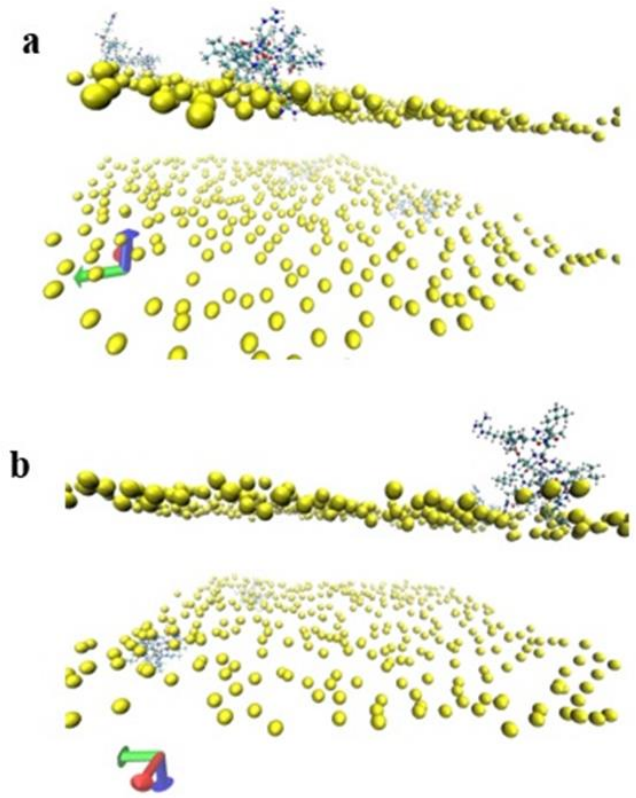

Figure 9. After the NET1 peptide molecule is positioned on the bacterial membrane and in water, the result of the molecular simulation for ~ 46 ns

a) side view, b) different angle view. Water molecules and lipids are turned off while visualizing, phosphate molecules are yellow VDW balls, peptides are shown with CPK atoms.

4.3. HPLC

Firstly, the determination of peptide purity after synthesis, the analytical HPLC was performed. After analytical HPLC, the semi-preparative HPLC.

4.3.1. Analytical HPLC

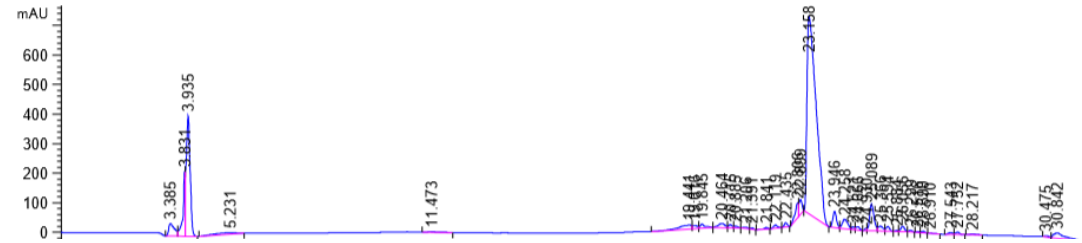

Figure 10. NET1 1 mg/ml

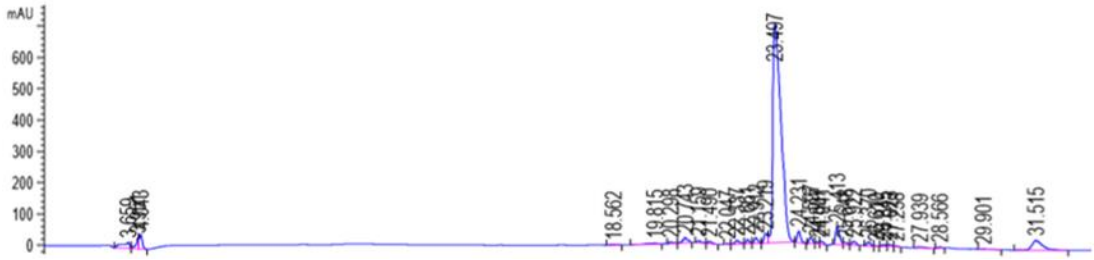

Figure 11. NET2 1 mg/ml

After analytical HPLC, a single peak was obtained for each peptide, indicating that the peptides are of high purity.

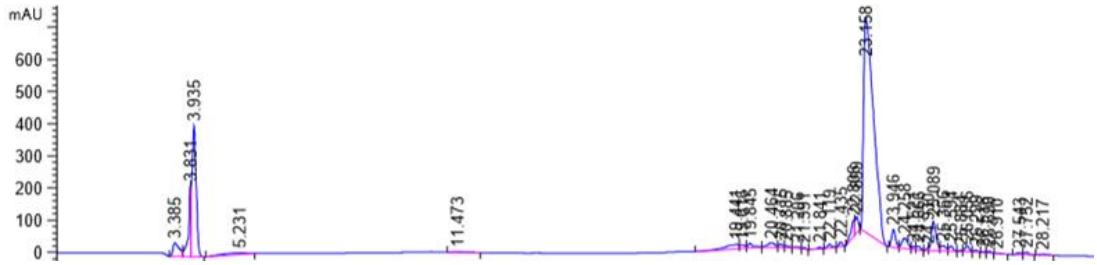

Figure 12. NET3 1 mg/ml

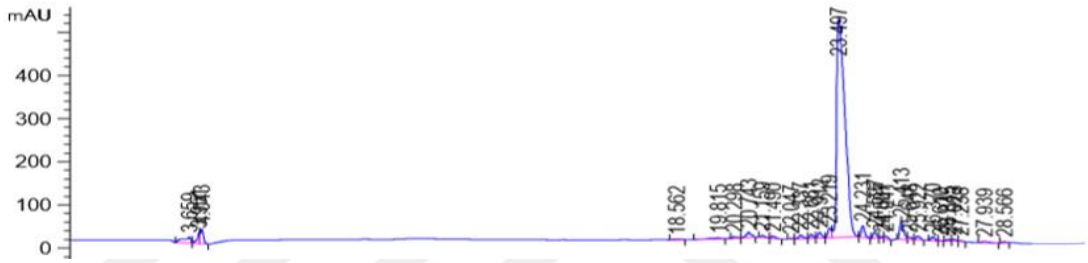

Figure 13. NET4 1 mg/ml

4.3.2. Semi-preparative HPLC

The solvent in which the peak peptide that comes between 3-8 minutes dissolves is DMSO peak. Then, between 20-22 minutes, the peptide peak comes. Semi-prep HPLC results of all 4 peptides are shown in Figure 14, 15, 16,17.

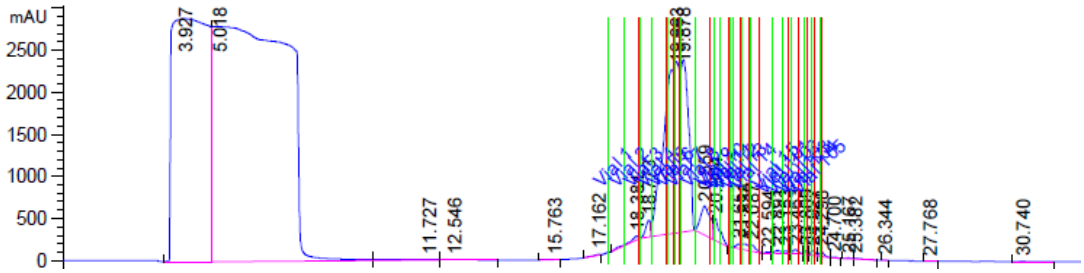

Figure 14. NET1 10 mg/ml semi-preparatif HPLC

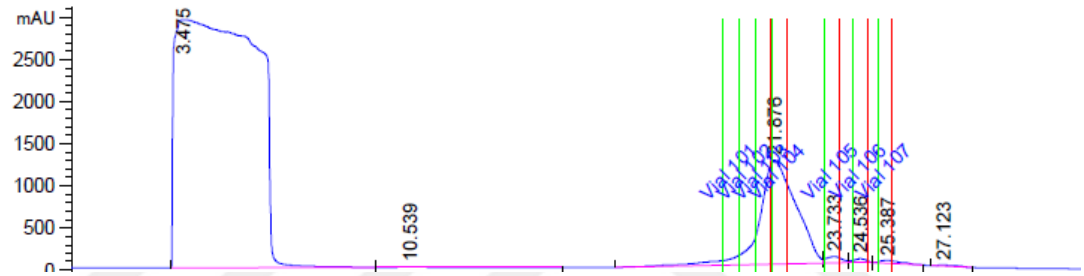

Figure 15. NET2 10 mg/ml semi-preparatif HPLC

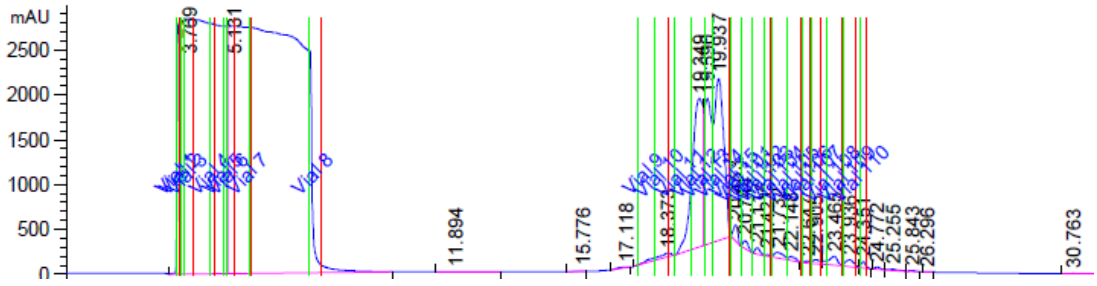

Figure 16. NET3 10 mg/ml semi-preparatif HPLC

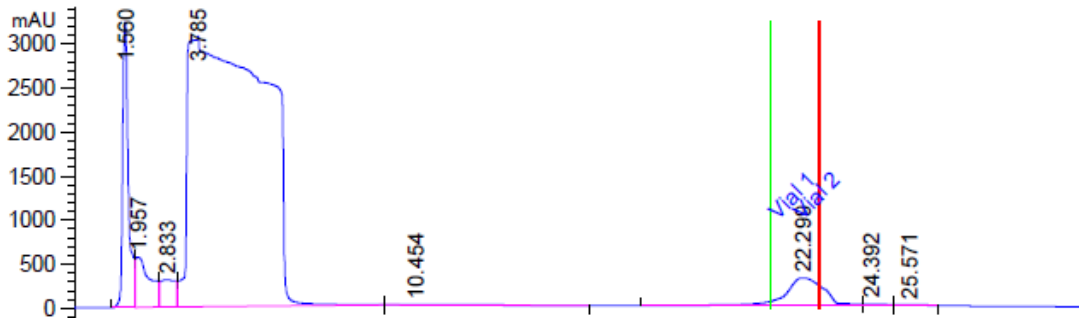

Figure 17. NET4 1 mg/ml semi-preparatif HPLC

4.4. Peptide Concentration Assay

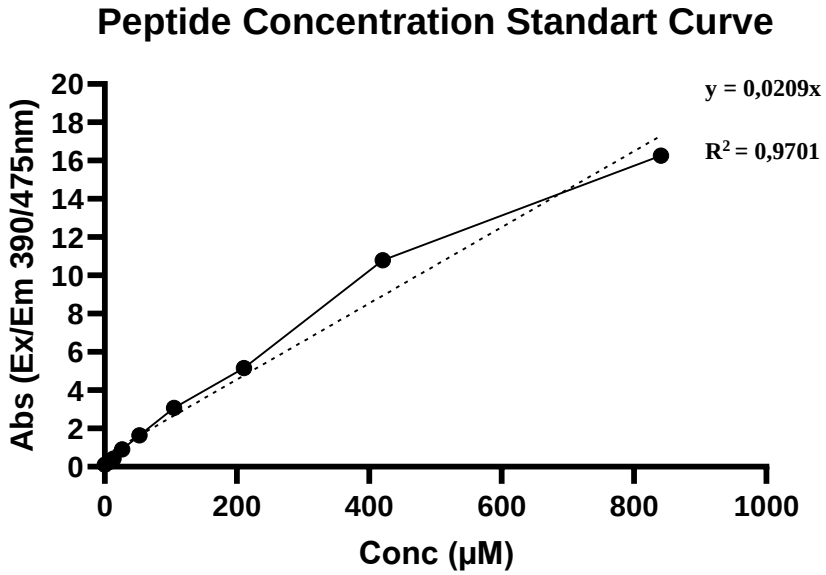

Figure 18. Peptide concentration standard curve

In the standard graph drawn with the peptide concentration kit, the absorbance values on the Y-axis are compared to the concentration value in µM on the X-axis (Figure 18). Based on the absorbance values for NET1, NET2, NET3, and NET4, the corresponding concentration value in µM is found for these peptides. To convert this value in µg / ml, the concentration in µg / ml, the concentration value in µM is multiplied by the molecular weight of the peptide (2085.75 g / mol) and divided by 10^{-6}. The peptide concentrations obtained as a result are given in Table 8.

Table 8. Pure peptide concentrations (mg/ml)

Peptide	Absorbance value	Calculated peptide concentration (µm)	Total peptide concentration (mg/ml)
NET1	19,69	942,33	1,96
NET2	19,25	918,66	1,91
NET3	22,13	1058,97	2,20
N3T4	19,13	913,87	1,90

4.5. LC / MS

The peak of NET1 peptide in LC / MS can be seen in Figure 19. The peptide appears to be pure since the peak is sharp and unique. However, to understand whether this peak belongs to NET1 or not, the ionization - mass graph of the peak should be examined. Peak fragments of NET1 are seen in figure 20. The mass values

of the fragments match the mass values obtained by ionizing the peptide. Since all peptides have the same molecular weight and degree of ionization, fragment masses in Table 7 are considered for all 4 peptides. Calculated in Table 7 for NET1, 1042.88 m/z^{+2}, 695.25 m/z^{+3}, 521.44 m/z^{+4}, 417.15 m/z^{+5}, 347.63 m/z^{+6} 260.72 m/z^{+8} fragments were detected. The molecular weight of 2085.75 m/z^{+1} was seen when the NET1 peptide was loaded at 1 mg / ml.

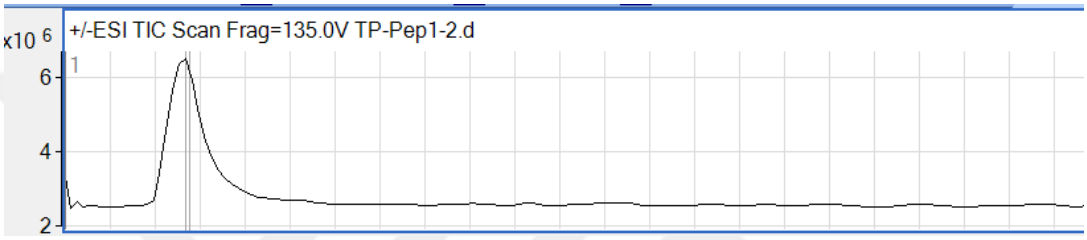

Figure 19. NET1 peak wiev 0.2 mg/ml

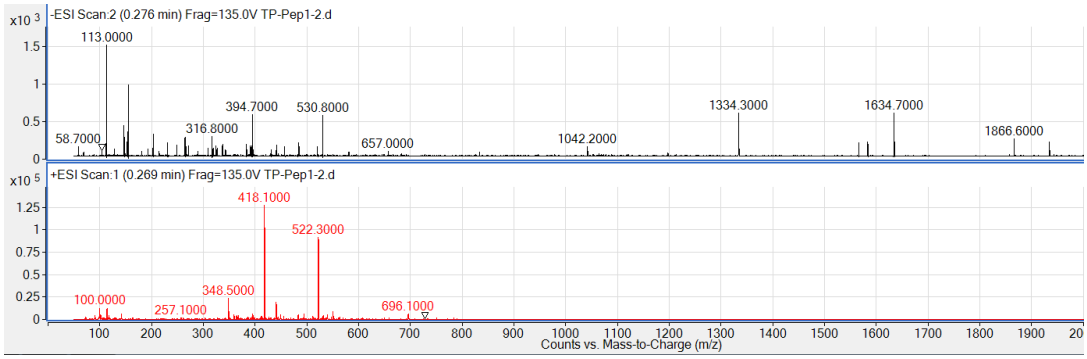

Figure 20. NET1 peak content

The peak of NET2 peptide in LC / MS can be seen in Figure 21. The peptide appears to be pure since the peak is sharp and unique. However, to understand whether this peak belongs to NET2 or not, the ionization - mass graph of the peak should be examined. Peak fragments of NET2 are seen in Figure 22. The mass values of the fragments match the mass values obtained by ionizing the peptide. Since all peptides have the same molecular weight and degree of ionization, fragment masses in Table 7 are considered for all 4 peptides. Calculated in Table 7 1042.88 m/z^{+2}, 695.25 m/z^{+3}, 521.44 m/z^{+4}, 417.15 m/z^{+5}, 347.63 m/z^{+6} fragments were detected. The molecular weight of 2085.75 m/z^{+1} was seen when the NET2 peptide was loaded at 1 mg / ml.

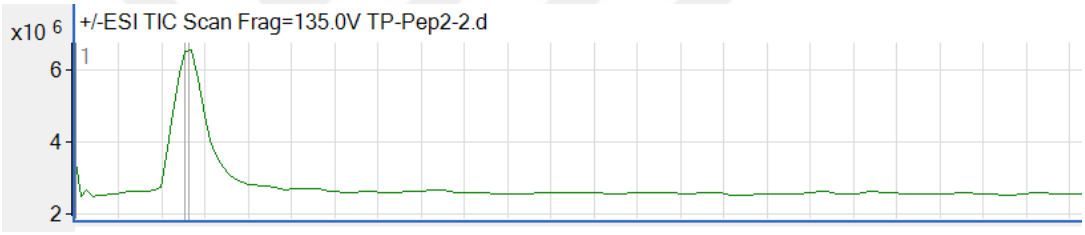

Figure 21. NET2 peak wiev 0.2 mg/ml

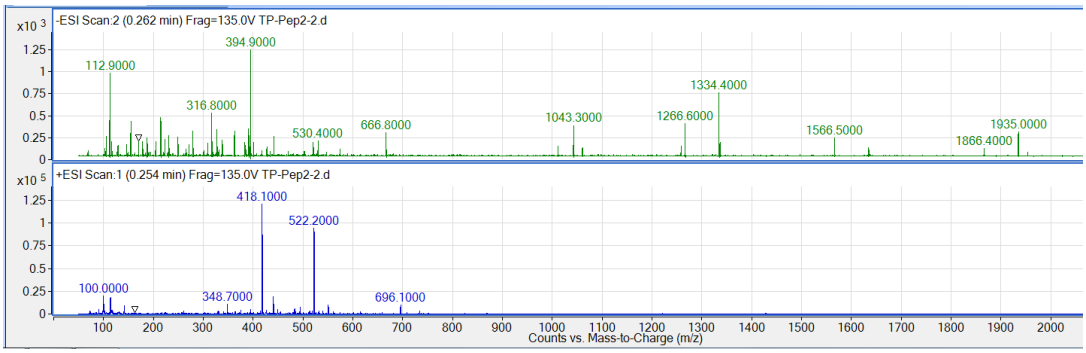

Figure 22. NET2 peak content

The peak of NET3 peptide in LC / MS can be seen in Figure 23. The peptide appears to be pure since the peak is sharp and unique. However, to understand whether this peak belongs to NET3 or not, the ionization - mass graph of the peak should be examined. Peak fragments of NET3 are seen in Figure 24. The mass values of the fragments match the mass values obtained by ionizing the peptide. Since all peptides have the same molecular weight and degree of ionization, fragment masses in Table 7. Calculated in Table 7 1042.88 m/z^{+2}, 695.25 m/z^{+3}, 521.44 m/z^{+4}, 417.15 m/z^{+5}, 347.63 m/z^{+6}, 260.72 m/z^{+8} fragments were detected. The molecular weight of 2085.75 m/z^{+1} was seen when the NET3 peptide was loaded at 1 mg / ml.

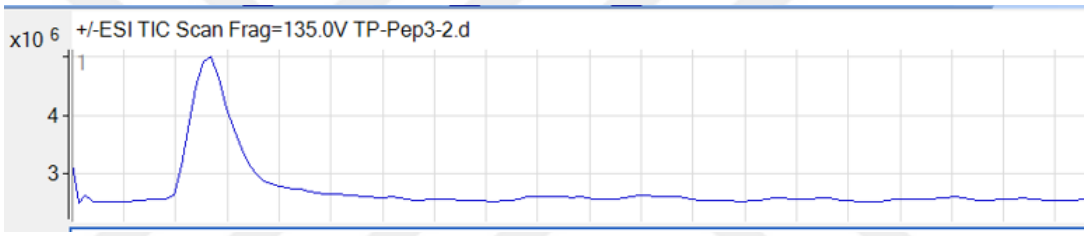

Figure 23.NET3 peak wiev 0.2 mg/ml

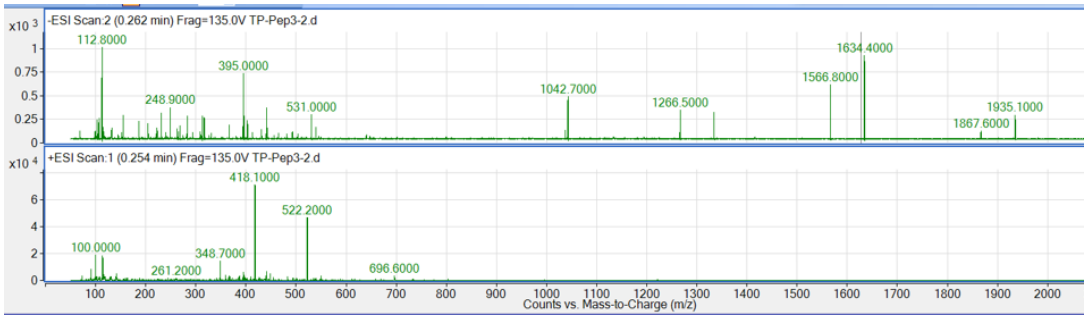

Figure 24. NET3 peak content

The peak of NET4 peptide in LC / MS can be seen in Figure 25. The peptide appears to be pure since the peak is sharp and unique. However, to understand whether this peak belongs to NET4 or not, the ionization - mass graph of the peak should be examined. Peak fragments of NET4 are seen in figure 26. The mass values of the fragments match the mass values obtained by ionizing the peptide. Since all peptides have the same molecular weight and degree of ionization, fragment masses in Table 7. Calculated in Table 7 1042.88 m/z^{+2}, 695.25 m/z^{+3}, 521.44 m/z^{+4}, 417.15 m/z^{+5}, 347.63 m/z^{+6}, 260.72 m/z^{+8} fragments were detected. The molecular weight of 2085.75 m/z^{+1} also was seen when the NET4 peptide was loaded at 0.2 mg/ml.

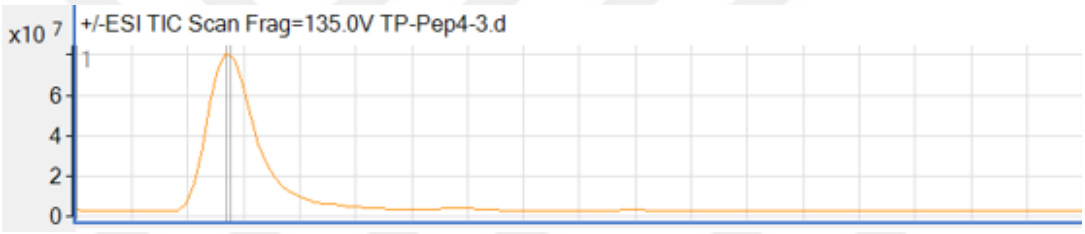

Figure 25. NET4 peak wiev 0.2 mg/ml

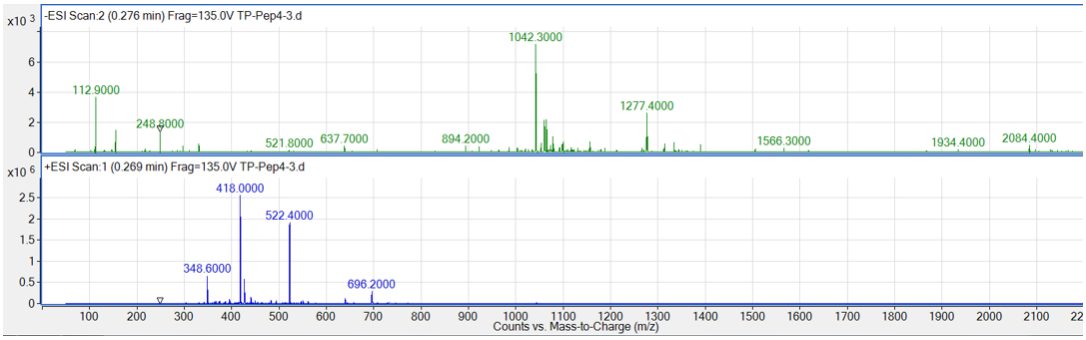

Figure 26. NET4 peak content

4.6. Detection of Antibacterial Activity (MIC)

The antibiogram result for 4 peptides on 5 bacterial strains are seen in Figure 27. It is observed that 4 peptides are effective on 5 bacteria at a concentration of 1 mg / ml with the zone they create (Figure 26). When the zone sizes are examined, we can comment that the zones belonging to the NET4 peptide remain smaller, so that it will have a lower antibacterial effect. In order to determine the minimum inhibition concentration of peptides with bactericidal action at 1 mg / ml, the MIC experiment was performed with serial dilution starting from 64 μg / ml.

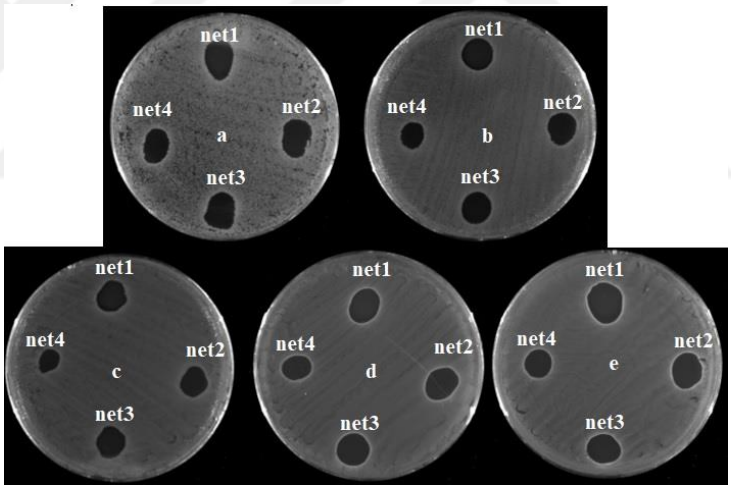

Figure 27. Antibiogram of 1 mg/ml NET1, NET2, NET3, NET4 peptides

on a) *E.coli ATCC25922 strain b) E.coli NTCC13846, c) S.aureus ATCC25923 c) S.aureus ATCC29213 d) S. aureus MRSA*

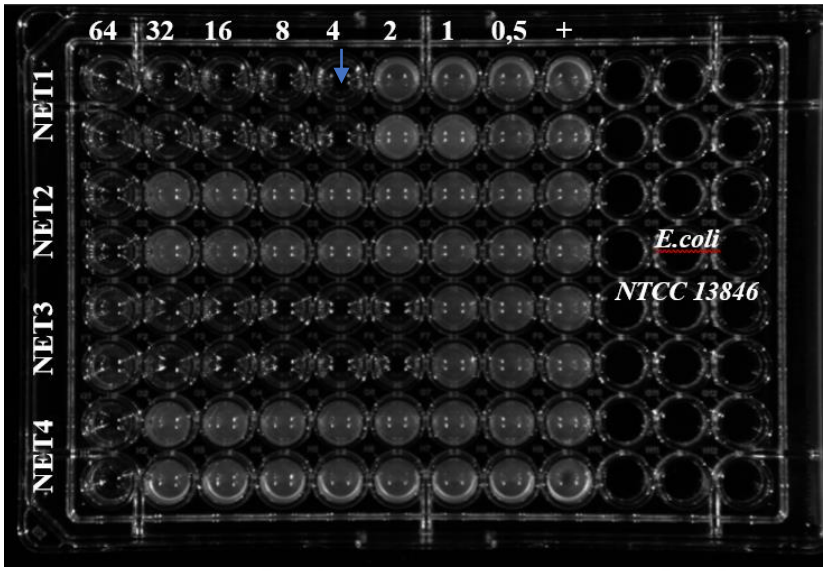

Figure 28. NET1, NET2, NET3, NET4 peptides MIC assay w/ E.coli NTCC 13846 epi -white chemidoc image

NET4 peptide serial dilution starting from 32 µg while other peptides starting from 64 µg concentration (Figure 28).

Table 9. MIC values of NET1, NET2, NET3, NET4 peptides

	NET1	**NET2**	**NET3**	**NET4**
E.coli ATCC 25922	2	64	4	8
S.aureus ATCC 25923	4	32	2	16
S.aureus MRSA	2	64	2	16
S.aureus 29213	2	64	2	16
E.coli NTCC13846	4	64	2	32

According to the results in Table 9, NET1 and NET3 peptides gave the best results (2-4 μg / ml), while NET2 and NET4 were effective generally more than 16 μg / ml.

4.7. SEM Images

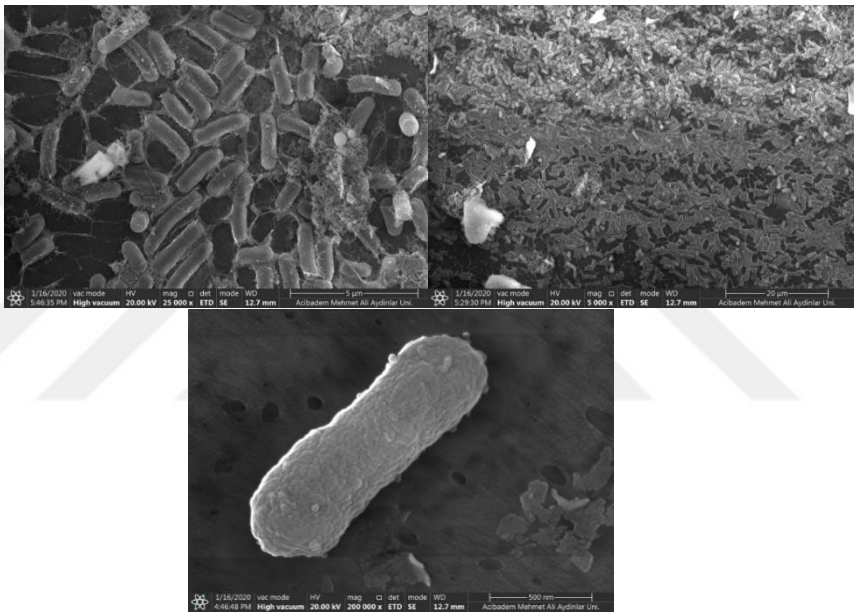

Figure 29. *E.coli* 5.000X, 25.000X, 200.000X SEM images

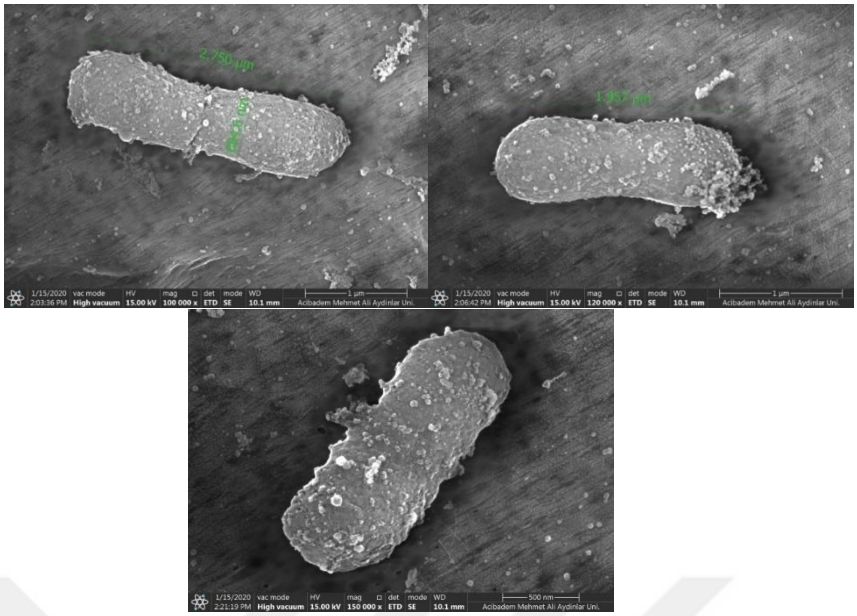

Figure 30. *E.coli* NET1 16 µg/ml 100.000X, 120.000X, 150.000X SEM images

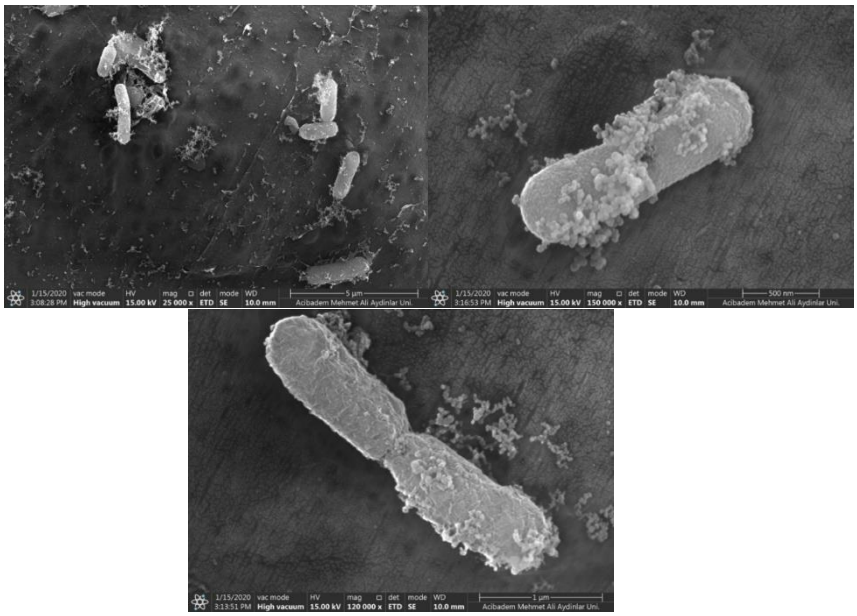

Figure 31. *E.coli* NET2 128 µg/ml 25.000X, 150.000X, 120.000X SEM images

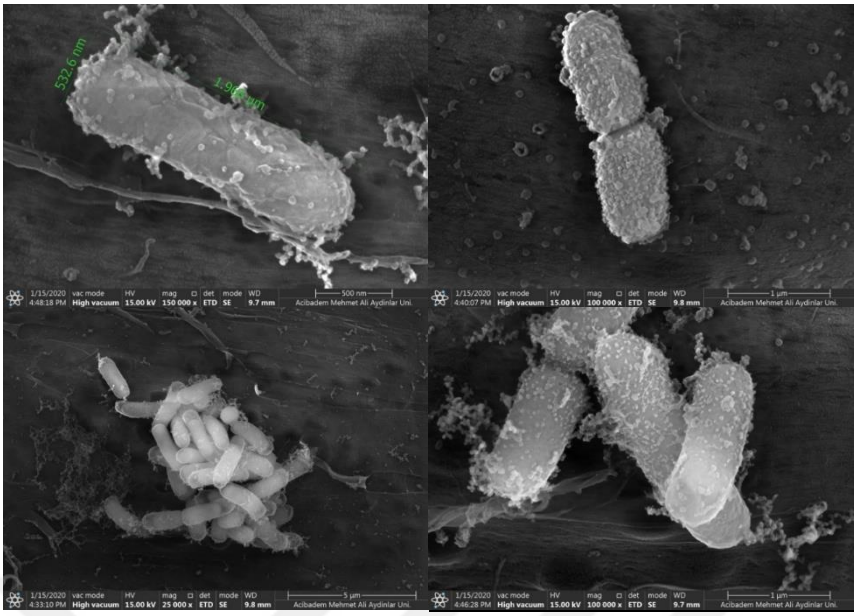

Figure 32. *E.coli* NET3 16 µg/ml 25.000X, 100.000X, 150..000X SEM images

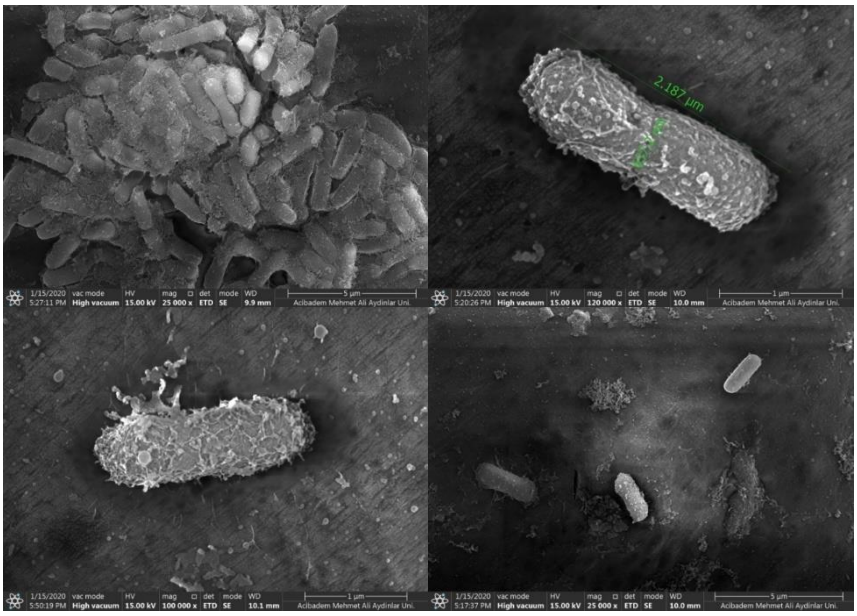

Figure 33. *E.coli* NET4 32 µg/ml 25.000X, 100.000X, 120.000X SEM images

When the taken images were examined, it was observed that *E.coli* used as a control had a smoother surface than those treated with peptides (Figure 29). In *E. coli* treated with peptide, it was observed that bubbles and holes were formed on the surfaces and the surface smoothness was lost (figure 30, figure 31, figure 32, figure 33). With the SEM image, it was observed that the peptides caused a change in the integrity of the membrane of *E.coli* bacteria.

4.8. Protease Resistant Assay

Four peptides synthesized in D and L form were used in protease resistance assays. The analytical HPLC examination results of the peptides after treated with proteinase K, comparing the D and L forms, are given in the following Figure 34, Figure 35, Figure 36, Figure 37. According to HPLC analysis, while NET2 peptide consisting of L-form aminocides was degraded, other peptides showed resistance against proteases.

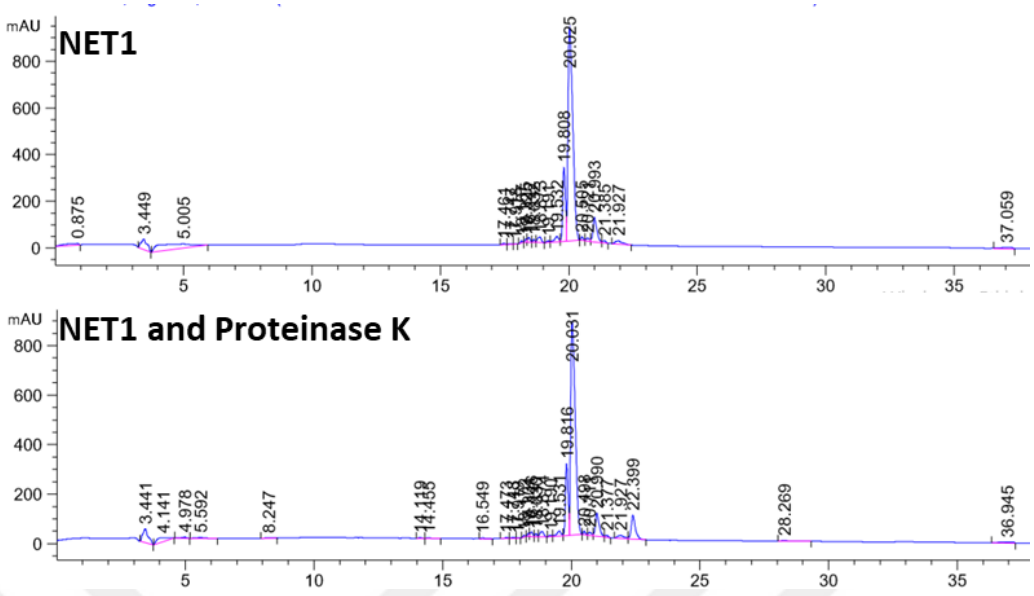

Figure 34. . NET1 peptide proteinase K assay HLC results

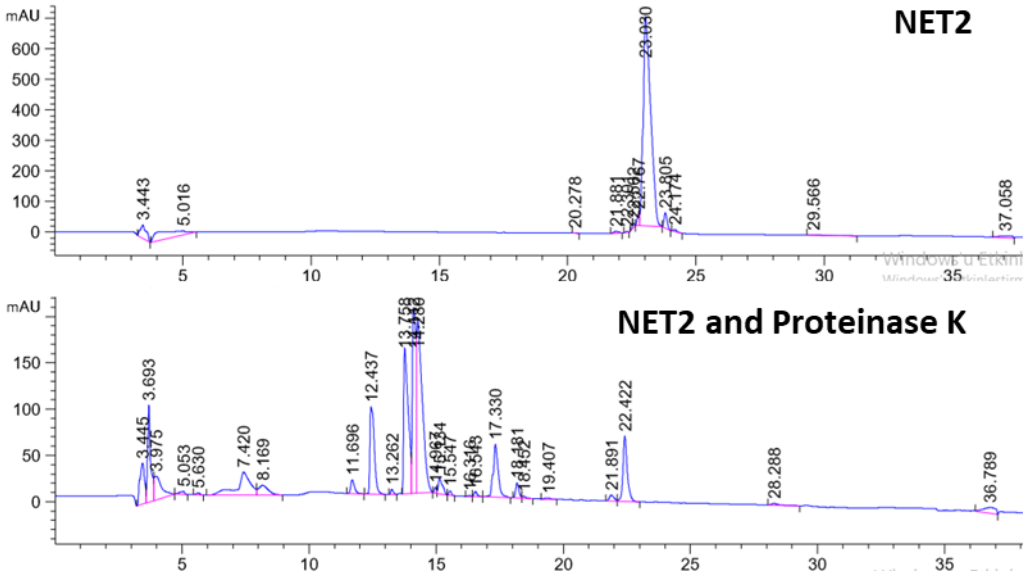

Figure 35. NET2 peptide proteinase K assay HLC results

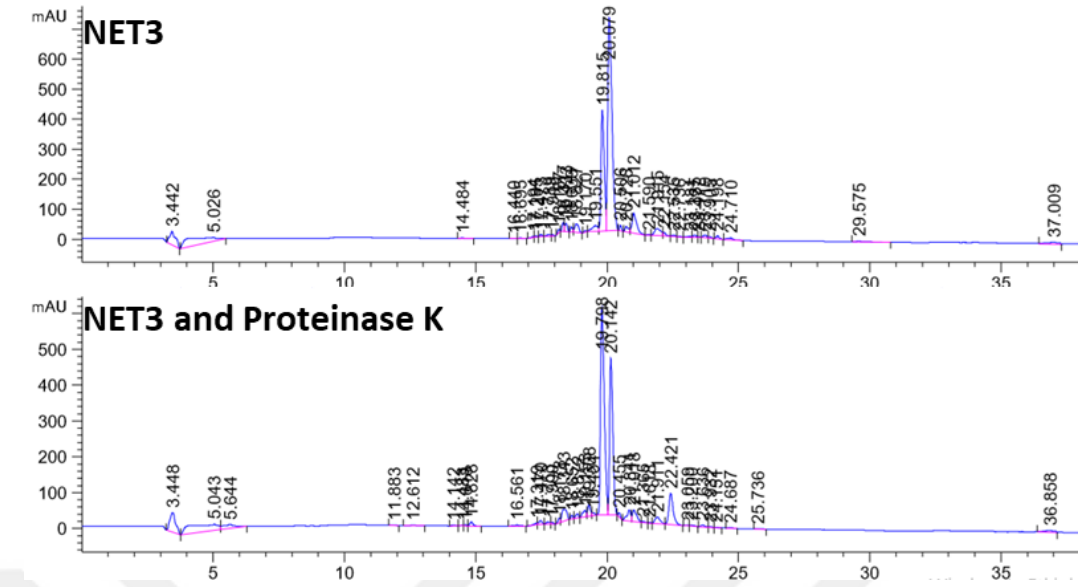

Figure 36. NET3 peptide proteinase K assay HLC results

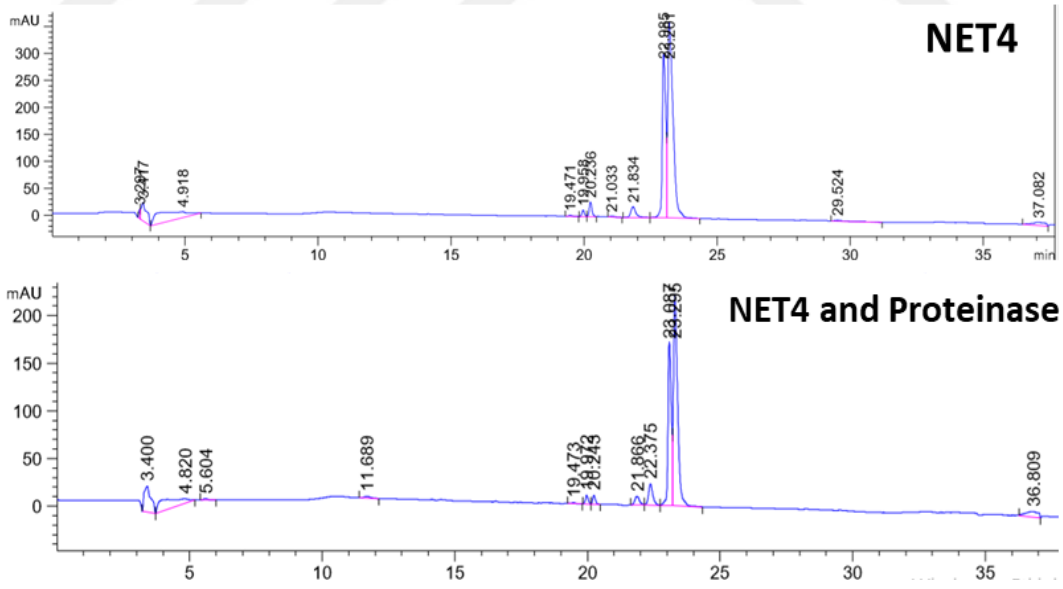

Figure 37. NET4 peptide proteinase K assay HLC results

4.9. Detection of Hemolysis

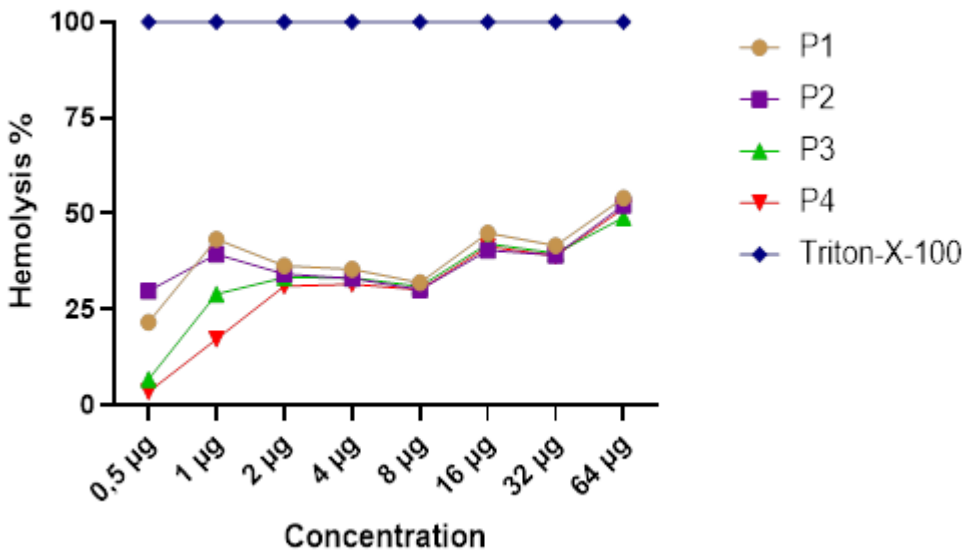

Figure 38. NET1, NET2, NET3, NET4 and Triton X-100 % lysis rates

Having checked the results, it is seen that the HC_{50} value of 3 peptides except NET3 peptide is 64 ug. However, even if the NET3 peptide does not exceed the HC_{50} value, it is very close. For NET1 and NET3 peptides, this concentration is 4-16 times the mic values, indicating that up to 4-16 times the mic values can be used for the antibacterial function of the peptides. In contrast, the NET2 peptide does not show hemolysis up to 4 times the mic values of *E.coli 25922* and *S.aureus 25923* strains, but causes hemolysis at the mic value required for resistant bacteria, is 64 µg. For NET4 peptide, since the minimum mic value is 2 and the maximum mic value is 32, it does not cause hemolysis up to 2-32 times.

4.10. Detection of Cytotoxicity

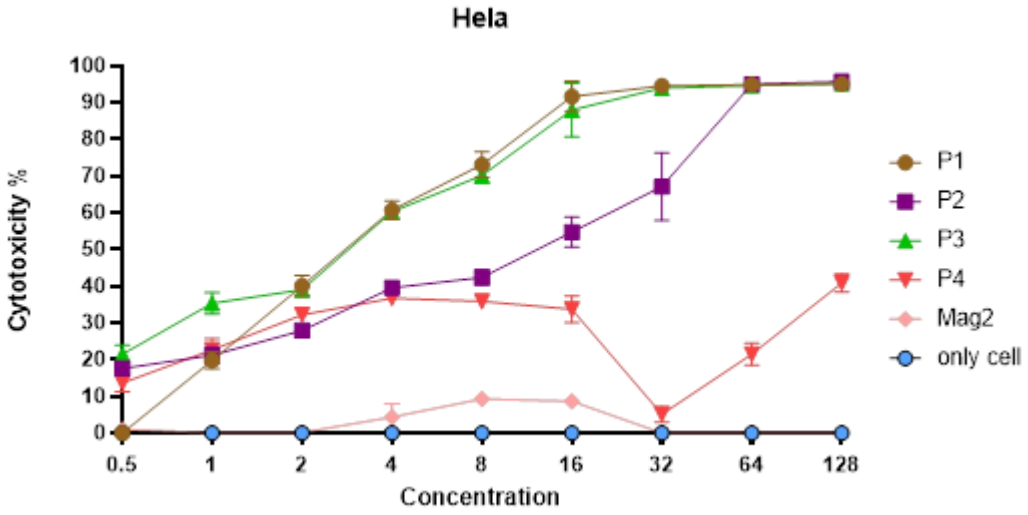

Figure 39. Cytotoxicity rates for NET1, NET2, NET3, NET4, Magainin 2 and only cell in Hela cell line

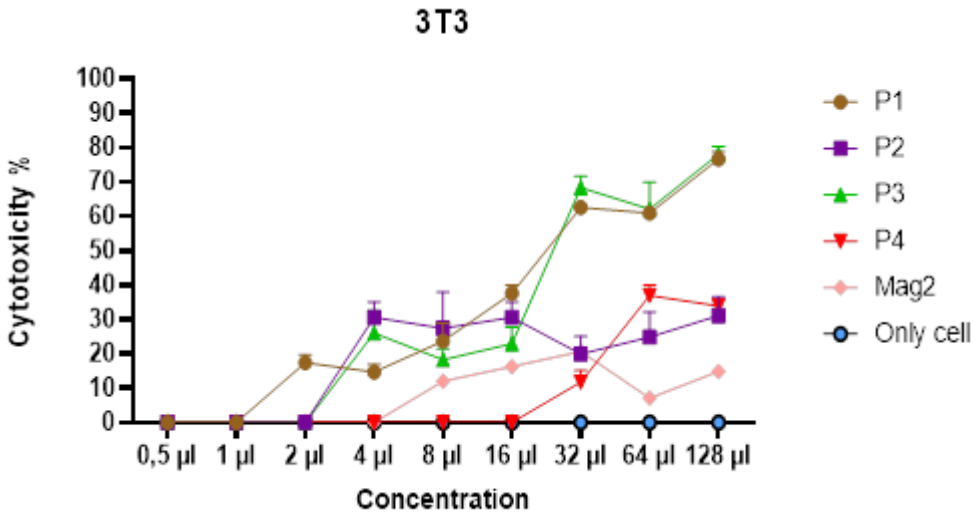

Figure 40. Cytotoxicity rates for NET1, NET2, NET3, NET4, Magainin 2 and only cell in 3T3 cell line

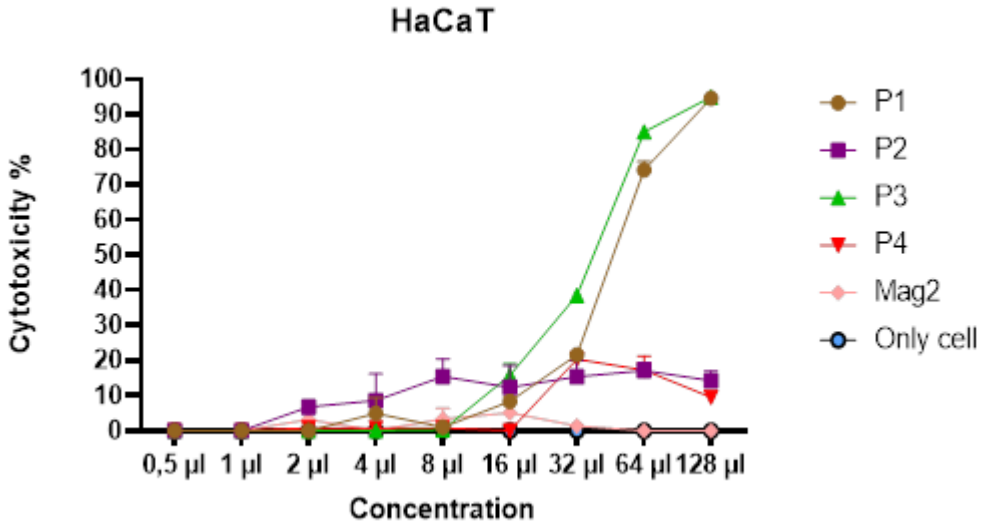

Figure 41. % Cytotoxicity rates for NET1, NET2, NET3, NET4, Magainin 2 and only cell in HaCaT cell line

When the results of peptides whose cytotoxicity rates were studied on 3 cell lines, it is seen that peptides create a cytotoxic effect at low concentrations on the toilet cancer cell. When looking at the IC_{50} values of peptides on the Hela cell line, it is seen that it is 4 µg for NET1, 16 µg for NET2, 4 µg for NET3 and 128 µg for NET4 (Figure 39). In the HaCaT cell line, it is seen that the IC_{50} values of the peptides are 64 µg for NET1, > 128 µg for NET2, 64 µg for NET3 and > 128 µg for NET4 (Figure 40). Finally, the IC_{50} values of peptides in the 3T3 fibroblast cell line appear to be 32 µg for NET1,> 128 µg for NET2, 32 µg for NET3, and > 128 µg for NET4 (Figure 41).

4.11. Detection of Minimum Biofilm Inhibition and Eradication

4.11.1 Minimum Biofilm Inhibiton Assay

It is aimed to inhibit the bacteria that are triggered to form biofilms with fructose added to the medium with peptides added to the medium. In parallel with the high mic values of NET2 and NET4 peptides, biofilm inhibition values are given in table 10. NET1 and NET3 peptides were also effective at low concentrations for biofilm inhibition.

Table 10. Minimum Biofilm Inhibition Values (ug/ml) by CV method

	**NET1**	**NET2**	**NET3**	**NET4**
E.coli ATCC 25922	4	128	8	16
S.aureus ATCC 25923	4	128	4	128
S.aureus MRSA	2	128	2	128
S.aureus 29213	2	128	2	128
E.coli NTCC13846	8	128	4	64

In addition to the biofilm inhibition experiment with CV, the Congo red broth method, which does not have any washing step and is based on the starting point of the biofilm was designed. For the optimization of this method, NaClO and

Ciproflaxaxin were used in the first step, and it was observed that there was a difference between the addition of antimicrobial agent at the stage of the planktonic stage and the addition of the biofilm at the starting point. Since it was observed that *S.aureus ATCC 29213* bacteria started biofilm formation at the starting concentration of 0.5 Mcfarland at the 8th hour, the antimicroial agent was added at the 7th hour (Figure 43). The results were also repeated with the CV to compare with the traditional method (Figure 44).

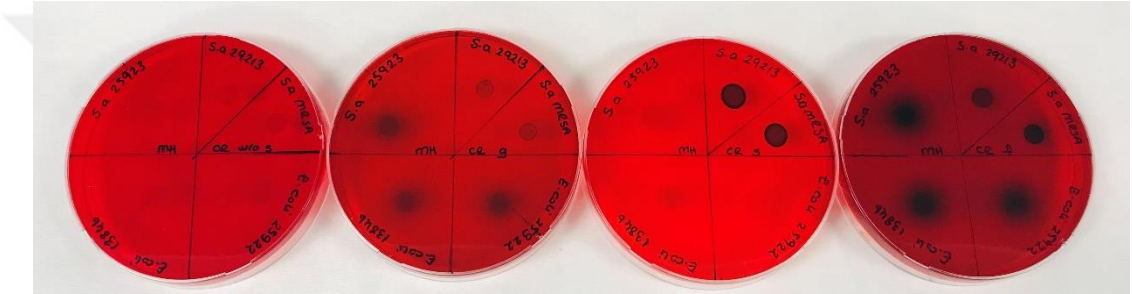

Figure 42. MHCRA black colony biofilm formation *S.aureus ATCC25923*, *S.aureus ATCC29213*, *S.aureus MRSA*, *E.coli ATCC25922*, *E.coli ATCC13846* bacteria strains on MHCR w/os, MHCR w/g, MHCR w/s, MHCR w/f

Table 12 shows the results obtained with the MHCRA method to determine the most suitable conditions for biofilm formation. According to this table, the carbon source that adapts to all bacteria for biofilm formation was determined as fructose.

Table 11. Dark sport formation on MHCRA with different carbon sources

MHB	w/o s	w/g	w/s	w/f
E.coli ATCC 25922	-	+	-	+
S.aureus ATCC 25923	-	-	+	+
S.aureus MRSA	-	-	+	+
S.aureus 29213	-	+	-	+
E.coli NTCC13846	-	+	-	+

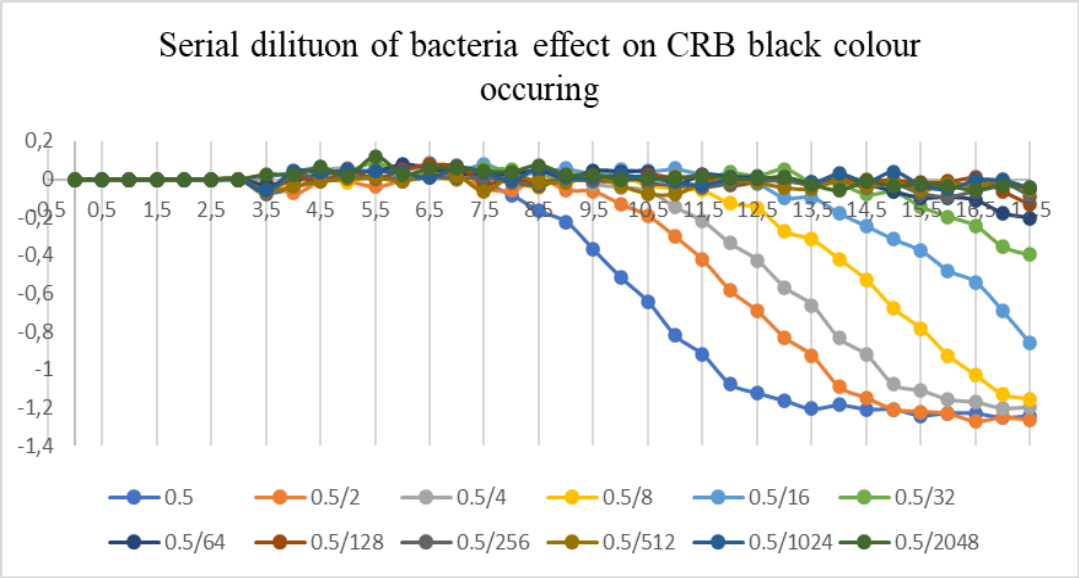

Figure 43. Serial dilituon of bacteria effect on CRB black colour occuring

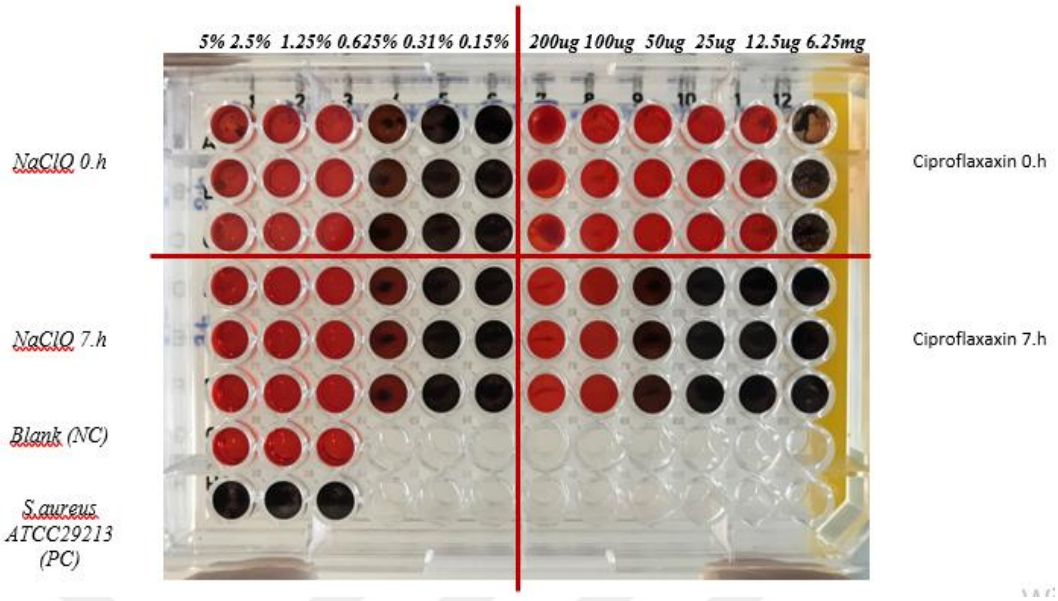

Figure 44. The NaClO and Ciproflaxxain treatment at 0. h and 7. hour by Congo red method

After this optimisations the congo red broth method was worked with four peptides. The real biofilm inhibition concentration results are given in Table 12. Comparint to this results with CV staining method, the four peptides MBIC values is so different from their MIC value unlike CV staining. Since the peptide added at the point of startin biofilm formation gave the beter reliable results than CV. At least bacterial growth was seen in the wells even not black coluor occurring, so that this method may be accepted as the method target specifically to biofil inhibisiton. Still the optimizations continue.

Table 12. Minimum Biofilm Inhibition Values (ug/ml) by CRB- MBIC method

	NET1	NET2	NET3	NET4
E.coli ATCC 25922	64	>256	128	>256
S.aureus ATCC 25923	64	>256	128	>256
S.aureus MRSA	64	>256	128	>256
S.aureus 29213	64	>256	128	>256
E.coli NTCC13846	64	>256	128	>256

4.11.2. Minimum Biofilm Eradication Assay

In the biofilm eradication assay performed to remove the biofilm from the environment after biofilm formation, it was observed that biofilm was removed at higher concentrations than the biofilm inhibition test. The results of biofilm eradication are given in Table 13.

Table 13. Minimum Biofilm Eradication Concentration (ug/ml) by CV method

	NET1	NET2	NET3	NET4
E.coli ATCC 25922	>128	>128	>128	>128
S.aureus ATCC 25923	>128	>128	>128	>128
S.aureus MRSA	>128	>128	>128	>128
S.aureus 29213	64	>128	128	>128
E.coli NTCC13846	>128	>128	>128	>128

4.12. Peptide Characterization and Self-assembly (FT-IR & SEM)

4.12.1. Peptide characterization

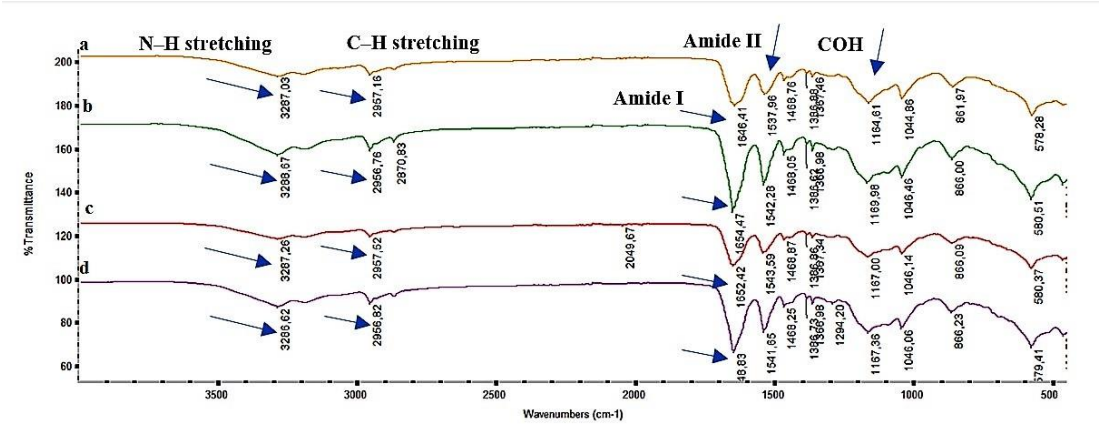

Figure 45. a) NET1 b) NET2 c) NET3 d) NET4 peptides FT-IR

Table 14. FT-IR wavenumbers and infrared peaks

Wavenumber cm^{-1}	**İnfrared Peaks**
~ 3286	Amide, N–H stretching
~ 2956	C–H stretching
~ 1680–1620	Amide I
~ 1580–1480	Amide II band (N–H bending vibration coupled with C–N stretching vibration
~ 1167	COH

4.11.2. Self-Assembly by Drip Method

4.12.2.1. Self-assembly by drip method at 25°C

When the self-assembly results of all 4 peptides were examined, a peak of the peptide was observed before washing which disappeared after washing (Figure 46). This indicates that the peptide powder remained on the catheter surface after the peptide solvent evaporated from the room, and the removal by washing indicates that the peptide was not adsorbed.

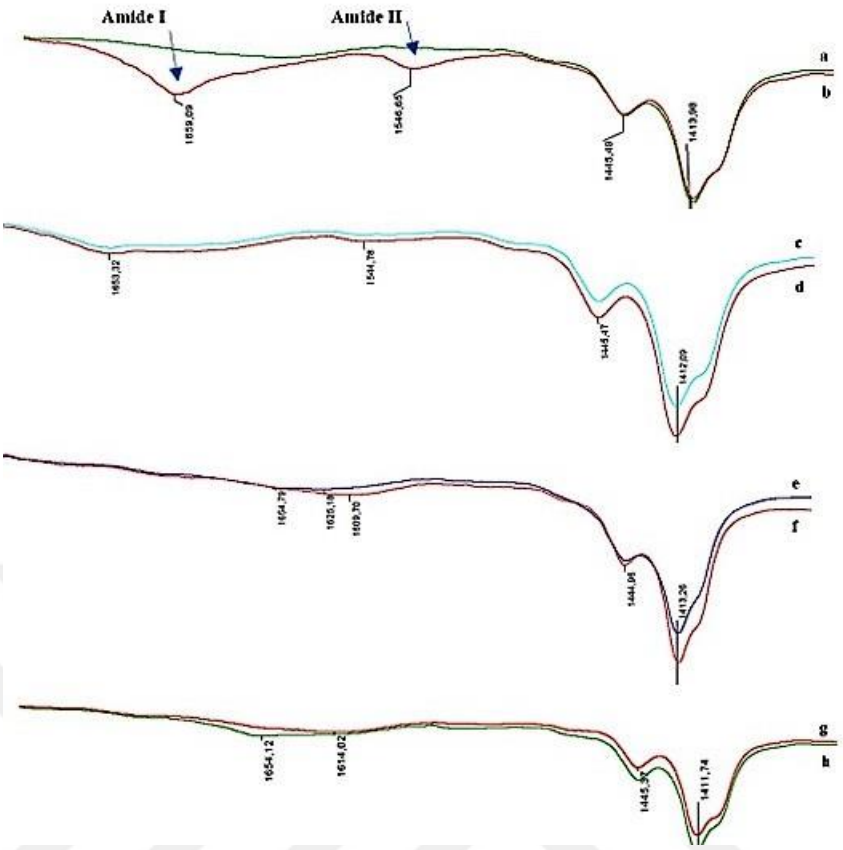

Figure 46. Peptide self-assembly on catheter at 25°C FT-IR results a) NET1 washed b) NET1 c) NET2 washed d) NET2 e) NET3 washed f) NET3 g) NET4 washed h) NET4

4.12.2.2. Self-assembly by drip method at 37°C

When the self-assembly results of all 4 peptides at 37°C were examined, a small peak of the peptide was observed before washing which disappeared after washing (Figure 47). This indicates that the peptide powder remained on the catheter surface after the peptide solvent evaporated from the room, and the removal by washing indicates that the peptide was not adsorbed.

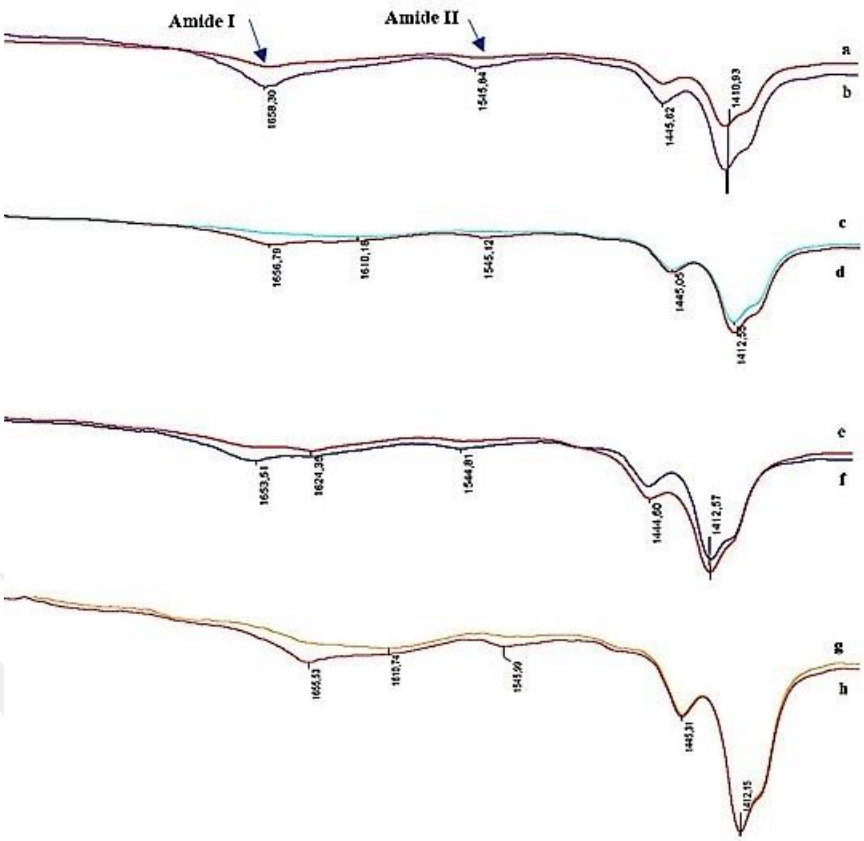

Figure 47. Peptide self-assembly on catheter at 37°C FT-IR results a) NET1 washed b) NET1 c) NET2 washed d) NET2 e) NET3 washed f) NET3 g) NET4 washed h) NET4

4.12.3. Self-assembly with soaking method in peptide solution

In order to test binding at higher concentrations, 6.4 mg / ml NET1 peptide was dropped on the catheter surface and incubated at 37 ° C. When the measurement was taken the next day, a significant peptide peak was burned. However, it was observed that the peak disappeared again after washing. This shows that the peptide does not have a self-assembly feature (Figure 50, Figure 51).

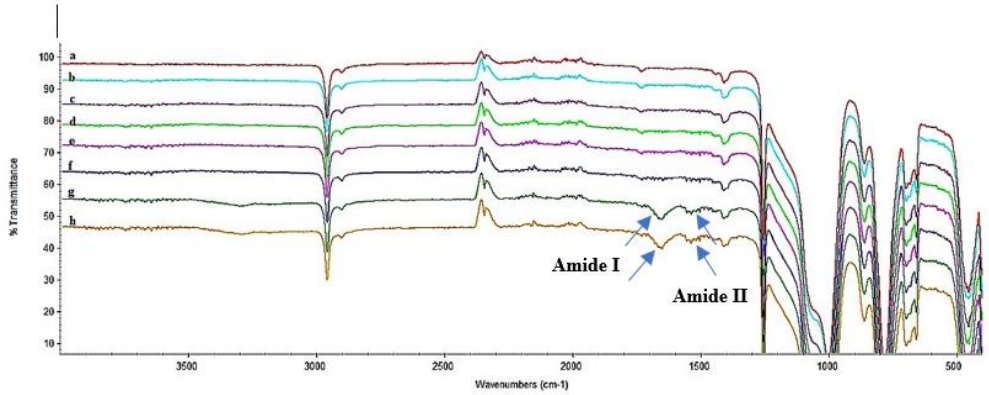

Figure 48. Self-assembly with soaking method in NET1 peptide solution at 37°C FT-IR results

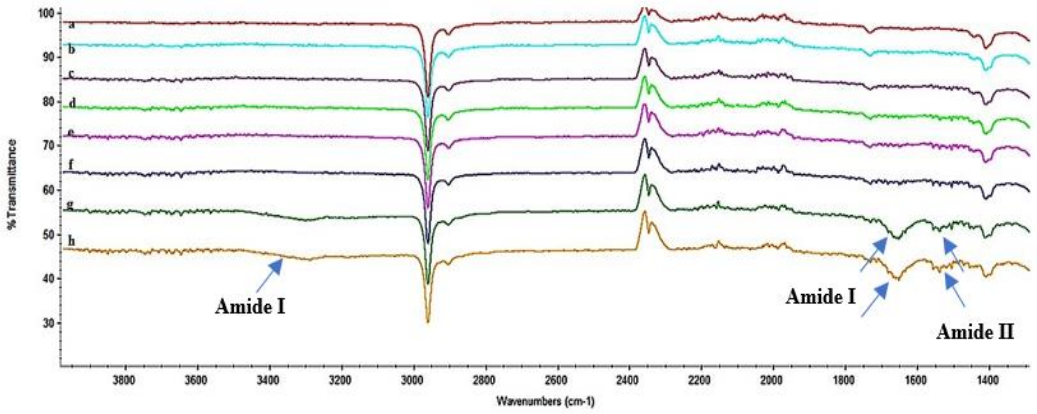

Figure 49. Self-assembly with soaking method in NET1 peptide solution at 37°C FT-IR results, zoom in Figure 48

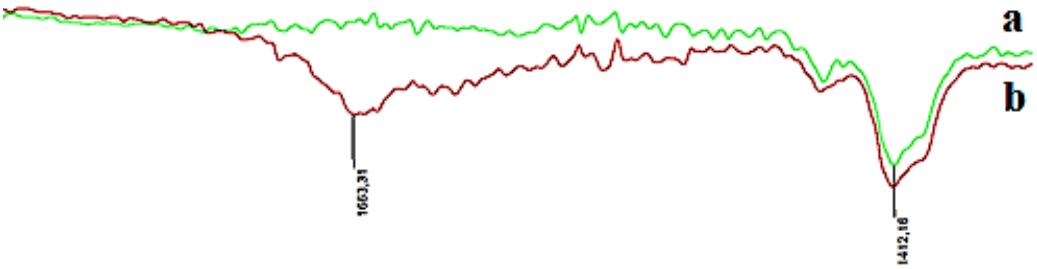

Figure 50. 6.4 mg/ml NET1 peptide self-assembly on catheter at 37°C a) NET1 washed b) NET1

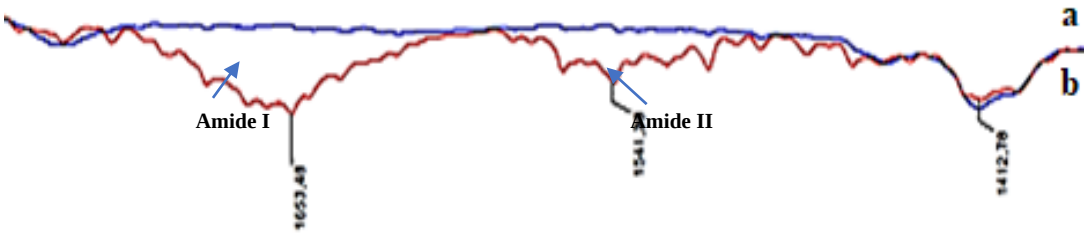

Figure 51. 10 mg/ml NET1 peptide self-assembly on catheter at 37°C a) NET1 washed b) NET1

4.12.4. Self-assembly EDS analysis

In the result analysis of the self-assembly experiment of 4 peptides to the silicon catheter surface, no numerical result was taken in FT-IR measurement, and a peak-based evaluation was attempted. Subsequently, the percentages of carbon (C),

nitrogen (N), oxygen (O), and silicon (Si) atoms on the catheter surface were calculated with the EDS analysis, which can give a more precise and numerical value. In the experiment, 4 peptides were tested at 25 ° C and 37 ° C, washed and unwashed, at 4 different conditions for each peptide. An empty catheter and an empty catheter washed with ACN were used as blanks. As the most important atom to be seen in these measurements is the nitrogen (N) atom, the adsorption rates of the peptide to the surface depending on the % change in the N atom were calculated. These rates are given in Table 15.

Table 15. EDS analytics based on N % to detect self-assembled peptide rate

		Percentage of peptide adsorbed (based on N %)	**The amount of peptide detached from the surface at 2 mg / ml**
25 ° C	NET1	40,56	1.20 mg /ml
	NET2	57,58	0,84 mg/ml
	NET3	38,64	1,22 mg/ml
	NET4	8,33	1,83 mg /ml
37 ° C	NET1	58,76	0,88 mg /ml
	NET2	31,39	1.37 mg /ml
	NET3	50,56	0,98 mg /ml
	NET4	52,92	0,94 mg /ml

5. DISCUSSION AND CONCULUSION

In this study, to create AMPs for biofilm-forming bacteria, we tried 4 peptides that have the same sequence with 2 amino acids combination of D- and L-forms. We tested the antibacterial activity, hemolytic activity, cytotoxicity rates in 3 different cell lines, both biofilm inhibition and biofilm eradication of these 4 peptides. After testing it in every aspect, we analyzed the effect of amino acid content on the behavior of the peptide. The use of amino acids in the D- and L- form resulted in good results of the peptide in some ways, while in others it had the opposite effect. Due to the presence of L-form amino acids in the human body, instead of using D-form amino acids, which we anticipate to have toxic effects on the entire peptide, we have turned to one of the two amino acids in its structure (NET1-NET3). Again, in line with our prediction, we synthesized a peptide made entirely of D-form (NET4). In addition to all these combinations, we also synthesized the peptide consisting entirely of L-form amino acids that can be synthesized in the body (NET2). Since D-form amino acids are not recognized by proteases, it also ensures that the peptide is resistant to proteases. In this peptide structure, we aimed to increase antimicrobial activity by using D form amino acids together with L form amino acids while also aiming to be resistant to proteases. As a result of the treatment of 4 peptides with Proteinase K, analytical HPLC analysis showed that the NET2 peptide consisting of full L form was cleaved, and NET1, NET3 and NET4 peptides containing at least one D form amino acid in their structure were resistant to protease.

Firstly, the MIC experiment was performed to compare peptides with the same sequence but different amino acid content in many ways. When looking at the data from the MIC experiment, the antibacterial effect was detected at low concentrations of NET1 and NET3 peptides in which the D and L form coexist, while the NET4 peptide consisting of the full D-form gave an average result among them. The NET2

peptide, which consists of full L-form, was the peptide with the lowest antibacterial effect. Based on this result, it has been observed that the combination of D and L form amino acids for this peptide sequence greatly enhances the antibacterial effect. We can predict that the change in the orientation of amino acids in the peptide structure contributes to the corkscrew-like structure in the increase of this effect. The change in the orientation of the branches of the peptide, which spirals due to its α-helix structure, increases the effective area of peptide branching, increasing the antibacterial effect of the peptide 8-16 times compared to the full D-form and 16-32 times compared to the full L-form. In the study by Takayuki Manabe and Kiyoshi Kawasaki (160), peptides in full L and full D form with the same sequence were synthesized, and the peptide consisting of D form amino acids were observed to have 16 times better activity in *S.aureus* bacteria and 2 times better in *E.coli* is shown. However, in the other 3 peptides used in the same study, the D and L forms showed equivalent antibacterial effects. In another study (192), the full L and full D form of LL-37 peptide were studied, and the activity of the D form was observed to be 10 times lower. As a result, there is no clear conclusion of whether form D or L form will work better.

A hemolytic activity assay was performed to determine whether peptides showing antibacterial effect at minimum 2, and maximum 64 μg cause degradation on human red blood cells, and if so, the concentration exceeding the HC_{50} value. According to this experiment, it was observed that the HC_{50} value of four peptides differing in mic values was 64 ug. Since this value is 16-32 times their own mic value for NET1 and NET3 peptides, the peptides remain in a safe range at the concentrations they exert an antibacterial effect. Since this HC_{50} value for NET2 peptide is 2-8 times the mic value, it can be said that it is in the safe range at its own mic value. However, for the NET4 peptide, the mic value in 4 out of 5 bacteria was determined as 64 μg, it seems that NET4 at the mic value corresponds to the HC_{50} value and it is not safe.

The cytotoxicity values of the peptides were then tested in 3 different cell lines. IC_{50} values were higher than expected for all 4 peptides in Hela cancer cell line. NET1 and NET3 peptides reached IC_{50} value in the Hela cell line at a concentration of 4 µg. In contrast to other healthy cell lines, it is desirable to determine the IC_{50} value at low concentrations in this cell line. The IC_{50} values of NET1 and NET3 peptides in HACAT and 3T3 cell lines, respectively, are 64 µg and 32 µg. It is desired that the IC50 value be high in these healthy cell lines, that is, the peptide does not create cytotoxic effects even at high concentrations. Since 64 and 32 µg concentrations are 16-32 times the mic values for both peptides, the peptides remain in the safe range in mic values in both cell lines. The IC_{50} value of the NET2 peptide is 16 µg in the Hela cell line, and > 128 µg in the HaCaT and 3T3 cell lines, respectively. It appears that it does not affect the cytotoxicity at > 2-4 times its mic value. NET4 peptide has IC50 values of 128µg, > 128µg, > 128µg in Hela, 3T3, and HaCaT cell lines, respectively.NET4 peptide does not show cytotoxic effect in all 3 cell lines at concentrations 4-16 times its own amount.

When looking at the biofilm inhibition and eradication experiments, it is seen that the MBIC and MBEC concentrations of the peptides change in parallel with the mic concentrations. While MBIC values remained the same as MIC values for NET3, MBIC values for NET1 increased twice the MIC values in 3 bacteria. MBIC values for NET2 peptide doubled in 4 of 5 bacteria tested, and increased 4 times in 1 bacterium. For the NET4 peptide, MBIC values increased 2 times the MIC value in 2 bacteria, 4 times the MIC value in two bacteria, and 2 times the MIC value in 1 bacteria. It appears that bacteria are more resistant to peptides in biofilm-forming conditions. During the literature review, the simultaneous addition of bacteria and peptide in biofilm inhibition study with the CV method and the difference of only 10-fold between the initial concentrations explains this difference between MBIC and MIC values. With the molecular modeling method, it is modeled that peptides show an antibacterial effect within nanoseconds. In addition, with SEM Imaging, it was reported that bacteria were damaged or killed after 3 hours of peptide treatment.

Based on these results, the idea that the peptide added simultaneously with the bacteria for the biofilm inhibition experiment kills the bacteria in the plantonic phase, and the bacteria that are not ready for biofilm formation are inhibited by stopping or slowing down bacterial growth. Based on this idea, the congo red broth method, which contains congo red dye that interacts with the secondary metabolite of c-di GMP and creates color change, has been developed. With this method, the bacteria are allowed to have the concentration that can form biofilms and the environment that the signal molecules contain, and the antimicrobial peptide added to the bacteria, which is ready for biofilm formation but not started, has been achieved with a true biofilm inhibition concentration. The MBIC results obtained in this experiment with the Congo red broth method were 64 µg for the NET1 peptide, 128 µg for the NET3 peptide, and > 256 for the NET2 and NET4 peptides. According to these results, NET1 peptide has the best MBIC value. Optimization studies of this method are ongoing.

When looking at the MBEC assay results, the biofilm eradication results of all peptides on 5 bacteria were 128µg or higher, while the concentration of NET1 peptide in *S.aureus 29213* was 64µg. NET1 peptide with D-leu in its structure disrupts the biofilm structure, which becomes difficult to remove after it has been formed, by showing better activity than NET3 peptide with D-arg in its structure. In the light of all this information, especially the bacterial strains that have strong biofilm formation ability and that are reference bacterial strains have been studied in this thesis. 4 peptides that show strong activity against biofilm-forming bacteria, and at the same time, the comparable difference in the amino acid content was synthesized. With the antibacterial activity experiment, which is the first step, it was determined that NET1 and NET3 peptides together with D- and L-form amino acids showed the best activity. Although the other 2 peptides had low antibacterial effects, they could not give better results than these two peptides in HC50 and IC50 values. The use of 2 different forms of amino acids together has allowed them to show stronger activity.

Some peptides, especially peptides with alpha-helix or beta-sheet structure and showing amphipathic properties, may exhibit the ability to hold between themselves and with the surface on which they are located. Self-assembly is called self-assembly without using any chemicals or linkers in the environment. Peptides showing sel-assembly are generally amphipathic in their structures by containing ionic and hydrophobic groups. In antimicrobial peptides, positively charged cationic amino acids such as R or K are preferred as the counterpart of these ionic amino acids (154). The reason for this is to maximize the peptide membrane interaction as mentioned in the previous titles. Besides the properties of the peptide, the ionic strength of the solvent and the peptide concentration also affect it. The excess of ionic power in the environment causes hydrogenation formation. For this, the reproduction of ionic and hydrophobic amino acid residues used in the structure of peptides in aqueous environment supports the formation of self-assembly (154). Whether the 4 peptides designed within the scope of this thesis have self-assembly properties were tested on the catheter surface. As a result, it was observed that peptides were not adsorbed on the catheter surface, and peptide piles that were seen before washing disappeared with washing. Chemical studies required to bind these AMPs to the catheter surface continue within the scope of the project. In the self-assembly study of peptides, the self-assembly results of peptides on the catheter surface were evaluated as a result of the EDS performed for quantitative analysis after FT-IR. In the light of these results, it was determined that the rate of binding of peptides on the surface varies. The point analysis of the EDS on the catheter surface and the different values obtained in the repeated measurements show that the peptides are not homogeneously distributed on the catheter surface. For this reason, in the calculation made with the average of the measurements taken, it was calculated that the peptides expected to bind for self assmbly were bound around 50%, and the NET4 peptide showed the lowest binding at 25 °C. Different solvents, temperature values or surface activation protocols can be tried to increase self-assembly productivity of the peptide.

6. REFERENCES

1. Ganz, T. ve Lehrer, R.I., (1999). "Antibiotic peptides from higher eukaryotes: biology and applications", Mol Med Today 5: 292-297. Antibiotic peptides from higher eukaryotes: biology and applications.

2. Mookherjee N, Anderson MA, Haagsman HP, Davidson DJ. Antimicrobial host defence peptides: functions and clinical potential. Nat Rev Drug Discov. 2020 May;19(5):311–32.

3. Nguyen LT, Haney EF, Vogel HJ. The expanding scope of antimicrobial peptide structures and their modes of action. Trends Biotechnol. 2011 Sep;29(9):464–72.

4. Malmsten M. Antimicrobial peptides. Ups J Med Sci. 2014 May;119(2):199–204.

5. Isidro-Llobet A, Alvarez M, Albericio F. Amino acid-protecting groups. Chem Rev. 2009 Jun;109(6):2455–504.

6. Cammue BP, De Bolle MF, Schoofs HM, Terras FR, Thevissen K, Osborn RW, et al. Gene-encoded antimicrobial peptides from plants. Ciba Found Symp. 1994;186:91–6.

7. Dürr UHN, Sudheendra US, Ramamoorthy A. LL-37, the only human member of the cathelicidin family of antimicrobial peptides. Biochim Biophys Acta. 2006 Sep;1758(9):1408–25.

8. Wang G. Human antimicrobial peptides and proteins. Pharmaceuticals (Basel). 2014 May;7(5):545–94.

9. Nissen-Meyer J, Nes IF. Ribosomally synthesized antimicrobial peptides: their function, structure, biogenesis, and mechanism of action. Arch Microbiol. 1997;167(2–3):67–77.

10. Guillier F, Orain D, Bradley M. Linkers and cleavage strategies in solid-phase organic synthesis and combinatorial chemistry. Chem Rev. 2000 Jun;100(6):2091–158.

11. Synthesizer CLBAMP. Liberty Blue^{TM} Automated Microwave Peptide Synthesizer. Available from: https://cem.com/en/liberty-blue

12. Hassan M, Kjos M, Nes IF, Diep DB, Lotfipour F. Natural antimicrobial peptides from bacteria: characteristics and potential applications to fight against antibiotic resistance. J Appl Microbiol. 2012 Oct;113(4):723–36.

13. Database AP. No Title [Internet]. Available from: http://aps.unmc.edu/AP

14. McDermott AM. Antimicrobial compounds in tears. Exp Eye Res. 2013 Dec;117:53–61.

15. Romeo D, Skerlavaj B, Bolognesi M, Gennaro R. Structure and bactericidal activity of an antibiotic dodecapeptide purified from bovine neutrophils. J Biol Chem. 1988 Jul;263(20):9573–5.

16. Gennaro R, Zanetti M. Structural features and biological activities of the cathelicidin-derived antimicrobial peptides. Biopolymers. 2000;55(1):31–49.

17. Johansson J, Gudmundsson GH, Rottenberg ME, Berndt KD, Agerberth B. Conformation-dependent antibacterial activity of the naturally occurring human peptide LL-37. J Biol Chem. 1998 Feb;273(6):3718–24.

18. Larrick JW, Lee J, Ma S, Li X, Francke U, Wright SC, et al. Structural, functional analysis and localization of the human CAP18 gene. FEBS Lett [Internet]. 1996;398(1):74–80. Available from: http://www.sciencedirect.com/science/article/pii/S0014579396011994

19. Kuroda K, Okumura K, Isogai H, Isogai E. The human cathelicidin antimicrobial peptide LL-37 and mimics are potential anticancer drugs. Front Oncol. 2015;5(JUN).

20. Xiao Y, Cai Y, Bommineni YR, Fernando SC, Prakash O, Gilliland SE, et al. Identification and functional characterization of three chicken cathelicidins with potent antimicrobial activity. J Biol Chem [Internet]. 2006;281(5):2858—2867. Available from: https://doi.org/10.1074/jbc.M507180200

21. Chang C-I, Pleguezuelos O, Zhang Y-A, Zou J, Secombes CJ. Identification of a Novel Cathelicidin Gene in the Rainbow Trout, Oncorhynchus mykiss Infect Immun [Internet]. 2005 Aug 1;73(8):5053 LP – 5064. Available from: http://iai.asm.org/content/73/8/5053.abstract

22. Papagianni M. Ribosomally synthesized peptides with antimicrobial properties: biosynthesis, structure, function, and applications. Biotechnol Adv. 2003 Sep;21(6):465–99.

23. Cole AM, Wang W, Waring AJ, Lehrer RI. Retrocyclins: using past as prologue. Curr Protein Pept Sci. 2004 Oct;5(5):373–81.

24. Selsted ME, Harwig SS, Ganz T, Schilling JW, Lehrer RI. Primary structures of three human neutrophil defensins. J Clin Invest. 1985 Oct;76(4):1436–9.

2**5.** Zhao C, Wang I, Lehrer RI. Widespread expression of beta-defensin hBD-1 in human secretory glands and epithelial cells. FEBS Lett [Internet]. 1996;396(2–3):319—322. Available from: https://doi.org/10.1016/0014-5793(96)01123-4

26. Harwig SS, Swiderek KM, Kokryakov VN, Tan L, Lee TD, Panyutich EA, et al. Gallinacins: cysteine-rich antimicrobial peptides of chicken leukocytes. FEBS Lett. 1994 Apr;342(3):281–5.

27. Bevins CL. Antimicrobial peptides as agents of mucosal immunity. Ciba Found Symp. 1994;186:250–9.

28. Hajishengallis G, Russell MW. Chapter 15 - Innate Humoral Defense Factors.

In: Mestecky J, Strober W, Russell MW, Kelsall BL, Cheroutre H, Lambrecht BN, editors. Mucosal Immunology (Fourth Edition) [Internet]. Fourth Edi. Boston: Academic Press; 2015. p. 251–70. Available from: http://www.sciencedirect.com/science/article/pii/B978012415847400015X

29. vanderSpek JC, Wyandt HE, Skare JC, Milunsky A, Oppenheim FG, Troxler RF. Localization of the genes for histatins to human chromosome 4q13 and tissue distribution of the mRNAs. Am J Hum Genet. 1989 Sep;45(3):381–7.

30. Rieg S, Saborowski V, Kern W V, Jonas D, Bruckner-Tuderman L, Hofmann SC. Expression of the sweat-derived innate defence antimicrobial peptide dermcidin is not impaired in Staphylococcus aureus colonization or recurrent skin infections. Clin Exp Dermatol. 2014 Mar;39(2):209–12.

31. Nawrot R, Barylski J, Nowicki G, Broniarczyk J, Buchwald W, Goździcka-Józefiak A. Plant antimicrobial peptides. Folia Microbiol (Praha). 2014 May;59(3):181–96.

32. Rivas L, Luque-Ortega RJ, Fernandez-Reyes M, Andreu D. Membrane-active peptides as anti-infectious agents. J Appl Biomed [Internet]. 2010;8(3):159–67. Available from: https://jab.zsf.jcu.cz/artkey/jab-201003-0005.php

33. Montesinos E. Antimicrobial peptides and plant disease control. FEMS Microbiol Lett [Internet]. 2007 May 1;270(1):1–11. Available from: https://doi.org/10.1111/j.1574-6968.2007.00683.x

34. Barbosa Pelegrini P, Del Sarto RP, Silva ON, Franco OL, Grossi-de-Sa MF. Antibacterial peptides from plants: what they are and how they probably work. Biochem Res Int. 2011;2011:250349.

35. Majewski J, Stec B. X-ray scattering studies of model lipid membrane interacting with purothionin provide support for a previously proposed mechanism of membrane lysis. Eur Biophys J. 2010;39(8):1155–65.

36. Fernandez de Caleya R, Gonzalez-Pascual B, García-Olmedo F, Carbonero P. Susceptibility of phytopathogenic bacteria to wheat purothionins in vitro. Appl Microbiol. 1972 May;23(5):998–1000.

37. Oard S, Rush MC, Oard JH. Characterization of antimicrobial peptides against a US strain of the rice pathogen Rhizoctonia solani. J Appl Microbiol [Internet]. 2004;97(1):169–80. Available from: https://sfamjournals.onlinelibrary.wiley.com/doi/abs/10.1111/j.1365-2672.2004.02291.x

38. Xu X, Lai R. The chemistry and biological activities of peptides from amphibian skin secretions. Chem Rev. 2015 Feb;115(4):1760–846.

39. Holthausen DJ, Lee SH, Kumar VT, Bouvier NM, Krammer F, Ellebedy AH, et al. An Amphibian Host Defense Peptide Is Virucidal for Human H1 Hemagglutinin-Bearing Influenza Viruses. Immunity. 2017 Apr;46(4):587–95.

40. Halverson T, Basir YJ, Knoop FC, Conlon JM. Purification and

characterization of antimicrobial peptides from the skin of the North American green frog Rana clamitans. Peptides. 2000 Apr;21(4):469–76.

41. Steinborner ST, Currie GJ, Bowie JH, Wallace JC, Tyler MJ. New antibiotic caerin 1 peptides from the skin secretion of the Australian tree frog Litoria chloris. Comparison of the activities of the caerin 1 peptides from the genus Litoria. J Pept Res. 1998 Feb;51(2):121–6.

42. Zasloff M. Magainins, a class of antimicrobial peptides from Xenopus skin: isolation, characterization of two active forms, and partial cDNA sequence of a precursor. Proc Natl Acad Sci U S A. 1987 Aug;84(15):5449–53.

43. Conlon JM, Kolodziejek J, Nowotny N. Antimicrobial peptides from the skins of North American frogs. Biochim Biophys Acta - Biomembr [Internet]. 2009;1788(8):1556–63. Available from: http://www.sciencedirect.com/science/article/pii/S0005273608003118

44. Conlon JM, Kolodziejek J, Nowotny N. Antimicrobial peptides from ranid frogs: taxonomic and phylogenetic markers and a potential source of new therapeutic agents. Biochim Biophys Acta. 2004 Jan;1696(1):1–14.

45. Haney EF, Hunter HN, Matsuzaki K, Vogel HJ. Solution NMR studies of amphibian antimicrobial peptides: linking structure to function? Biochim Biophys Acta. 2009 Aug;1788(8):1639–55.

46. Kang S-J, Son W-S, Han K-D, Mishig-Ochir T, Kim D-W, Kim J-I, et al. Solution structure of antimicrobial peptide esculentin-1c from skin secretion of Rana esculenta. Mol Cells. 2010 Nov;30(5):435–41.

47. Simmaco M, Mignogna G, Barra D, Bossa F. Antimicrobial peptides from skin secretions of Rana esculenta. Molecular cloning of cDNAs encoding esculentin and brevinins and isolation of new active peptides. J Biol Chem. 1994 Apr;269(16):11956–61.

48. Marenah L, Flatt PR, Orr DF, Shaw C, Abdel-Wahab YHA. Skin secretions of Rana saharica frogs reveal antimicrobial peptides esculentins-1 and -1B and brevinins-1E and -2EC with novel insulin releasing activity. J Endocrinol. 2006 Jan;188(1):1–9.

49. Patocka J, Nepovimova E, Klimova B, Wu Q, Kuca K. Antimicrobial Peptides: Amphibian Host Defense Peptides. Curr Med Chem. 2019;26(32):5924–46.

50. Martinez B, Rodriguez A, Suárez E. Antimicrobial Peptides Produced by Bacteria: The Bacteriocins. In 2016. p. 15–38.

51. Perez RH, Zendo T, Sonomoto K. Novel bacteriocins from lactic acid bacteria (LAB): various structures and applications. Microb Cell Fact. 2014 Aug;13 Suppl 1(Suppl 1):S3.

52. Cotter PD, Ross RP, Hill C. Bacteriocins - a viable alternative to antibiotics? Nat Rev Microbiol. 2013 Feb;11(2):95–105.

53. Diaz M, Valdivia E, Martínez-Bueno M, Fernández M, Soler-González AS,

Ramírez-Rodrigo H, et al. Characterization of a new operon, as-48EFGH, from the as-48 gene cluster involved in immunity to enterocin AS-48. Appl Environ Microbiol. 2003 Feb;69(2):1229–36.

54. Nissen-Meyer J, Rogne P, Oppegård C, Haugen HS, Kristiansen PE. Structure-function relationships of the non-lanthionine-containing peptide (class II) bacteriocins produced by gram-positive bacteria. Curr Pharm Biotechnol. 2009 Jan;10(1):19–37.

55. Maldonado-Barragán A, Cárdenas N, Martínez B, Ruiz-Barba JL, Fernández-Garayzábal JF, Rodríguez JM, et al. Garvicin A, a novel class IId bacteriocin from Lactococcus garvieae that inhibits septum formation in L. garvieae strains. Appl Environ Microbiol. 2013 Jul;79(14):4336–46.

56. Oppenheim JJ, Biragyn A, Kwak LW, Yang D. Roles of antimicrobial peptides such as defensins in innate and adaptive immunity. Ann Rheum Dis. 2003 Nov;62 Suppl 2(Suppl 2):ii17-21.

57. Corrales-Garcia LL, Possani LD, Corzo G. Expression systems of human β-defensins: vectors, purification and biological activities. Amino Acids. 2011 Jan;40(1):5–13.

58. Jarczak J, Kościuczuk EM, Lisowski P, Strzałkowska N, Jóźwik A, Horbańczuk J, et al. Defensins: natural component of human innate immunity. Hum Immunol. 2013 Sep;74(9):1069–79.

59. Kountouras J, Deretzi G, Gavalas E, Zavos C, Polyzos SA, Kazakos E, et al. A proposed role of human defensins in Helicobacter pylori-related neurodegenerative disorders. Med Hypotheses. 2014 Mar;82(3):368–73.

60. Srinivasan DK, Ojo OO, Owolabi BO, Conlon JM, Flatt PR, Abdel-Wahab YHA. [I10W]tigerinin-1R enhances both insulin sensitivity and pancreatic beta cell function and decreases adiposity and plasma triglycerides in high-fat mice. Acta Diabetol [Internet]. 2016;53(2):303–15. Available from: https://doi.org/10.1007/s00592-015-0783-3

61. Panteleev P V, Bolosov IA, Balandin S V, Ovchinnikova T V. Structure and Biological Functions of β-Hairpin Antimicrobial Peptides. Acta Naturae. 2015;7(1):37–47.

62. Reinholz M, Ruzicka T, Schauber J. Cathelicidin LL-37: an antimicrobial peptide with a role in inflammatory skin disease. Ann Dermatol. 2012 May;24(2):126–35.

63. Sengupta D, Leontiadou H, Mark AE, Marrink S-J. Toroidal pores formed by antimicrobial peptides show significant disorder. Biochim Biophys Acta - Biomembr [Internet]. 2008;1778(10):2308–17. Available from: http://www.sciencedirect.com/science/article/pii/S0005273608001764

64. Antibiotic peptides from higher eukaryotes: biology and applications.

65. Hancock RE, Diamond G. The role of cationic antimicrobial peptides in innate host defences. Trends Microbiol. 2000 Sep;8(9):402–10.

66. L.B. Charles GD. Mammalian Antimicrobial Peptides. In: Peptides Antibiotics Discovery, Modes of Action and Aplications. 2002. p. 145–92.

67. Pag, U. ve Sahl H. Lanthionine-Containing Bacterial Peptides. In: Peptide Antibiotics Discovery, Modes of Action and Aplications. 2002. p. 47–80.

68. Nes, I.F., Holo, H., Fimland, G., Hauge, H.H., ve Meyer JN. Unmodified Peptide-Bacteriocins (Class II) Produced by Lactic Acid Bacteria. In: Peptide Antibiotics Discovery, Modes of Action and Aplication. 2002. p. 81–116.

69. Taber HW. Introduction to the Peptide Antibiotics. In: Peptide Antibiotics Discovery, Modes of Action and Aplication. 2002.

70. Pelegrini PB, Franco OL. Plant gamma-thionins: novel insights on the mechanism of action of a multi-functional class of defense proteins. Int J Biochem Cell Biol. 2005 Nov;37(11):2239–53.

71. Poon IK, Baxter AA, Lay FT, Mills GD, Adda CG, Payne JA, et al. Phosphoinositide-mediated oligomerization of a defensin induces cell lysis. Elife. 2014 Apr;3:e01808.

72. Lee C-C, Sun Y, Qian S, Huang HW. Transmembrane pores formed by human antimicrobial peptide LL-37. Biophys J. 2011 Apr;100(7):1688–96.

73. Wang G, Mishra B, Epand RF, Epand RM. High-quality 3D structures shine light on antibacterial, anti-biofilm and antiviral activities of human cathelicidin LL-37 and its fragments. Biochim Biophys Acta. 2014 Sep;1838(9):2160–72.

74. Stewart SE, Kondos SC, Matthews AY, D'Angelo ME, Dunstone MA, Whisstock JC, et al. The perforin pore facilitates the delivery of cationic cargos. J Biol Chem. 2014 Mar;289(13):9172–81.

75. Segev-Zarko L, Saar-Dover R, Brumfeld V, Mangoni ML, Shai Y. Mechanisms of biofilm inhibition and degradation by antimicrobial peptides. Biochem J. 2015 Jun;468(2):259–70.

76. Brogden KA. Antimicrobial peptides: pore formers or metabolic inhibitors in bacteria? Nat Rev Microbiol. 2005 Mar;3(3):238–50.

77. Nyberg P, Rasmussen M, Björck L. alpha2-Macroglobulin-proteinase complexes protect Streptococcus pyogenes from killing by the antimicrobial peptide LL-37. J Biol Chem. 2004 Dec;279(51):52820–3.

78. Sieprawska-Lupa M, Mydel P, Krawczyk K, Wójcik K, Puklo M, Lupa B, et al. Degradation of human antimicrobial peptide LL-37 by Staphylococcus aureus-derived proteinases. Antimicrob Agents Chemother. 2004 Dec;48(12):4673–9.

79. Galván EM, Lasaro MAS, Schifferli DM. Capsular antigen fraction 1 and Pla modulate the susceptibility of Yersinia pestis to pulmonary antimicrobial peptides such as cathelicidin. Infect Immun. 2008 Apr;76(4):1456–64.

80. Joo H-S, Fu C-I, Otto M. Bacterial strategies of resistance to antimicrobial

peptides. Philos Trans R Soc London Ser B, Biol Sci. 2016 May;371(1695).

81. Jin T, Bokarewa M, Foster T, Mitchell J, Higgins J, Tarkowski A. Staphylococcus aureus resists human defensins by production of staphylokinase, a novel bacterial evasion mechanism. J Immunol. 2004 Jan;172(2):1169–76.

82. Otto M. Bacterial evasion of antimicrobial peptides by biofilm formation. Curr Top Microbiol Immunol. 2006;306:251–8.

83. Otto M. Molecular basis of Staphylococcus epidermidis infections. Semin Immunopathol. 2012 Mar;34(2):201–14.

84. Vuong C, Voyich JM, Fischer ER, Braughton KR, Whitney AR, DeLeo FR, et al. Polysaccharide intercellular adhesin (PIA) protects Staphylococcus epidermidis against major components of the human innate immune system. Cell Microbiol. 2004 Mar;6(3):269–75.

85. Cole JN, Pence MA, von Köckritz-Blickwede M, Hollands A, Gallo RL, Walker MJ, et al. M protein and hyaluronic acid capsule are essential for in vivo selection of covRS mutations characteristic of invasive serotype M1T1 group A Streptococcus. MBio. 2010 Aug;1(4).

86. Ogunleye A, Bhat A, Irorere VU, Hill D, Williams C, Radecka I. Poly-γ-glutamic acid: production, properties and applications. Microbiology. 2015 Jan;161(Pt 1):1–17.

87. Batoni G, Maisetta G, Brancatisano FL, Esin S, Campa M. Use of antimicrobial peptides against microbial biofilms: advantages and limits. Curr Med Chem. 2011;18(2):256–79.

88. Strempel N, Strehmel J, Overhage J. Potential application of antimicrobial peptides in the treatment of bacterial biofilm infections. Curr Pharm Des. 2015;21(1):67–84.

89. Di Luca M, Maccari G, Nifosì R. Treatment of microbial biofilms in the post-antibiotic era: prophylactic and therapeutic use of antimicrobial peptides and their design by bioinformatics tools. Pathog Dis. 2014 Apr;70(3):257–70.

90. Revilla-Guarinos A, Gebhard S, Alcántara C, Staron A, Mascher T, Zúñiga M. Characterization of a regulatory network of peptide antibiotic detoxification modules in Lactobacillus casei BL23. Appl Environ Microbiol. 2013 May;79(10):3160–70.

91. Leach AR. Molecular Modelling: Principles and Applications. 2001.

92. Allen, M.P. ve Tildesley DJ. Computer Simulation of Liquids, Oxford. 1990.

93. Monasse B. Description of a Molecular Dynamics Simulation System - AA Scale - Description of a Molecular Dynamics Simulation System - AA Scale - HAL Id : hal-00773174. 2015.

94. Hockney, R.W. ve Eastwood JW. Computer simulations using particles. : Bristol. 1988.

95. Karatan E, Watnick P. Signals, regulatory networks, and materials that build and break bacterial biofilms. Microbiol Mol Biol Rev. 2009 Jun;73(2):310–47.

96. López D, Vlamakis H, Kolter R. Biofilms. Cold Spring Harb Perspect Biol. 2010 Jul;2(7):a000398.

97. Hall-Stoodley L, Costerton JW, Stoodley P. Bacterial biofilms: from the natural environment to infectious diseases. Nat Rev Microbiol. 2004 Feb;2(2):95–108.

98. Watnick P, Kolter R. Biofilm, city of microbes. J Bacteriol. 2000 May;182(10):2675–9.

99. Nyström T. Aging in bacteria. Curr Opin Microbiol. 2002 Dec;5(6):596–601.

100. Chang C-Y. Surface Sensing for Biofilm Formation in Pseudomonas aeruginosa. Front Microbiol [Internet]. 2018;8:2671. Available from: https://www.frontiersin.org/article/10.3389/fmicb.2017.02671

101. Briandet R, Herry J-M, Bellon-Fontaine M-N. Determination of the van der Waals, electron donor and electron acceptor surface tension components of static Gram-positive microbial biofilms. Colloids Surf B Biointerfaces. 2001 Aug;21(4):299–310.

102. Takahashi H, Suda T, Tanaka Y, Kimura B. Cellular hydrophobicity of Listeria monocytogenes involves initial attachment and biofilm formation on the surface of polyvinyl chloride. Lett Appl Microbiol. 2010 Jun;50(6):618–25.

103. Gupta P, Sarkar S, Das B, Bhattacharjee S, Tribedi P. Biofilm, pathogenesis and prevention--a journey to break the wall: a review. Arch Microbiol. 2016 Jan;198(1):1–15.

104. Veerachamy S, Yarlagadda T, Manivasagam G, Yarlagadda PK. Bacterial adherence and biofilm formation on medical implants: a review. Proc Inst Mech Eng Part H, J Eng Med. 2014 Oct;228(10):1083–99.

105. Gu H, Hou S, Yongyat C, De Tore S, Ren D. Patterned biofilm formation reveals a mechanism for structural heterogeneity in bacterial biofilms. Langmuir. 2013 Sep;29(35):11145–53.

106. Hall CW, Mah T-F. Molecular mechanisms of biofilm-based antibiotic resistance and tolerance in pathogenic bacteria. FEMS Microbiol Rev. 2017 May;41(3):276–301.

107. Hammer BK, Bassler BL. Quorum sensing controls biofilm formation in Vibrio cholerae. Mol Microbiol. 2003 Oct;50(1):101–4.

108. Nealson KH, Platt T, Hastings JW. Cellular control of the synthesis and activity of the bacterial luminescent system. J Bacteriol. 1970 Oct;104(1):313–22.

109. Balamurugan P, Praveen Krishna V, Bharath D, Lavanya R, Vairaprakash P, Adline Princy S. Staphylococcus aureus Quorum Regulator SarA Targeted

Compound, 2-[(Methylamino)methyl]phenol Inhibits Biofilm and Down-Regulates Virulence Genes. Front Microbiol. 2017;8:1290.

110. Chu Y-Y, Nega M, Wölfle M, Plener L, Grond S, Jung K, et al. A new class of quorum quenching molecules from Staphylococcus species affects communication and growth of gram-negative bacteria. PLoS Pathog. 2013;9(9):e1003654.

111. Cook LC, Federle MJ. Peptide pheromone signaling in Streptococcus and Enterococcus. FEMS Microbiol Rev. 2014 May;38(3):473–92.

112. Ha J-H, Eo Y, Grishaev A, Guo M, Smith JAI, Sintim HO, et al. Crystal structures of the LsrR proteins complexed with phospho-AI-2 and two signal-interrupting analogues reveal distinct mechanisms for ligand recognition. J Am Chem Soc. 2013 Oct;135(41):15526–35.

113. Atkinson S, Williams P. Quorum sensing and social networking in the microbial world. J R Soc Interface. 2009 Nov;6(40):959–78.

114. Samanta S, Dey P, Gupta N, Mouleeswaran KS, Nijhawan R. Micronucleus in atypical squamous cell of undetermined significance. Diagn Cytopathol. 2011;39(4):242–4.

115. Sturme MHJ, Kleerebezem M, Nakayama J, Akkermans ADL, Vaughan EE, de Vos WM. Cell to cell communication by autoinducing peptides in gram-positive bacteria. Antonie Van Leeuwenhoek [Internet]. 2002;81(1):233–43. Available from: https://doi.org/10.1023/A:1020522919555

116. Taga ME, Miller ST, Bassler BL. Lsr-mediated transport and processing of AI-2 in Salmonella typhimurium. Mol Microbiol. 2003 Nov;50(4):1411–27.

117. Ishihama A. Adaptation of gene expression in stationary phase bacteria. Curr Opin Genet Dev. 1997 Oct;7(5):582–8.

118. Zambrano MM, Kolter R. GASPing for life in stationary phase. Cell. 1996 Jul;86(2):181–4.

119. Camilli A, Bassler BL. Bacterial small-molecule signaling pathways. Science. 2006 Feb;311(5764):1113–6.

120. Shank EA, Kolter R. New developments in microbial interspecies signaling. Curr Opin Microbiol. 2009 Apr;12(2):205–14.

121. Papenfort K, Bassler BL. Quorum sensing signal–response systems in Gram-negative bacteria. Nat Rev Microbiol [Internet]. 2016;14(9):576–88. Available from: https://doi.org/10.1038/nrmicro.2016.89

122. Jenal U. Cyclic di-guanosine-monophosphate comes of age: a novel secondary messenger involved in modulating cell surface structures in bacteria? Curr Opin Microbiol. 2004 Apr;7(2):185–91.

123. Jenal U, Malone J. Mechanisms of cyclic-di-GMP signaling in bacteria. Annu Rev Genet. 2006;40:385–407.

124. **Joubert L-M, Wolfaardt GM, Botha A. Microbial exopolymers link predator and prey** in a model yeast biofilm system. Microb Ecol. 2006 Aug;52(2):187–97.

125. Van Colen C, Underwood G, Serodio J, Paterson DM. Ecology of intertidal microbial biofilms: mechanisms, patterns and future research needs. J Sea Res. 2014;92:2–5.

126. Cooksey KE, Wigglesworth-Cooksey B. Adhesion of bacteria and diatoms to surfaces in the sea: A review. Aquat Microb Ecol. 1995;9(1):87–96.

127. Fanning S, Mitchell AP. Fungal biofilms. PLoS Pathog. 2012;8(4):e1002585.

128. Chandra J, Kuhn DM, Mukherjee PK, Hoyer LL, McCormick T, Ghannoum MA. Biofilm formation by the fungal pathogen Candida albicans: development, architecture, and drug resistance. J Bacteriol. 2001 Sep;183(18):5385–94.

129. Phototropic biofilm [Internet]. Available from: https://en.wikipedia.org/wiki/Phototrophic_biofilm

130. Roeselers G, Norris TB, Castenholz RW, Rysgaard S, Glud RN, Kühl M, et al. Diversity of phototrophic bacteria in microbial mats from Arctic hot springs (Greenland). Environ Microbiol. 2007 Jan;9(1):26–38.

131. Wolcott RD, Rhoads DD, Bennett ME, Wolcott BM, Gogokhia L, Costerton JW, et al. Chronic wounds and the medical biofilm paradigm. J Wound Care. 2010 Feb;19(2):45-46,48-50,52-53.

132. Hrv R, Devaki R, Kandi V. Evaluation of Different Phenotypic Techniques for the Detection of Slime Produced by Bacteria Isolated from Clinical Specimens. Cureus. 2016 Feb;8(2):e505.

133. Mozioğlu E. Fluorescence-based real-time monitoring of Pseudomonas aeruginosa and a simple, continuous screening method for detection of antibiofilm activity. Int J Environ Anal Chem [Internet]. 2020;100(4):383–92. Available from: https://doi.org/10.1080/03067319.2019.1685091

134. Djordjevic D, Wiedmann M, McLandsborough LA. Microtiter plate assay for assessment of Listeria monocytogenes biofilm formation. Appl Environ Microbiol. 2002 Jun;68(6):2950–8.

135. Hassan A, Usman J, Kaleem F, Omair M, Khalid A, Iqbal M. Evaluation of different detection methods of biofilm formation in the clinical isolates. Brazilian J Infect Dis an Off Publ Brazilian Soc Infect Dis. 2011;15(4):305–11.

136. Freeman DJ, Falkiner FR, Keane CT. New method for detecting slime production by coagulase negative staphylococci. J Clin Pathol. 1989 Aug;42(8):872–4.

137. Singer G, Besemer K, Hödl I, Chlup A, Hochedlinger G, Stadler P, et al. Microcosm design and evaluation to study stream microbial biofilms. Limnol Oceanogr Methods [Internet]. 2006;4(11):436–47. Available from:

https://aslopubs.onlinelibrary.wiley.com/doi/abs/10.4319/lom.2006.4.436

138. Wiggli M, Smallcombe A, Bachofen R. Reflectance spectroscopy and laser confocal microscopy as tools in an ecophysiological study of microbial mats in an alpine bog pond. J Microbiol Methods. 1999;34(3):173–82.

139. Mandakhalikar KD. Medical Biofilms. ACS Symp Ser. 2019;1323(1):83–99.

140. Pozo JL Del. Biofilm-related disease. Expert Rev Anti Infect Ther [Internet]. 2018;16(1):51–65. Available from: https://doi.org/10.1080/14787210.2018.1417036

141. Fux CA, Stoodley P, Hall-Stoodley L, Costerton JW. Bacterial biofilms: a diagnostic and therapeutic challenge. Expert Rev Anti Infect Ther. 2003 Dec;1(4):667–83.

142. Raad II, Bodey GP. Infectious complications of indwelling vascular catheters. Clin Infect Dis an Off Publ Infect Dis Soc Am. 1992 Aug;15(2):197–208.

143. Gristina AG, Naylor P, Myrvik Q. Infections from biomaterials and implants: a race for the surface. Med Prog Technol. 14(3–4):205–24.

144. Tumbarello M, Posteraro B, Trecarichi EM, Fiori B, Rossi M, Porta R, et al. Biofilm production by Candida species and inadequate antifungal therapy as predictors of mortality for patients with candidemia. J Clin Microbiol. 2007 Jun;45(6):1843–50.

145. Uppuluri P, Srinivasan A, Ramasubramanian A, Lopez-Ribot JL. Effects of fluconazole, amphotericin B, and caspofungin on Candida albicans biofilms under conditions of flow and on biofilm dispersion. Antimicrob Agents Chemother. 2011 Jul;55(7):3591–3.

146. Andersson DI, Hughes D. Microbiological effects of sublethal levels of antibiotics. Nat Rev Microbiol. 2014 Jul;12(7):465–78.

147. Adams WPJ, Haydon MS, Raniere JJ, Trott S, Marques M, Feliciano M, et al. A rabbit model for capsular contracture: development and clinical implications. Plast Reconstr Surg. 2006 Apr;117(4):1211–4.

148. Arslan SY, Leung KP, Wu CD. The effect of lactoferrin on oral bacterial attachment. Oral Microbiol Immunol. 2009 Oct;24(5):411–6.

149. Overhage J, Campisano A, Bains M, Torfs ECW, Rehm BHA, Hancock REW. Human host defense peptide LL-37 prevents bacterial biofilm formation. Infect Immun. 2008 Sep;76(9):4176–82.

150. Okuda K, Zendo T, Sugimoto S, Iwase T, Tajima A, Yamada S, et al. Effects of bacteriocins on methicillin-resistant Staphylococcus aureus biofilm. Antimicrob Agents Chemother. 2013 Nov;57(11):5572–9.

151. Mansour SC, Pena OM, Hancock REW. Host defense peptides: front-line immunomodulators. Trends Immunol. 2014 Sep;35(9):443–50.

152. Brancatisano FL, Maisetta G, Di Luca M, Esin S, Bottai D, Bizzarri R, et al.

Inhibitory effect of the human liver-derived antimicrobial peptide hepcidin 20 on biofilms of polysaccharide intercellular adhesin (PIA)-positive and PIA-negative strains of Staphylococcus epidermidis. Biofouling. 2014;30(4):435–46.

153. Zhu C, Tan H, Cheng T, Shen H, Shao J, Guo Y, et al. Human β-defensin 3 inhibits antibiotic-resistant Staphylococcus biofilm formation. J Surg Res. 2013 Jul;183(1):204–13.

154. McCloskey AP, Gilmore BF, Laverty G. Evolution of antimicrobial peptides to self-assembled peptides for biomaterial applications. Pathogens. 2014;3(4):792–821.

155. Yeaman MR, Yount NY. Mechanisms of antimicrobial peptide action and resistance. Pharmacol Rev. 2003 Mar;55(1):27–55.

156. Hollmann A, Martinez M, Maturana P, Semorile LC, Maffia PC. Antimicrobial peptides: Interaction with model and biological membranes and synergism with chemical antibiotics. Front Chem. 2018;6(JUN):1–13.

157. Turner J, Cho Y, Dinh NN, Waring AJ, Lehrer RI. Activities of LL-37, a cathelin-associated antimicrobial peptide of human neutrophils. Antimicrob Agents Chemother. 1998 Sep;42(9):2206–14.

158. de Breij A, Riool M, Cordfunke RA, Malanovic N, de Boer L, Koning RI, et al. The antimicrobial peptide SAAP-148 combats drug-resistant bacteria and biofilms. Sci Transl Med. 2018 Jan;10(423).

159. Hamamoto K, Kida Y, Zhang Y, Shimizu T, Kuwano K. Antimicrobial activity and stability to proteolysis of small linear cationic peptides with D-amino acid substitutions. Microbiol Immunol. 2002;46(11):741–9.

160. Manabe T, Kawasaki K. D-form KLKLLLLLKLK-NH(2) peptide exerts higher antimicrobial properties than its L-form counterpart via an association with bacterial cell walfile:///C:/Users/PC/Downloads/1471-2180-11-114.pdfl components. Sci Rep. 2017 Mar;7:43384.

161. Kim J-Y, Park S-C, Yoon M-Y, Hahm K-S, Park Y. C-terminal amidation of PMAP-23: translocation to the inner membrane of Gram-negative bacteria. Amino Acids. 2011 Jan;40(1):183–95.

162. Yoo J, Cui Q. Chemical versus Mechanical Perturbations on the Protonation State of Arginine in Complex Lipid Membranes: Insights from Microscopic pKa Calculations. Biophys J [Internet]. 2010;99(5):1529–38. Available from: http://www.sciencedirect.com/science/article/pii/S0006349510007915

163. Li J, Koh JJ, Liu S, Lakshminarayanan R, Verma CS, Beuerman RW. Membrane active antimicrobial peptides: Translating mechanistic insights to design. Front Neurosci. 2017;11(FEB):1–18.

164. Milletti F. Cell-penetrating peptides: classes, origin, and current landscape. Drug Discov Today. 2012 Aug;17(15–16):850–60.

165. Thévenet P, Shen Y, Maupetit J, Guyon F, Derreumaux P, Tufféry P. PEP-

FOLD: an updated de novo structure prediction server for both linear and disulfide bonded cyclic peptides. Nucleic Acids Res. 2012 Jul;40(Web Server issue):W288-93.

166. Phillips JC, Braun R, Wang W, Gumbart J, Tajkhorshid E, Villa E, et al. Scalable molecular dynamics with NAMD. J Comput Chem [Internet]. 2005;26(16):1781–802. Available from: https://onlinelibrary.wiley.com/doi/abs/10.1002/jcc.20289

167. Humphrey W, Dalke A, Schulten K. VMD: Visual molecular dynamics. J Mol Graph [Internet]. 1996;14(1):33–8. Available from: http://www.sciencedirect.com/science/article/pii/0263785596000185

168. van Meer G, Voelker DR, Feigenson GW. Membrane lipids: where they are and how they behave. Nat Rev Mol Cell Biol. 2008 Feb;9(2):112–24.

169. Hwang H, Paracini N, Parks JM, Lakey JH, Gumbart JC. Distribution of mechanical stress in the Escherichia coli cell envelope. Biochim Biophys acta Biomembr. 2018 Dec;1860(12):2566–75.

170. Sheppard RC. Peptide synthesis. Nature. 1979;282(5734):116.

171. High-performance liquid chromatography [Internet]. Available from: https://en.wikipedia.org/wiki/High-performance_liquid_chromatography

172. Difference between C8 and C18 column used in HPLC system [Internet]. Available from: https://www.pharmaguideline.com/2018/05/difference-between-c8-and-c18-columns.html

173. Freeze-drying [Internet]. Available from: https://en.wikipedia.org/wiki/Freeze-drying

174. Information IP. Pierce Quantitative Fluorometric Peptide Assay. Thermofisher Sci [Internet]. 2014;3723(815):1–5. Available from: https://tools.thermofisher.com/content/sfs/manuals/23290_quantpeptide_fluor_UG.pdf

175. Hyphenated Separation Techniques. In: Fundamentals of Contemporary Mass Spectrometry [Internet]. John Wiley & Sons, Ltd; 2007. p. 151–94. Available from: https://onlinelibrary.wiley.com/doi/abs/10.1002/9780470118498.ch5

176. Basics of LC/MS.

177. Teh CH, Nazni WA, Nurulhusna AH, Norazah A, Lee HL. Determination of antibacterial activity and minimum inhibitory concentration of larval extract of fly via resazurin-based turbidometric assay. BMC Microbiol. 2017;17(1):1–8.

178. de Lucio H, Gamo AM, Ruiz-Santaquiteria M, de Castro S, Sánchez-Murcia PA, Toro MA, et al. Improved proteolytic stability and potent activity against Leishmania infantum trypanothione reductase of α/β-peptide foldamers conjugated to cell-penetrating peptides. Eur J Med Chem [Internet]. 2017;140:615–23. Available from: http://www.sciencedirect.com/science/article/pii/S0223523417307468

179. Scanning electron microscope [Internet]. 2020. Available from: https://en.wikipedia.org/wiki/Scanning_electron_microscope

180. Wang Q, Xu Y, Dong M, Hang B, Sun Y, Wang L, et al. HJH-1, a Broad-Spectrum Antimicrobial Activity and Low Cytotoxicity Antimicrobial Peptide. Molecules. 2018 Aug;23(8).

181. Eren T, Som A, Rennie JR, Nelson CF, Urgina Y, Nüsslein K, et al. Antibacterial and Hemolytic Activities of Quaternary Pyridinium Functionalized Polynorbornenes. Macromol Chem Phys [Internet]. 2008;209(5):516–24. Available from: https://doi.org/10.1002/macp.200700418

182. MTT Assay for Cell Viability and Proliferation [Internet]. Available from: https://www.sigmaaldrich.com/technical-documents/protocols/biology/roche/cell-proliferation-kit-i-mtt.html

183. Kirshenbaum AS, Kessler S. ., Goff JP, Mercalfe D. Demonstration of the origin of human mast cells from CD34 + bone marrow progenitor Information about subscribing to The Journal of Immunology is online at : DEMONSTRATION OF THE ORIGIN OF HUMAN MAST CELLS FROM CD34 +. J Immunol. 1991;146:1410–5.

184. Bacalum M, Radu M. Cationic antimicrobial peptides cytotoxicity on mammalian cells: An analysis using therapeutic index integrative concept. Int J Pept Res Ther. 2015;21(1):47–55.

185. Mathur T, Singhal S, Khan S, Upadhyay DJ, Fatma T, Rattan A. Detection of biofilm formation among the clinical isolates of staphylococci: An evaluation of three different screening methods. Indian J Med Microbiol. 2006;24(1):25–9.

186. Cruz CD, Shah S, Tammela P. Defining conditions for biofilm inhibition and eradication assays for Gram-positive clinical reference strains. BMC Microbiol. 2018;18(1):1–9.

187. Stepanović S, Vuković D, Dakić I, Savić B, Švabić-Vlahović M. A modified microtiter-plate test for quantification of staphylococcal biofilm formation. J Microbiol Methods [Internet]. 2000;40(2):175–9. Available from: http://www.sciencedirect.com/science/article/pii/S0167701200001226

188. Kaiser TDL, Pereira EM, dos Santos KRN, Maciel ELN, Schuenck RP, Nunes APF. Modification of the Congo red agar method to detect biofilm production by Staphylococcus epidermidis. Diagn Microbiol Infect Dis [Internet]. 2013;75(3):235–9. Available from: http://www.sciencedirect.com/science/article/pii/S073288931200497X

189. Riaz T, Zeeshan R, Zarif F, Ilyas K, Safi SZ, Rahim A, et al. FTIR analysis of natural and synthetic collagen. 2018;4928. Available from: https://doi.org/10.1080/05704928.2018.1426595

190. Pallandre A, Glinel K, Jonas AM, Nysten B. Binary Nanopatterned Surfaces Prepared from Silane Monolayers. Nano Lett. 2004;4(2):365–71.

191. Peptide prediction PEP-FOLD3 [Internet]. Available from: https://bioserv.rpbs.univ-paris-diderot.fr/services/PEP-FOLD3/

192. Dean SN, Bishop BM, van Hoek ML. Natural and synthetic cathelicidin peptides with anti-microbial and anti-biofilm activity against Staphylococcus aureus. BMC Microbiol. 2011;11(May):114.

7. CURRICULUM VITAE